The South Indian Convergence Zone and Relationship with Rainfall variability in Mozambique

Atanásio João Manhique

Thesis Presented for the Degree of Doctor of Philosophy in the
Department of Oceanography, Faculty of Science
University of Cape Town

Cape Town, South Africa,

August 2008

ABSTRACT

Southern Hemisphere atmospheric circulation and sea surface temperatures in the South Indian Ocean, associated with the South Indian Convergence Zone (SICZ), the main rain producing system over southern Africa, and links with rainfall over Mozambique, are analysed. Cluster analysis applied to gridded outgoing long-wave radiation data, were used to identify convective activity related to the tropical temperate troughs that collectively form the SICZ. Intra-seasonal and inter-annual variability of these systems and their contribution to the anomalies of rainfall over Mozambique were explored using composite, correlation and regression analyses for both the early (October to December) and the late (January to March) summer.

Positive anomalies of rainfall are observed over southern and central Mozambique when the SICZ is positioned over southern Africa. Large scale atmospheric circulation patterns that contribute to generate and maintain the SICZ over southern Africa, are linked to La Niña and Southern Hemisphere planetary waves. A wavenumber-3 or -4 pattern was observed to strengthen and shift the South Indian Ocean anticyclone westward, thus contributing to strengthening the easterly winds over the tropical and subtropical Indian Ocean. Both La Niña and the Southern Hemisphere planetary waves force the main sea surface temperature anomaly patterns over the South Indian Ocean, which may explain much of the significant relationship between the sea surface temperature and rainfall over southern Africa.

Negative anomalies of rainfall are observed over southern Africa, when the SICZ is shifted towards the Southwest Indian Ocean. The mechanism contributing to the north-eastward shift of the SICZ appears to be associated with sea surface temperature forcing over the central South Indian Ocean, particularly associated with El Niño. Warm anomalies of sea surface temperature force wind and moisture convergence over the central South Indian Ocean, which weakens the onshore winds and moisture fluxes towards southern Africa.

Declaration

I declare that this thesis is my own, and that I have received no assistance except as acknowledged. It has not been submitted before for any degree or examination in any other university.

ACKNOWLEDGEMENTS

A number of people have given their valuable contribution for the accomplishment of this study to who I am very grateful.

I would like to thank my supervisors Prof. Chris Reason and Prof. Lars Rydberg for their guidance throughout the research and patient reviews of my writing. I would also like to thank Dr. Yves Richard and Dr. Nicolas Fauchereau of the Centre of Climate Research (CRC) at the University of Bourgogne, France, for their help on techniques of statistical analysis. The help and collaboration of the staff at the Departments of Oceanography at UCT and at the University of Gothenburg, and also the staff at the CRC at the University of Bourgogne is very much appreciated.

A word of gratitude to Dr. Mathieu Rouault who provided some of the Matlab scripts used to read the NETCDF files, to Dr. Nicolas Fauchereau who provided the Matlab scripts used to compute the cluster analysis and to Dr. Nathalie Philippon who provided the Matlab scripts used to compute the wet spells.

I am grateful to the Mozambique Institute of Meteorology for allowing me to carry out this study and for providing the rainfall station data used in the study.

Financial support for this research was provided by Sida/SAREC initially through the project: “Coastal and Marine Processes for Management of Coastal Resources” and later through the program: “The Development of Biological and Oceanographic Research Capacity”, at UEM in Mozambique. I would like to express my gratitude for the funding and also to the coordinators of the project/program who organized my trips to carry out this research study. I am also grateful to the project IPSC of the CRC, for funding my visits to the University of Bourgogne, which helped me in developing the necessary skills in statistical analysis necessary to handle the large number of different datasets used in this study.

Lastly and wholeheartedly, a big thank to my family and friends, particularly to my wife Horácia, my children Tânia, Chilton and Atanásio, for their support and for enduring the long periods of my absence to accomplish my studies.

In memory of my parents

João Manhique and

Marta Zandamela

CONTENTS

Appendices

List of abbreviations and frequently used symbols

AAO	Antarctic Annular Oscillation
AMJ	April to May season
ASO	August to September season
BMI	Brandon-Marion index
CA	Cluster Analysis
CGCM	Coupled General Circulation Model
CMAP	Merged Analysis of Precipitation
CPC	Climate Prediction Centre
CRU	Climate Research Unit (at University of East Anglia)
DJF	December to January season
EACC	East African Coast Current
ECC	Equatorial Counter Current
ENSO	El Niño Southern Oscillation
EOF	Empirical orthogonal functions
FMA	February to March season
GCM	General Circulation Model
HadSST	Hadley Centre Sea Surface Temperature dataset
ITCZ	Inter-tropical Tropical Convergence Zone
JFM	January to March season
LBCZ	Land based convergence zone
MAM	March to May season
MJJ	May to July season
NCAR	National Center for Atmospheric Research
NCEP	National Centre for Environmental Prediction
NDJ	November to January season

NH	Northern Hemisphere
JAS	July to September season
JJA	June to August season
OLR	Outgoing long-wave radiation
OND	October to December season
PCA	Principal Component Analysis
r	Correlation coefficient
QBO	Quasi-Biennial Oscillation
SACZ	South Atlantic Convergence Zone
SEC	South Equatorial Current
SH	Southern Hemisphere
SICZ	South Indian Convergence Zone
SIOD	Subtropical Indian Ocean dipole
SO	Southern Oscillation
SON	September to November season
SPCZ	South Pacific Convergence Zone
SST	Sea surface temperature
SWIO	South-West Indian Ocean
TTT	Tropical temperate troughs

List of Figures

List of Tables

Chapter One

1. Introduction

1.1 General introduction

Climate variability over southern Africa, particularly rainfall variability is fairly well understood. A significant number of references discussing the climate variability at different space and time scales are available (e.g. Harrison, 1984; Lindesay, 1988; Jury, 1992; Rocha and Simmonds, 1997; Makarau and Jury, 1997; Reason 1998 and 2002; Reason et al., 2000; Mulenga et al., 2003; Richard et al., 2000, 2001; Reason and Jagadheesha, 2005; Cook, 2000 and 2001). A summary of more significant results can be found in Reason et al. (2006a, b). The rainfall variability in Mozambique has a different regime to most of southern Africa countries, given its coastal location, facing the warm Indian Ocean, the varying altitude (see Fig. 3.1), and its long latitudinal extension. Thus, the northern part is more influenced by tropical weather systems and the southern part more influenced by mid-latitude systems or by interactions with both. For example, the central and northern regions in Mozambique receive between 400 and 600 mm more annual mean rainfall than the southern part (see Fig.1.2). Furthermore, a significant number of dry spells is observed in the southern part while in the northern part rains are more regular (e.g. Usman and Reason, 2004).

Rainfall anomalies occur regularly in Mozambique on different space and time scales. These anomalies have a significant impact on food security and subsistence of rural communities. During the last few decades, the country has experienced recurrent severe climate events with dramatic effects on the economy and human life. Some examples are the droughts in 1982-83 and 1991-1992 and more recently the floods (due to excessive rainfall) in 1999-2000, 2000-2001 and 2006-2007 in the central and southern parts of the country. These claimed hundreds of lives and caused hundreds of millions of US dollars in

destruction of infrastructure (e.g. Mozambique News Agency reports 2000, 2001 and 2007). Also, outbreak of some diseases such as malaria and cholera often occur in Mozambique during years with above average rainfall. Treatment and mitigation of these diseases outbreaks is very costly and lead to significant strain on government health resources. That has cost enormous financial resources, necessary for the development of the country. These events also hampered the government's efforts to improve the economic and social conditions for the people.

Mozambique has a large potential for agriculture and more than 75% of the population lives in rural areas (see the website for the Mozambique National statistics Institute: http://www.ine.gov.mz/Ingles/censos_dir/agro-pecuaria/agro-pec/) with the majority dependent on rain fed subsistence agriculture. Rainfall is a key issue for agriculture and infrastructure development in Mozambique.

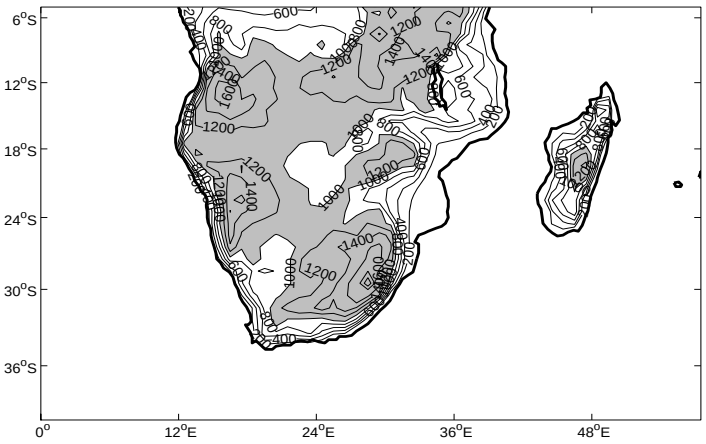

Fig.1.1 Topography of southern Africa. Shaded areas indicate areas equal or above 1000 m of altitude. Contours are 200 m.

Tropical temperate troughs (TTT) have been recognised as the main summer synoptic rain producing systems over southern Africa (e.g. Harrison, 1984; Washington and Todd 1999; Reason et al., 2006a). Collectively over the austral summer, they contribute to the South Indian Convergence Zone (SICZ - Cook, 2000). Here the term TTT is used when discussing multiple systems and their variability, and SICZ, is used when referring collectively to the broad feature.

Understanding the mechanisms that generate these systems and their inter-annual variability is important for a better appreciation of rainfall variability over southern Africa.

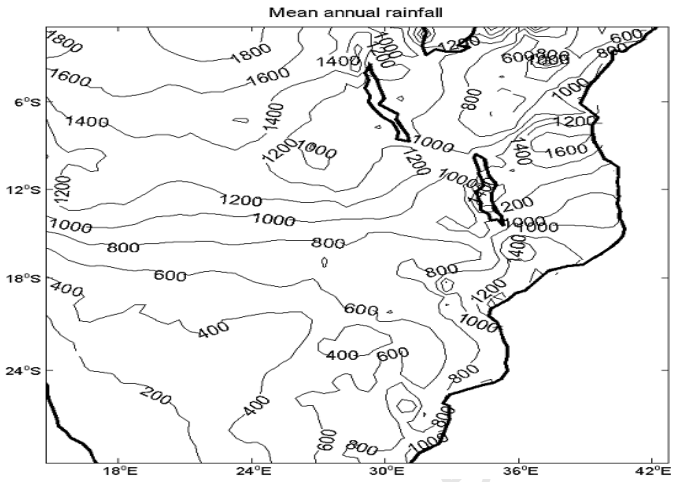

Fig. 1.2 Annual mean (1961 – 2000) rainfall (mm) over southern Africa. CRU TS 2.0 monthly data

1.2 Statement of the problem

Despite the importance of TTT for rainfall over southern Africa, only recently have they received significant attention from the scientific community. This interest might have been fuelled by the recent availability of large amount of data that was made possible by development of meteorological and oceanographic remote sensing techniques, reanalysis projects such as that from NCEP-NCAR (Kalnay et al., 1996), development of global circulation models and developments in computing, which make it possible to cope with huge amounts of data. The importance of TTT for rainfall over southern Africa has been long recognised (e.g. Harrison, 1984), but detailed descriptions of the atmospheric circulation and rainfall linked to them has only recently been investigated (e.g. Todd and Washington, 1999; Tyson and Preston-Whyte, 2000; Todd et al. 2004; Reason et al., 2006a; Fauchereau et al. 2008). However, links between TTT over southern Africa and SST over the surrounding oceans have not been thoroughly addressed. This aspect is important as a number of studies have

shown significant statistical links between rainfall and sea surface temperature (SST) over the South Indian Ocean (e.g. Jury et al. 1996; Rocha and Simmonds, 1997; Reason and Mulenga, 1999). Although other studies using numerical models have supported these links (e.g. Rocha and Simmonds, 1997; Reason, 2002; Washington and Preston, 2006), physical explanations remain in general unclear. Therefore, studying the relationships between SST and TTT (being the main rain producing systems) would help to unveil the mechanisms linking rainfall and SST over southern Africa. Another important aspect less studied is the inter-annual variability of the TTT. A better comprehension of this aspect would help in understanding the physical mechanisms behind rainfall relationships with ENSO and also with Southern Hemisphere (SH) atmospheric modes. These two topics are both analysed in the present study, with emphasis to the rainfall variability in Mozambique. This thesis is entirely based on diagnostic work of observed data and reanalysis products from NCEP II as a first approach to understand the complex links between the frequencies of TTT, rainfall variability in Mozambique and large scale atmospheric and oceanic patterns, therefore no numerical model is used.

1.3 Objectives

The main aim of this study is to explore the statistical and physical links between the South Indian Convergence Zone and sea surface temperatures (SST) over the Indian Ocean, and in particular the rainfall variability associated with the TTT. A second aim is to explore the links between these systems and inter-annual frequency of wet spells and of dry days over Mozambique. The reason why dry days are used instead of dry spells is explained in Chapter 3.

To achieve the main goals of this study, the following objectives are formulated:

1. To define the convective patterns associated with the TTT over southern Africa in general and particularly over Mozambique using OLR data as a proxy for convective activity.
2. Explore the atmospheric mechanisms associated with the SICZ.
3. Explore the intra-seasonal and inter-annual variability of the TTT and their links with frequency of wet spells and dry days over Mozambique.
4. Explore statistical and physical links between regional SST and the SICZ over southern Africa and South-West Indian Ocean (SWIO).

1.4 Outline of the chapters

This thesis is divided into seven chapters:

Chapter 2 This chapter reviews the work on rainfall variability over southern Africa, the relationship between rainfall variability and the SICZ and links with atmospheric circulation and SST

Chapter 3 This chapter describes the data and methods used to analyse the data.

Chapter 4 This chapter shows the composite anomalies of atmospheric patterns associated with the SICZ.

Chapter 5 This chapter analyses inter-annual variability of the SICZ and its relationship with atmospheric circulation, ENSO and Indian Ocean SST modes.

Chapter 6 This chapter explores links between the frequencies of wet spells and dry days over Mozambique and the SICZ.

Chapter 7 Summary and conclusions are presented.

Chapter Two

2. Literature review

2.1 Atmospheric circulation

Weather-producing systems are distinguished by their characteristic scales and circulation patterns. These patterns are caused by energy imbalances which produce temperature and, therefore pressure variations. Pressure gradients generate winds. The wind systems occur at a variety of scales ranging from microscales to the global scale. At the global scale, the winds are generally characterised by easterly winds in the tropics, westerly winds in mid latitudes and polar easterly winds in high latitudes (Tyson and Preston-Whyte, 2000). South Africa and southern Mozambique location in the subtropics ensures that are affected by circulation systems prevailing in both the tropics to the north and mid-latitudes to the south (e.g. Reason et al., 2006a).

2.1.1 General aspects of Southern Hemisphere atmospheric circulation affecting southern Africa

Atmospheric circulation over southern Africa is dominated by the presence of the subtropical anticyclones over the South Indian and South Atlantic Oceans, which are elements of the discontinuous high pressure belt that circles the Southern Hemisphere (SH) at about 30°S and the seasonally migratory Inter-tropical Convergence Zone (ITCZ). The two anticyclones vary significantly in position throughout the year. The South Indian anticyclone undergoes a semi-annual variation in its latitudinal movement, but also an annual oscillation in its longitudinal displacement while the South Atlantic anticyclone exhibits a yearly cycle in both (Tyson and Preston-Whyte, 2000). Figure 2.1 derived from the NCEP-NCAR reanalysis data set shows the SH mean sea level pressure (annual, October to December - OND and January to March - JFM). The shifts are evident in both the South Indian and the South Atlantic anticyclones from the

OND to JFM averages, but they are more accentuated in the South Indian anticyclone, particularly the latitudinal shift.

Tyson and Preston-Whyte (2000) indicate that disturbances in the tropical easterly flow occurring around the northern margins of the subtropical anticyclones take the form of easterly waves and lows and are associated with the ITCZ and the warm humid easterly winds between this zone and the subtropical high-pressure belt (see Fig. 2.2). Furthermore they argue that easterly waves over southern Africa are semi-stationary while tropical disturbances are almost exclusively a summer phenomenon with an annual cycle peaking between December and February.

At mid-latitudes, westerly waves dominate the Southern Hemisphere circulation throughout the year. Tyson and Preston-Whyte (2000) divide the westerly waves into two categories: Long, semi-stationary forced barotropic waves and shorter, transient, baroclinic travelling waves, with the latter steered by the semi-stationary waves and large scale flow. They argue that shifts in phase (longitudinally) or in amplitude (latitudinally) of the long waves or changes in variance on the short-wave disturbances have effects on weather and climate of southern Africa.

Thompson and Wallace (2000) suggest that leading modes of the extratropical circulation in both hemispheres are characterised by deep zonally symmetric or “annular” structures, with geopotential height perturbations of opposing signs in the polar cap region and in the surrounding zonal ring centred near 45° of latitude. The SH mode is known as the Antarctic Annular Oscillation (AAO) or the Southern Annular mode (e.g. Kidson, 1999; Gong and Wang, 1999). Thompson and Wallace (2000) argue that the annular modes exist throughout the year in the troposphere, amplifying with height, upward into the stratosphere during seasons (late spring) in which the strength of the zonal flow is leading to strong planetary wave-mean flow interaction. They also suggest that the annular modes modulate the Lagrangian mean circulation in the lower

stratosphere, total column ozone and tropopause height over mid and high latitudes and the strength of the trade winds on their respective hemispheres.

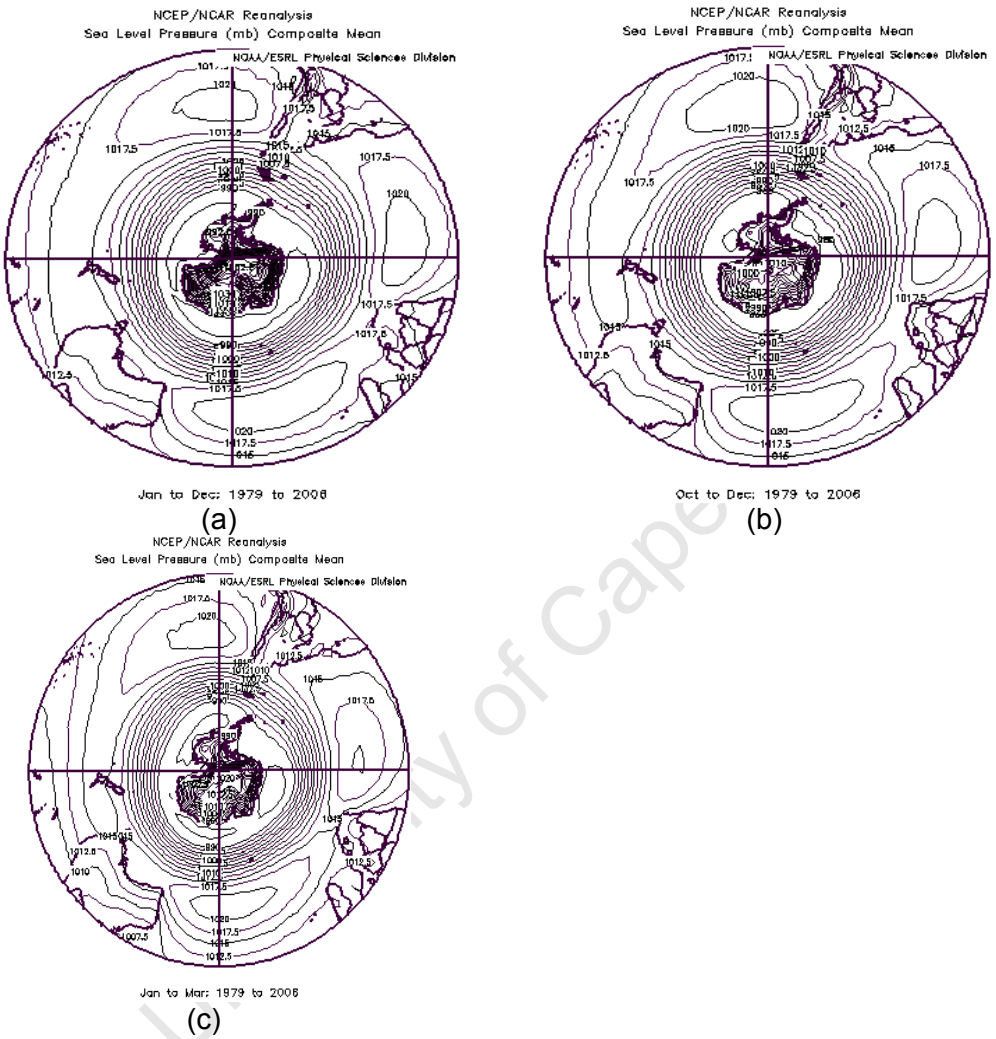

Fig.2.1 Mean sea level pressure (contour interval is 2.5 mb) over the Southern Hemisphere (NCEP/NCAR reanalysis) for the period 1979-2006 (a) annual; (b) October – December; (c) January – March .

EOF1 of 500 hPa geopotential height of Mo (2000) shows an annular structure with a phase reversal between anomalies in the Southern Hemisphere high and mid-latitudes. He indicates that this mode appears in the inter-decadal band and the 50 day low-pass filtered data. Ghil and Mo (1991) suggest that the dominant mode of intra-seasonal oscillation in the Southern Hemisphere has a

period of 23 days, with a zonal wavenumber-4 structure and the second mode has 40 days period and is dominated by wavenumbers-3 and -4.

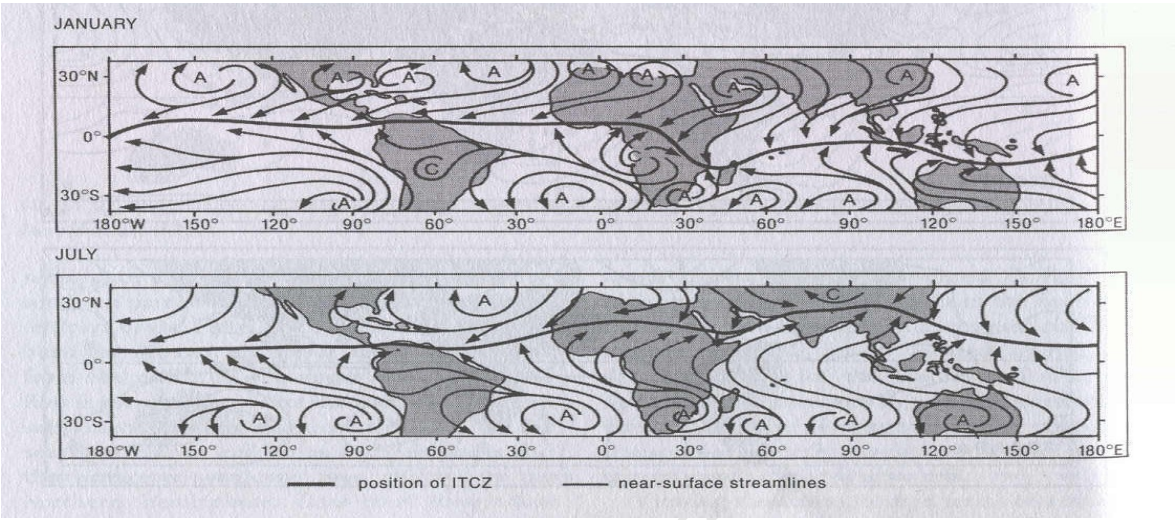

Fig.2.2 Schematic representation of streamlines of near-surface flow in the global tropics in January and July to show mean Inter-Tropical Convergence Zone (ITCZ). A denotes an anticyclonic centre, C denotes a cyclonic centre (after Tyson and Preston-Whyte, 2000)

Cai and Watterson (2002) suggest that 500-hPa geopotential height modes of variability, including the AAO can be generated by atmospheric internal dynamics alone, whereas the oceanic dynamics, air-sea interactions, and ENSO forcing are not essential.

Van Loon et al. (1993) noticed an intensification of the zonal wavenumber-3 at higher latitudes and in the semi-annual wave in pressure and winds during 1970s and 1980s. They also noticed a widespread fall in pressure in summer over Indian Ocean.

Both easterly and westerly waves have significant impact in the variability of the subtropical convergence zones (see next section).

2.1.2 Subtropical convergence zones and Tropical temperate troughs

Subtropical convergence zones are important features of the global atmospheric circulation. Kodama (1999) suggests the existence of three subtropical convergence zones, one in the Northern Hemisphere (NH) and two in

the Southern Hemisphere (SH). The NH subtropical convergence zone is the Baiu/Mei-yu frontal zone (BFZ) over East Asia and western North Pacific. The SH zones are the subtropical part of the South Pacific Convergence Zone (SPCZ) over the South Pacific and the South Atlantic Convergence Zone (SACZ), over the southern part of Brazil and South Atlantic. Figure 2.3 from Kodama (1999) shows these convergence zones. Cook (2000) suggests a third convergence zone over SH, the South Indian convergence zone, over southern Africa and the South-West Indian Ocean (SWIO). Figure 2.4 shows satellite image displaying cloud bands associated with this convergence zone. Subtropical convergence zones are regions of significant convective activity, cloudiness and rainfall. The SICZ is an austral summer feature while the SPCZ and the SACZ are also observed in winter although they are more active in austral summer (see e.g. Lenters and Cook, 1995; Vincent, 1994; Cook, 2000).

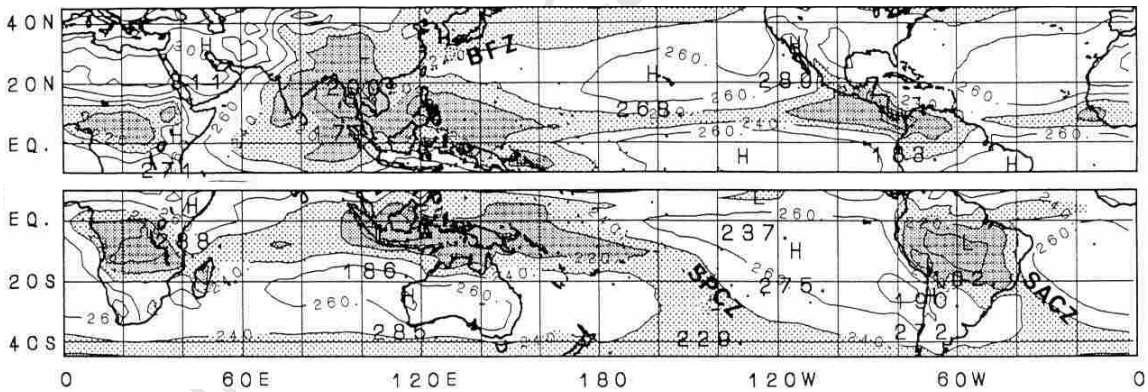

Fig. 2.3 OLR distribution averaged for the Northern Hemisphere summer (Jun-Aug; upper panel), and Southern Hemisphere summer (Dec-Mar; lower panel) for the period 1979-1986; from Kodama, (1999). Contour interval is 20 Wm^{-2} and dark (light) shading indicates OLR less than 220 Wm^{-2} (240 Wm^{-2}).

Different theories on the origin and maintenance of subtropical convergence zones have been developed. Some studies suggest SST gradients as an important forcing mechanism. These studies argue that SST gradients produce pressure gradients which in turn drive low level winds that result in moisture convergence. The role of SST gradients is in general associated with the ITCZ or subtropical zonal convergence zones (e.g. Lindzen and Nigam,

1987; Grodsky and Carton, 2003); however Lenters and Cook (1995) suggest that SSTs affect both the position and intensity of the SACZ.

Generation of continental heat lows, particularly in summer has been shown to be an important forcing of the subtropical convergence zones. The mechanism proposed here is associated with enhancement of pressure gradients between the subtropical highs (particularly over their north-western side) and the continents. This contributes to wind convergence and advection of warm air and moisture over the eastern part of the continents, which may then generate vertical motion and set up the convergence zones (e.g. Lenterss and Cook, 1995; Kodama, 1999; Cook, 2000).

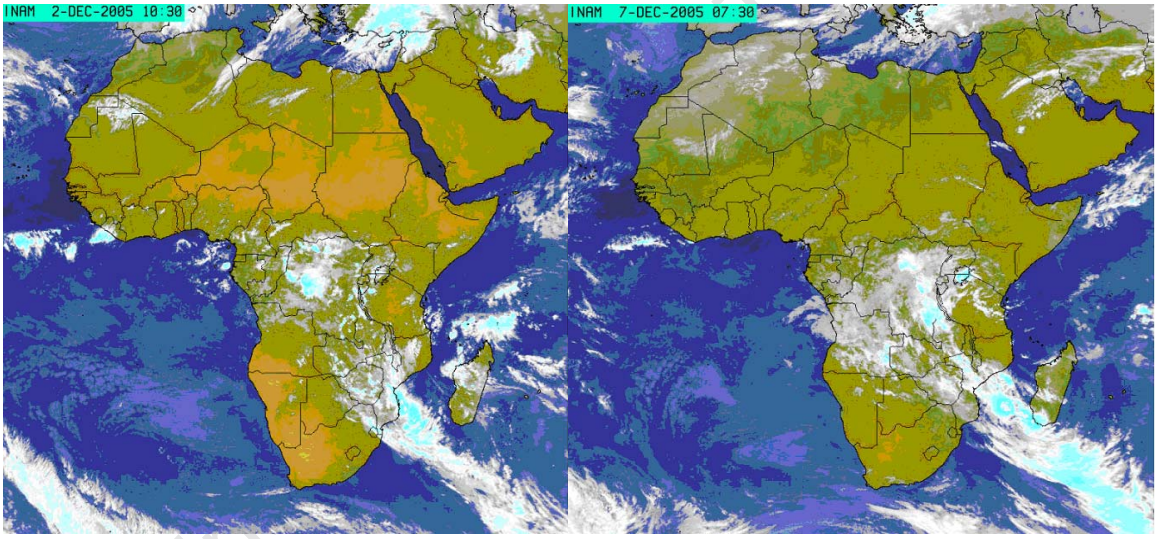

Fig.2.4 Satellite images showing cloud bands over southern Africa typical of TTT on 2nd and 7th December 2005. Courtesy of Mozambique weather service.

The most discussed hypothesis for the origin of the subtropical convergence zones and troughs is associated with interactions between tropical and middle latitude systems. For example Kiladis et al. (1989) argue that when a tropical convergence zone frequently interacts with transient troughs in the middle latitude westerlies, this interaction will be manifested as a “cloud band” extending into the middle latitudes. This argument has been defended in a

number of other studies (e.g.; Liebmann et al., 1999; Todd and Washington, 1999; Todd et al., 2004).

Although recognised to be the main summer rain producing systems, only recently have a few studies discussed in detail the variability of TTT over southern Africa. For example, Washington and Todd (1999) argue that the leading mode of empirical orthogonal functions (EOF) of daily rainfall variability for November-March over southern Africa and SWIO (15 – 40°S, 10–70°E) is a dipole mode characterised by tropical-temperature links in all months. Collectively over the austral summer, they contribute to the South Indian Convergence Zone (SICZ - Cook, 2000). Todd et al. (2004) suggest that TTT events facilitate a substantial water vapour flux from the tropics into middle latitudes. Furthermore, they argue that these systems are major regions of moisture convergence.

Cook (2000) argues that the SICZ is a land based convergence zone (LBCZ) with position and intensity partially determined by surface conditions over southern Africa. Furthermore, she argues that the zonal wind convergence between the flow in the subtropical high to the east of the continent and the thermal low supports a root zone for the LBCZ over the land surface, and the extension out over the ocean is primarily due to the partially compensating influences of moisture advection and moist transient eddy activity, with the meridional convergence wind also contributing. Tyson and Preston-Whyte (2000) suggest that a conjunction between tropical and westerly disturbances is needed for the formation of elongated tropical-temperate trough and extended cloud bands linking tropical and middle latitudes over southern Africa.

The position of the TTT over southern Africa exhibits both intra-seasonal and inter-annual variations. The intra-seasonal variations have been attributed to the zonal shifts of the South Indian Ocean anticyclone (e.g. Todd and Washington, 1999). At inter-annual time scales, Tyson and Preston-Whyte (2000) have shown shifts in the position of the SICZ forced by the different phases of ENSO and associated changes in the Walker Cell circulation (see Fig.

2.5). Cook (2001) also observed north-eastward shifts of the SICZ as a result of weakening of the western portion in the South Indian Ocean high pressure cell as result of ENSO-like warming in the eastern Pacific. Fauchereau et al. (2008) have indicated an increase in frequency of TTT over southern Africa during La Nina conditions, with a consequent increase in probability of wet spells. However, they argue that El Niño conditions do not significantly increase the frequency of TTT over the SWIO. Todd and Washington (1999) indicate that TTT are relatively infrequent, occurring on average twice per month, and can be stationary or propagating.

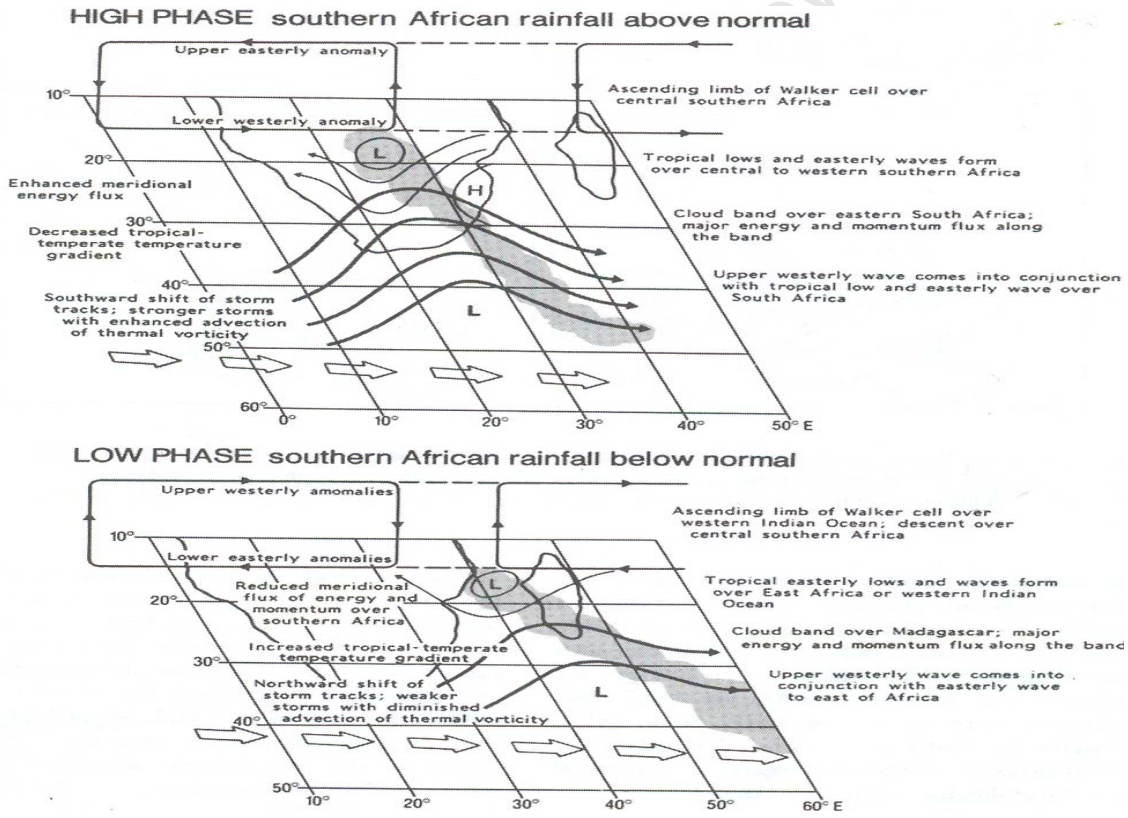

Fig.2.5 Schematic representation of anomalous Walker Circulation over southern Africa, showing the different phases of ENSO and resulting shifts in the mean position of main rainfall producing cloud bands (extracted from Tyson and Preston-Whyte, 2000).

2.1.3 Inter-annual variability of SICZ and links with ENSO and rainfall

At the inter-annual scale, the Southern Oscillation (atmospheric counterpart of ENSO) is the most significant mode of atmospheric variability affecting circulation over southern Africa (e.g. Lindesay, 1988b; Shinoda and Kawamura, 1996; Jury et al., 1996; Reason et al., 2000). The influence of ENSO on global atmospheric circulation is through a modulation of the Walker Cell (see Fig.2.6). Technically, only the overturning cell in the Pacific is referred to as the Walker Cell although this term is often used to refer to similar cells over the Indian and Atlantic basins and this usage is also employed here. In the austral summer, during the low phase of Southern Oscillation (SO) or an El Niño event, positive anomalies of pressure develop throughout the troposphere over central southern Africa. During the high phase (La Niña), the opposite is observed (e.g. Lindesay, 1988b; Shinoda and Kawamura, 1996). This leads to suppressed (enhanced) convective activity over southern Africa during El Niño (La Niña) events.

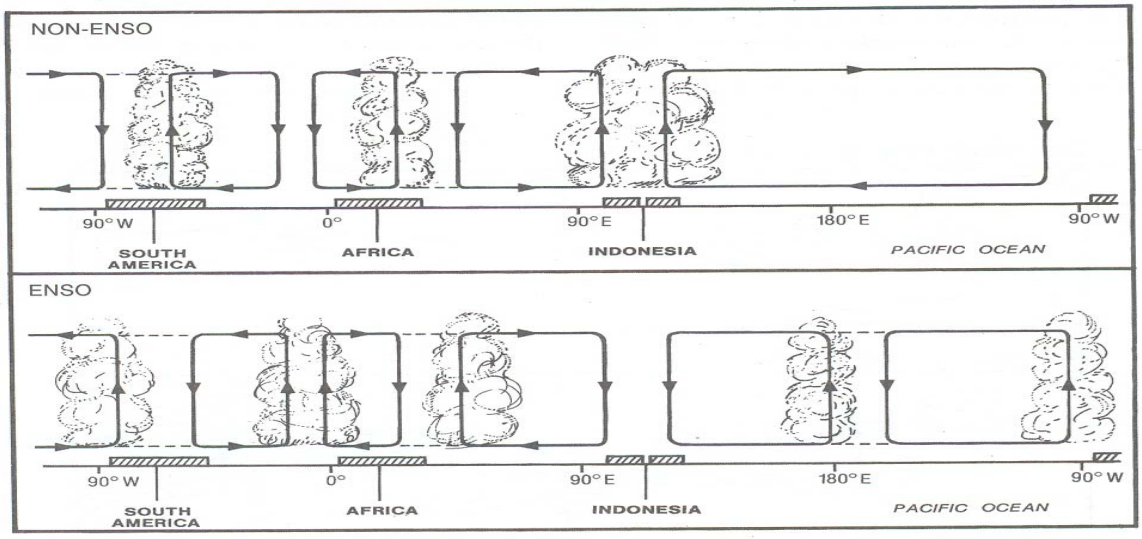

Fig.2.6 Schematic representation of the Walker Circulation along the equator during La Niña (upper panel) and El Niño(lower panel) events (From Tyson and Preston-Whyte, 2000)

As pointed out above, dry and wet conditions have been linked to shifts in the SICZ position (see Fig.2.5); wet conditions associated with La Niña over

southern Africa tend to be synchronous with wet conditions over Australia and southeast parts of South America (Tyson and Preston-Whyte, 2000). This result is in line with Todd and Washington (1999) who suggest that the November-January TTT rainfall over southern Africa/SWIO may be in phase with similar rainfall dipole structures observed in the South Pacific and South Atlantic convergence zones.

In a study of dry spells over subtropical southern Africa, Usman and Reason (2004) found highest (lowest) dry spell frequencies during El Niño (La Niña) seasons over most of the region. Using 20 Pacific ENSO events during 1901-1990, Nicholson and Kim (1997) identified 15 regions over Africa where rainfall is modulated by ENSO. Over southern Africa, about 9 regions are identified. Over Mozambique, about 4 regions are identified with different temporal response to ENSO. They show that there is a strong tendency for positive rainfall anomalies to occur during the first half of the El Niño conditions and negative during the second half over the bulk of southern Africa. In Mozambique, the ENSO signal is strongest over the southern and central regions (see e.g. Rocha and Simmonds, 1997). Positive rainfall anomalies are observed in the months preceding and following the El Niño onset and negative in the late months (mature phase) or following its decaying.

Reason et al. (2000) divided ENSO into quasi-biennial (2-2.5 years) and low-frequency (2.5-7 years) bands and showed that southern Africa rainfall exhibits stronger response in the quasi-biennial band, mainly in January-March (JFM). Their results also show that the response to ENSO is significant in the low frequency band in October-December (OND) over southern and central Mozambique. However, Tyson and Preston-Whyte (2000) suggest that the stratospheric Quasi-Biennial Oscillation (QBO) may modulate the effects of ENSO over southern Africa. For example, they argue that when the QBO is westerly more than 36% of the inter-annual rainfall variability in late summer (January -March), over large areas of the summer rainfall region, may be ascribed to the effects of ENSO. Furthermore, they argue that when the QBO is

easterly, the ENSO-rainfall weakens and becomes statistically not significant. Reason and Jagadheesha (2005) suggest that the rainfall response over southern Africa to ENSO is associated with the way a particular ENSO event modulates the Angola low. They argue that in some ENSO years, modulation of the Angola low is weak, therefore the impact of those ENSO events in southern Africa rainfall is less obvious.

Rocha and Simmonds (1997) derived an atmospheric index over Indian Ocean by differencing the monthly normalized time series of mean sea level pressure of the St Brandon station (16°27' S, 59°37'E) and Marion Island (46°54'S, 37°44'E). They argue that this index that they name Brandon-Marion Index (BMI) is a measure of the position of the mid-latitude trough associated with standing waves 1 and 3 which is also linked to the TTT (see e.g. Fig. 2.5). Furthermore, Rocha and Simmonds (1997) suggest that the BMI has stronger correlation with rainfall over southeast southern Africa than the Southern Oscillation Index. This is why changes in those systems that modulate the South Indian Ocean anticyclone may impact TTT over southern Africa.

2.2 Sea surface temperatures and links with rainfall

The ocean is the dominant source of atmospheric moisture, and the latent heat released when the moisture condenses, is the primary driving force for the atmospheric circulation. The winds in turn affect SST in several different ways; and the SST largely controls the magnitude and spatial distribution of the moisture to the atmosphere (Tomczak and Godfrey, 1994). The SST plays a fundamental role in the exchange of energy, momentum, and moisture between the ocean and the atmosphere. It largely controls the magnitude and spatial distribution of the moisture flux to the atmosphere and it is a central determinant of air-sea interactions and climate variability (Wentz et al., 2000).

Lindzen and Nigam (1987) argue that if the tropical lower troposphere is well mixed in the vertical, the horizontal gradients of temperature beneath the

trade inversion are expected to resemble their surface pattern, hence pressure gradients, proportional to sea surface temperature would arise in the boundary layer and drive low level winds. Webster (1981) suggests that the local atmospheric response to SST anomaly diminishes with increasing latitude. He argues that the weak atmospheric response to SST anomaly placed at high latitude is related to the zonal circulation and the latitude of the forcing due to rotational limitations on the relative scale of the vertical velocity. Von Storch and Navarra (1999) argue that in the mid latitudes the atmospheric variability appears to be mainly generated by internal atmospheric dynamics with the SST often responding to rather than significantly altering the low frequency atmospheric variability. Webster (1981) argues that the local atmosphere response to an SST anomaly in the extratropical regions is seasonal dependent. He suggests that the extratropical regions of the summer hemisphere are quite sensitive to the local thermal forcing.

SST in the Indian Ocean display significant variability on both seasonal and inter-annual scales (e.g. Behera et al. 2001). Loschnigg and Webster (2000) argue that the annual cycle in the North Indian Ocean SST is regulated by strong oceanic advection across the equator and by changes in the upper ocean storage. These changes regulate the monsoon circulation over Indian Ocean and adjacent continents (see Fig.2.7).

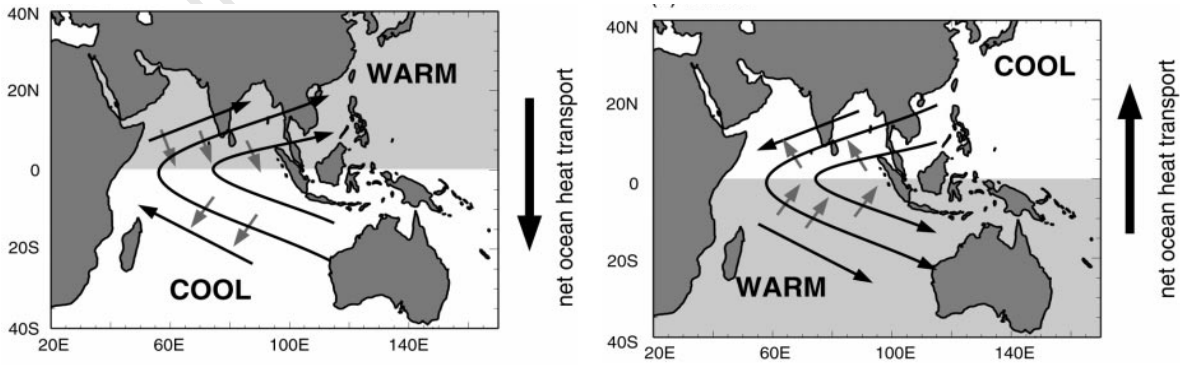

Fig. 2.7 A regulatory model of the annual cycle of the Indian Ocean monsoon system for (a) SH winter and (b) SH summer. From Loschnigg and Webster (2000).

Intra-seasonal changes in the position of the South Indian Ocean anticyclone appear to be in response to these changes. For example, SST shows a seasonal march between OND and JFM (see Fig. 2.8) consistent with the observed southward and eastward shift in the position of the South Indian Ocean anticyclone. Over the South Indian Ocean, SST displays a near zonal orientation. Tomczak and Godfrey (1994) attribute the zonal orientation to a lack of upwelling along the western coast of Australia.

On the inter-annual scale, the main modes of tropical SST variability over the Indian Ocean are associated with El Niño (e.g. Reason et al., 2000; Xie et al., 2002) and the Indian Ocean Zonal Dipole Mode (Saji et al., 1999; Webster et al.,1999). During El Niño (La Niña), warm (cool) conditions prevail over the bulk of the tropical and subtropical Indian Ocean (e.g. Reason et al., 2000; Venzke et al., 2000). Reason et al. (2000) argue that atmospheric changes (mainly cloud cover and wind) induced by ENSO are the main mechanism responsible for the SST changes. Venzke et al. (2000) argue that the signal is carried into Indian Ocean mainly through anomalous ENSO-related surface heat fluxes.

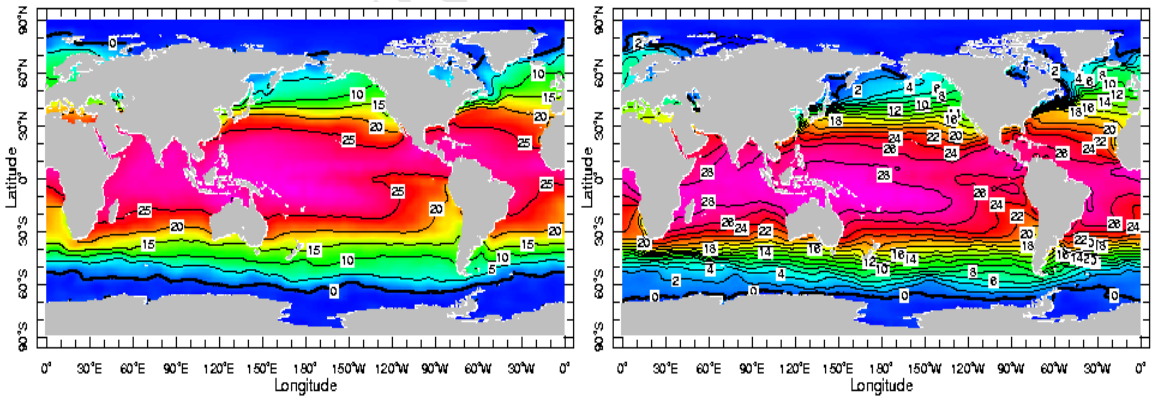

Fig.2.8 Global mean sea surface temperature for (a) OND (contour interval is 5°C) and (b) JFM (contour interval is 2°C) from 2005 World Ocean Atlas

Nicholson and Kim (1997) suggest that rainfall over Africa is associated with low- latitude SST fluctuations over Atlantic and Western Indian oceans linked to ENSO. Similarly, Reason et al. (2000) suggest that southern African

rainfall anomalies respond to SST anomalies in the surrounding Atlantic and Indian Oceans associated with ENSO. However they point out that it is the combination of SST and circulation anomalies across southern Africa and the adjacent western Indian Ocean that dictates the rainfall response. Rocha and Simmonds (1997) also showed significant relationships between ENSO and inter-annual summer rainfall over south-eastern Africa. However they point out that even after removing the ENSO effects, the relationship between the SST over the Indian Ocean and south-eastern Africa remains strong. Goddard and Graham (1999) argue that although the Pacific SST exerts some influence over the African region, it is the atmospheric response to the Indian Ocean variability that is essential for simulating the correct rainfall response over eastern, central and southern Africa.

Other SST patterns that have been argued as being independent from ENSO (Saji et al., 1999) ENSO have been identified in the Indian Ocean. These authors, identified the Indian Ocean Dipole mode in the tropical Indian Ocean characterised by SST anomalies of opposite sign in the east and the west of the basin. They argue that this mode is ENSO independent. However some studies consider this mode to be associated with ENSO (e.g. Allan et al., 2001; Baquero-Bernal et al., 2002). By applying empirical orthogonal function analysis to sea surface height, Rao et al. (2002) also identified the Indian Ocean Dipole mode and they also argue that the mode is ENSO independent. Some studies have shown association between the Indian Ocean Dipole and rainfall over eastern Africa, including north Mozambique and elsewhere (e.g. Saji and Yamagata, 2003; Ashok et al., 2003, Ummenhofer et al., 2008).

Schott and McCreary (2001) identified an upwelling region over the tropical South Indian Ocean. They suggest that this upwelling region results from negative curl between the south-easterly trade winds and equatorial westerlies, raising the thermocline in the west. Hermes and Reason (2008) indicate that the tropical South Indian Ocean upwelling is focused in the west during austral spring and summer. Furthermore, they argue that local divergence between the south-

easterly trade winds and the monsoon westerlies and also remote forcing through Rossby waves, have impacts on this upwelling region. It is important to mention that this region has been indicated as the main source of moisture for southern Africa during rainy days in summer (e.g. D'Abreton and Lindesay, 1993). Xie et al. (2002) argue that this upwelling does not lead to local SST minimum in the annual-mean, because it is relatively weak and its effect is masked by an equatorward gradient. Furthermore, Xie et al. (2002) suggest that SST on this upwelling region, influence rainfall anomalies over the western Indian Ocean and eastern Africa.

Behera and Yamagata (2001) have identified a dipole mode in the subtropical South Indian Ocean. The positive (negative) phase of this event is characterised by cool (warm) anomalies in the eastern part i.e. off Australia and warm (cool) anomalies in the western part, south of Madagascar. They suggest that stronger than normal winds are responsible for the evaporative and entrainment cooling in the eastern and central parts while decrease in seasonal heat loss due to reduced evaporation, and anomalous downwelling and Ekman transport of warmer water are responsible for the warming in the South-Western Indian Ocean.

Hermes and Reason (2005) suggest that the large scale forcing of the South Indian Ocean subtropical mode (SIOD) is associated with modulation of wavenumber-3 or -4 pattern in the Southern Hemisphere atmospheric circulation. They also found links between the SIOD and the Antarctic Oscillation (AAO) mode and they suggest that the relationship has strengthened since the mid-1970s.

Using a general atmospheric circulation model, Reason (2001, 2002) found increased rainfall as a result of enhanced convergence of moisture over southeast Africa associated with the positive phase of this subtropical dipole mode. The same study suggested that the negative phase of this mode is linked to decreased rainfall over the same region as result of increased low-level divergence. SST in the warm Agulhas Current region has been linked to rainfall

variability over subtropical southern Africa, particularly via enhancement of tropical temperate troughs and middle latitude westerly waves disturbances (e.g. Crimp et al., 1998; Reason and Mulenga, 1999).

2.3 Ocean circulation

Compared to the atmosphere, the ocean is much more efficient in conserving heat. This is redistributed by ocean circulation, in the upper ocean typically on seasonal to annual time-scales. Oceanic evaporation, in turn has an important role on rainfall. On average, ocean currents transport heat from equatorial regions towards the poles, tending to cool the tropics and heat polar-regions (Tomczak and Godfrey, 1994). The circulation in the ocean is slow compared with the atmosphere, however the strength of the currents vary, so inter-annual variations of the heat exchange are to be expected (Tomczak and Godfrey, 1994). The Indian Ocean displays significant seasonal and inter-annual variability and plays a major role (as compared to the Atlantic) in the rainfall variability and anomalies over southern Africa (e.g. Reason et al., 2006a). Therefore the analyses in this section focus on circulation aspects of the Indian Ocean.

The upper circulation in the South Indian Ocean is characterized by an anti-cyclonic wind-driven gyre (see Fig. 2.9). It is limited to the north by the South Equatorial Current (SEC), to the south by the subtropical convergence, and closed to the west by the poleward flow of the Agulhas Current. The South Equatorial Current forms a band of westward flow between 10°S and 20°S extending across the basin and it has its highest transport during the Southwest Monsoon (Schott and McCreary, 2001). In the east, the SEC is fed by the low salinity Indonesian throughflow waters. At times, Ekman divergence at the northern edge of the SEC appears to be strong enough to upwell subsurface waters into the mixed layer (Schott and McCreary, 2001).

The Agulhas Current is the strongest western boundary current in the Southern Hemisphere. It plays a significant role in regional ocean-atmosphere interactions (e.g. Reason, 2001; Rouault et al, 2003; Lutjeharms, 2006). As mentioned above, the SST over the Agulhas current has been associated with rainfall at different scales over southern Africa (e.g. Jury et al., 1993; Reason and Mulenga, 1999; Rouault et al., 2002). In the Mozambique Channel, the circulation is dominated by large (300-Km scale) eddies, about 4-5 per year, which progress southward eventually joining the Agulhas Current (e.g. Schott and McCreary, 2001; Lutjeharms, 2006). Warm eddies may intensify tropical cyclones which have caused floods and havoc over particularly Mozambique and Madagascar. Goni et al. (2008) have shown intensification of a tropical cyclone when passing over a warm eddy over the Mozambique Channel.

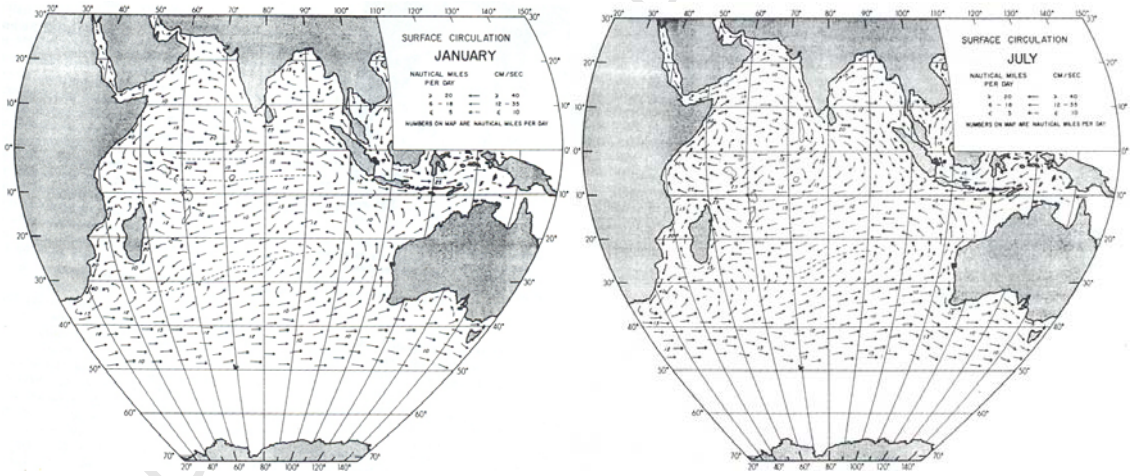

(a) (b)

Fig. 2.9 Observed large scale surface circulation during (a) Northeast and (b) Southwest monsoons in the Indian Ocean, from analysis of ship drift data (from Woodberry et al., 1989).

In the northern and equatorial Indian Ocean, the surface circulation displays the largest seasonal variation in the World Ocean. The maximum variations at 10° N and 10° S are associated with the monsoon over Indian Ocean and changes in the easterlies over the South Indian Ocean (Lee and Marotzke, 1998). Northward of the SEC, two major monsoonal currents are observed, the East African Coastal Current (EACC) and the Equatorial Counter

Current (e.g. Woodberry et al., 1989). The Equatorial Counter Current (ECC) lies between 3°N to 5° S, but from January to April it moves to 10°S (Schott and McCreary, 2001). Rossby waves propagate westward in the shear zone between the SEC and the ECC (e.g. Woodberry et al., 1989). Schott and McCreary (2001) suggest that during the Southwest Monsoon, SEC and EACC supply the northward flowing Somali Current, which turns offshore after crossing the equator at about 4°N, forming a cold upwelling wedge near the coast. This brings SST to values below 20°C during the Southwest Monsoon and results in an annual mean of below 28°C (Tomczak and Godfrey, 1994).

2.4 Summary

Statistical and modelling studies (e.g. Jury et al., 1996; Reason and Mulenga, 1999; Reaon, 2002; Washington and Preston, 2006) have shown significant relationships between rainfall anomalies in southern Africa and different SST patterns in the neighbouring oceans, particularly in the Indian Ocean, either linked or independent of ENSO. Warm (cool) anomalies over the central Indian Ocean have been associated with dry (wet) conditions over the bulk of southern Africa (e.g. Jury et al., 1996; Rocha and Simmonds, 1997; Mulenga et al., 2003; Washington and Preston, 2006).

The subtropical South Indian Ocean dipole, consisting of anomalies of opposite sign, has been shown to have significant influence in the rainfall anomalies in southern Africa (Behera and Yamagata, 2001). Positive (negative) anomalies of rainfall are observed when the warm (cool) pole is located to the west (east) and cool (warm) pole is located to the east (west) in the subtropical South Indian Ocean (Rocha and Simmonds, 1997; Reason, 2002; Washington and Preston, 2006). The physical mechanisms explaining these relationships are still not well understood.

General Circulation Models (GCMs) forced with the above mentioned patterns of SST in the Indian Ocean have been used to try to explain the physical

mechanisms linking these patterns of SST with the anomalies of rainfall in southern Africa (e.g. Reason, 2001, 2002). However, the climate variability over southern Africa is complex, with a multitude of forcing mechanisms (e.g. Reason, 2006a). While specific patterns of SST have been singled out and their role in the atmospheric circulation analysed in these modeling studies, the response of rainfall to the SST patterns is still not clear. For example, some studies suggest that the SIOD is mainly forced by the subtropical South Indian Ocean anticyclone, which is in turn forced by the Southern Hemisphere planetary waves (e.g. Fauchereau et al., 2003; Hermes and Reason, 2005). Cool anomalies of SST in the tropical South Indian Ocean, associated with La Niña, are forced by stronger easterlies which are in turn associated with stronger South Indian anticyclone (e.g. Reason et al., 2000). On the other hand, the SICZ, which is regarded as the main summer rain producing system over southern Africa (e.g. Washington and Todd, 1999; Reason and Mulenga, 1999; Cook, 2000), is strongly associated with seasonal variation and anomalies of the subtropical South Indian Ocean anticyclone (e.g. Todd and Washington, 1999; Cook, 2000).

The fact that the atmospheric circulation forcing the SST patterns associated with the rainfall anomalies is also forcing the main atmospheric system (SICZ) associated with the summer rainfall over southern Africa, casts doubt in the way these SST patterns may influence the rainfall over southern Africa. Feedbacks may exist between the atmosphere and SST anomalies, such that an initially atmospheric forced anomaly pattern of SST may later force atmosphere anomalies resulting in rainfall anomalies (see e.g. Fauchereau et al. 2003). However, these feedbacks are not considered in the GCMs used in the studies exploring relationship between SST and rainfall over southern Africa, as the anomalies of SST are prescribed (e.g. Rocha and Simmonds, 1997; Reason, 2002; Washington and Preston, 2006). Furthermore, the atmospheric response to the imposed SST pattern in the GCMs tends to be a convergence of the flow over the warm SST anomaly (e.g. Rocha and Simmonds, 1997; Reason and Mulenga, 1999; Reason, 2002) and a divergence of the flow over the cool

anomalies (e.g. Reason, 2002; Washington and Preston, 2006). It has been argued that this response of the atmosphere to SST anomalies is not always valid (e.g. Neelin et al, 1998).

This thesis studies the relationship between ENSO, the SST anomalies in the Indian Ocean and the South Indian Convergence Zone, with the aim to explore the main mechanisms (both atmospheric and oceanic) forcing summer rains in southern Africa. Here the patterns of TTT (associated with the main summer rainfall over southern Africa) are identified first (applying statistical analysis in OLR) and the associated atmospheric circulation and SST patterns are analysed independently, based on the temporal indices of observed TTT events. This procedure may not give clear physical connections between SST, the atmospheric circulation and rainfall anomalies, but from the emerging patterns, physical connections may be inferred. Furthermore, comparisons with the present knowledge of climate variability from both statistical and modeling studies, may give more clues as to physical mechanisms linking the rainfall over southern Africa and SST anomalies over southern Africa.

Chapter Three

3. Data and Methods

3.1 Data

The data used in the present study and respective sources, spatial and temporal resolutions are shown in Table 3.1.

Table 3.1 Data description

Data	Temporal resolution	Spatial resolution (lat x long)	Source
Outgoing long wave radiation (OLR)	Daily	2.5° x 2.5°	National Oceanic and Atmospheric Administration (NOAA)
Sea Surface Temperature (SST)	Monthly	1° x 1°	Hadley Centre for Climate Prediction and Research , Met Office, UK
Geopotential height	Daily/monthly	2.5° x 2.5°	NCEP -DOE reanalysis II
wind	Daily/monthly	2.5° x 2.5°	NCEP -DOE reanalysis II
Air temperature	Daily/monthly	2.5° x 2.5°	NCEP-DOE reanalysis II
Mean sea level pressure (MSLP)	Daily/monthly	2.5° x 2.5°	NCEP -DOE reanalysis II
Specific humidity	Daily/monthly	2.5° x 2.5°	NCEP -DOE reanalysis II
Rainfall	Daily/Monthly	2.5° x 2.5°; 0.5° x0.5°; stations	Climate Prediction Centre (CPC); CRU TS 2.0 at University of East Anglia, INAM (Mozambique)

Below a description of each data set is given.

3.1.1 NCEP-NCAR data

The National Centre for Environmental Prediction – National Center for Atmospheric Research (NCEP-NCAR) reanalysis (Kalnay et al., 1996) products have been used in a vast number of studies and the quality of these reanalysis

has also been extensively discussed. The reanalysis have been obtained by assimilation of all available observations data into the NCEP atmospheric model. Here the NCEP-DOE Atmospheric Model Intercomparison Project (AMIP- II) reanalysis, henceforth NCEPII is primarily used. This is an update of NCEPI with the correction of several errors and upgrades to the forecast model and a diagnostic package that has been developed since NCEPI (Kanamitsu et al., 2002). NCEPII starts only in 1979 and this has constrained most of the analyses in the present study to the period covered by these reanalysis products.

3.1.2 Outgoing long-wave radiation (OLR)

OLR has been used in a number of studies as a proxy for convective activity (e.g. Jury et al., 1996; Liebmann et al., 1999; Carvalho et al., 2004). Low OLR values in the tropics and summer sub-tropics indicate convective weather systems, in contrast to cloud free regions where warm surface emit high OLR (Jury et al., 1996). OLR data used here is calculated from the daily interpolated data from AVHRR satellite soundings for OLR; it is interpolated spatial and temporally to remove missing values (Liebmann and Smith, 1996).

3.1.3 Rainfall

The rainfall data used in the present study are comprised of Climate Research Unit (CRU TS 2.0), Climate Prediction Centre (CPC) Merged Analysis of Precipitation (CMAP) and Mozambique climatological station data. CRU TS 2.0 data (Mitchell et al., 2004) uses only land-based stations (19800 stations) from a variety of sources. In Mozambique, the stations used are mainly along the coast but there are a significant number of stations along the border with South Africa, Zimbabwe and Malawi (see Fig. 1 in New et al, 1999) that may have improved the quality of these data. The station data are interpolated as a function of latitude, longitude and elevation. The accuracy of the interpolations was assessed using cross validation and by comparison with other climatologies

(New et al., 1999). The period considered here for these data is 1961-2000. CMAP data used here is a merge of rain gauges measurements and estimates from variety of satellite observations (Xie and Arkin, 1997) and covers the period January 1979 – July 2003. Daily rainfall data from ten stations across Mozambique (Fig.3.1) are used to study the variability of wet spells and of dry days and to validate the analyses with the gridded data.

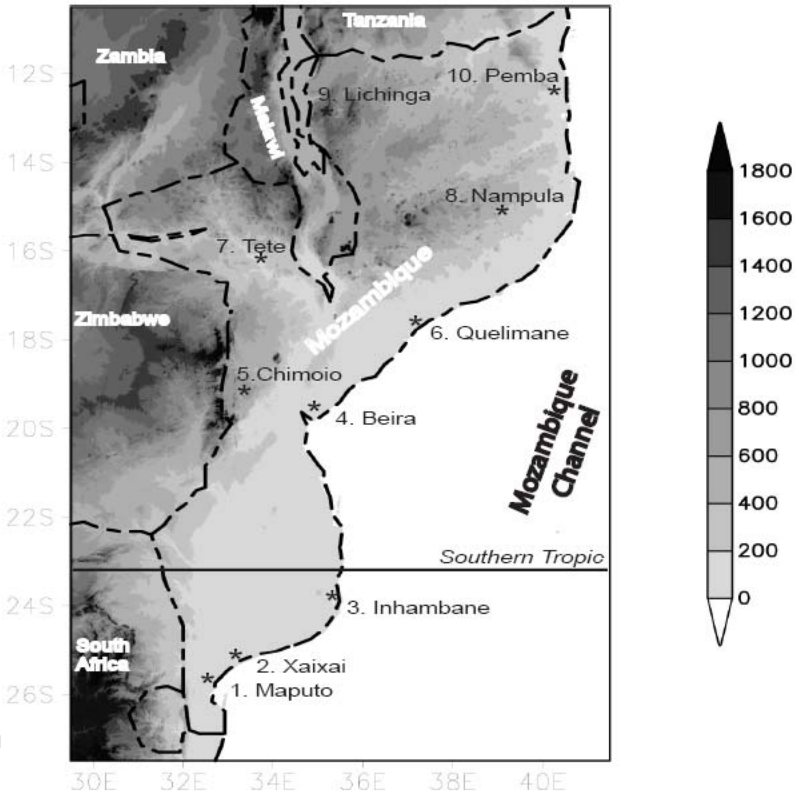

Fig.3.1 Map showing rainfall stations used in the study and topography (m)

The period considered for these data is between 1961 and 2004. To check the quality of the data, the annual number of rain days together with annual rainfall for January-March are plotted (Fig.3.2). Some gaps are observed for stations 4 and 5 in central Mozambique and for station 10 in the northern part of the country. This may affect the results for these stations, particularly station 4 in central Mozambique, which shows more missing data. However given the length

of the period considered (44 years) the influence of the missing data may be minimised. All the stations show significant correlation (see Fig.3.2) between the number of rain days and total rainfall and no significant trend is observed.

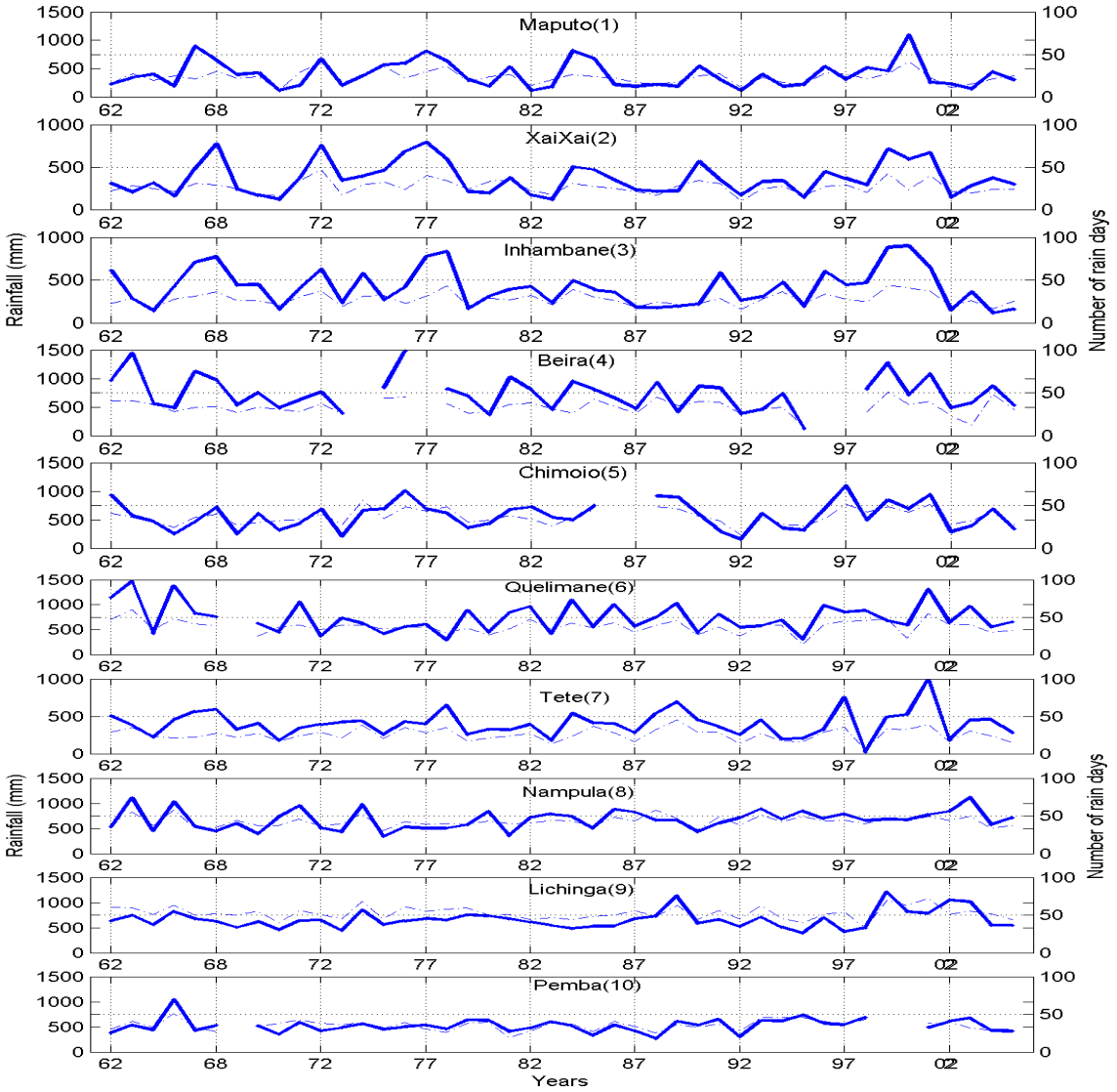

Fig.3.2 Seasonal (JFM) mean rainfall (mm) and inter-annual variability of number of rain days in each station. The heavy line show the rainfall (mm) and light dashed line the number of rain days.

The relationship is stronger for the northern stations. In general, years with extreme total annual rainfall over southern Mozambique are not associated with a high number of rain days (see for example the years 1967, 1968, 1977 and 1978 in the 4 southernmost stations). These weak relationships between the

number of rain days and rainfall amounts over the southern parts may suggest that, some years with extreme total rainfall may be associated with few extreme rainfall events.

3.1.4 Seas surface temperature (SST)

The SST data used here comes from the second Hadley Centre Sea Surface Temperature dataset (HadSST2) from the UKMO Hadley Centre for Climate Prediction and Research. These data are based on the International Comprehensive Ocean – Atmosphere Data Set (ICOADS) database (Rayner et al., 2006).

3.2 Methods

3.2.1 Analysis techniques

To define the patterns associated with the TTT, cluster analysis (CA) is used. However, prior to the cluster analysis, empirical orthogonal functions (EOF) are applied to the OLR data to reduce the number of variables. This is a common practice in cluster analysis (Michelangel et al., 1995; Solman and Menéndez, 2003; Fauchereau et al., 2008). Composites and linear correlations are used to explore the linear relationship between different variables. Student's t test is used in both composites and correlations to test the robustness of the results. Regression analyses are also used to isolate patterns, particularly those associated with ENSO; this has been done in other studies (e.g. Barreiro et al., 2002; Washington and Preston, 2006). A description of each statistical analysis technique is given below.

3.2.1.1 Cluster analysis

Cluster analysis is a multivariate method used in geophysical research to classify variables into homogeneous groups or clusters (e.g. Michelangel et

al.,1995; Solman and Menéndez, 2003). The data partition in this thesis follows the Michelangel et al. (1995) algorithm.

a) Distance measures

Clustering data points is based in the idea of distance. Clusters should be composed of points separated by small distances, relative to the distances between points (e.g. Wilks, 2006). In geophysical research, the Euclidean distance and correlation coefficient are the two measures of distance most frequently employed (Gong and Richman, 1995). The Euclidian distance is used in this study.

b) Clustering

There is a wide range of clustering techniques used in atmospheric science, for a review and comparison of these methods see Gong and Richman (1995). Here, a non-hierarchical method is used. Non-hierarchical methods start from either (1) an initial partition of items into groups or (2) an initial set of seed points, which will form the nuclei of clusters. One way to start is to randomly select seed points from among the items or to randomly partition the items into initial groups (Johnson and Wichern, 1982). The widely applied K- means method is here used, as follow (Gong and Richman, 1995; Wilks, 2006):

Step 1. Specify k seed points as a set of centroids. The seed points are randomly identified.

Step 2. Compute the Euclidian distance between the current data vector ($\boldsymbol{x}_i$, i=1,.....,n) items and each of the centroids; then assign each item to the cluster having the nearest centroid to attain the initial partition.

Step 3. If $\boldsymbol{x}_i$ is already a member of the group whose mean is closest, repeat step 2 for $\boldsymbol{x}_{i+1}$. Otherwise, $\boldsymbol{x}_i$ is reassigned to the group whose mean is closest, and step 1is repeated.

Clustering is applied in this study to OLR daily data to identify patterns of convective activity associated with TTT. Prior to clustering, empirical orthogonal functions are used in order to reduce the number of variables.

c) Clusters selection

To select the best partition the classifiability index is used. The classifiability index compares the similarity of the clusters for the members of each partition. The higher the classifiability index the more similar are the members of each partition and the more robust is the classification (Solman and Menéndez, 2003).

3.2.1.2 Empirical Orthogonal Functions

Empirical orthogonal Functions (EOF) also known as Principal component analysis (PCA) is a statistical tool for the analysis of spatial and temporal variability of physical fields. The technique became popular for analysis of atmospheric data following the paper by Edward Lorenz in 1956 (Preisendorfer, 1988). The purpose of PCA is to reduce a data set containing a large number of modes to a data set containing fewer new modes or patterns, but nevertheless representing a large fraction of the variability contained in the original data (Wilks, 2006).

3.2.1.3 Composite analysis

Composite analysis is a widely used method in climatology studies. The basic idea with composites is to construct 'typical' states of a variable conditional on the value of an external index (Von Storch and Zwiers, 2000). However, there may be considerable variability around each composite, so that the composite may not be representative of the typical state. In order to verify the significance of the composite, student's t test is used in general at 5% significance level, unless otherwise stated. Because the student's t test assume normal distribution (e.g.

Storch and Zwiers, 2000), and some of the variables analysed here are not normally distributed (e.g. precipitation), Monte Carlo Simulations (e.g. Von Storch and Zwiers, 2000) were also used for comparison.

3.2.1.4 Correlations

Linear correlation is a tool used to measure the degree of linear relationship between two variables. Here we use the Pearson coefficient of correlation (r) given by equation 3.1:

$$r = \frac{\frac{1}{n}\sum_{i=1}^{n}(x_i - \bar{x})(y_i - \bar{y})}{\sqrt{\frac{1}{n}\sum_{i=1}^{n}(x_i - \bar{x})^2}\sqrt{\frac{1}{n}\sum_{i=1}^{n}(y_i - \bar{y})^2}} \qquad (3.1)$$

where: $\bar{x}$ and $\bar{y}$ are the arithmetic means of the variables x and y.

The student's t test is also used to test the significance of the correlations performed here.

3.2.1.4 Linear regression

Linear regression is statistical technique used to derive linear relationship between two variables, an independent x and a dependent variable y. In the analyses here Niño 3.4 represents the independent variable and the dependent variables are either atmospheric variables or SST.

3.2.2 Analysis of water vapour balance and thermodynamics

The equations for balance of water vapour described here are from Peixoto and Oort (1992).

Precipitable water (*W*) in the atmosphere can be written as:

$$W(\lambda,\phi,t) = \int_0^{p_0} q \frac{dp}{g} \tag{3.2}$$

It represents the amount of liquid water that would result if all the water vapour in the unit column of the atmosphere were condensed.

The horizontal transport of water is given by:

$$\mathbf{Q}(\lambda,\phi,t) = \int_0^{p_0} q\mathbf{V} \frac{dp}{g} = Q_\lambda \mathbf{i} + Q_\phi \mathbf{j} \tag{3.3}$$

and the zonal and meridional components of **Q** are given by:

$$Q_\lambda = \int_0^{p_0} qu \frac{dp}{g} = \langle qu \rangle p_0 / g \tag{3.4}$$

$$Q_\phi = \int_0^{p_0} qv \frac{dp}{g} = \langle qv \rangle p_0 / g \tag{3.5}$$

Q_ϕ (ϕ=constant) represents the flux of water vapour across a latitudinal section and Q_λ (λ= constant) across a longitudinal section; p_0 is the surface pressure and g the gravitational acceleration; q is the specific humidity; u and v are the zonal and meridional wind respectively.

The simplified general balance equation of water vapour, averaged in time (Peixoto and Oort, 1992) is given by:

$$\overline{\frac{\partial W}{\partial t}} + div\overline{\mathbf{Q}} = \overline{E} - \overline{P} \tag{3.6}$$

where: E is the evaporation and P the precipitation. The over bars indicate averanging in time. Over long periods of time, such as a year, changes in storage in the land and in the atmosphere become small (Peixoto and Oort, 1992). The averanging period considered in this study refers to TTT events in different years (25 years), therefore changes in storage can be discarded and equation 3.6 rewritten as:

$$div\overline{\mathbf{Q}} \approx \overline{E} - \overline{P} \tag{3.7}$$

This equation shows that the divergence field of water vapour in the atmosphere depends on its relationship with the mean difference of evaporation and precipitation. Regions of positive mean divergence $(\overline{E}-\overline{P}>0)$ represent source regions of water vapour, while regions of convergence $(\overline{E}-\overline{P}<0)$ are sink regions of water vapour for the atmosphere.

Following Lenterss and Cook, (1995) and Cook (2000), the convergence of moisture vapour $-div\overline{\mathbf{Q}}$ is decomposed as:

$$-div\overline{Q}=\overline{C}+\overline{A}+\overline{T}+\overline{O} \tag{3.8}$$

where: $\overline{C}$ is the convergence term, $\overline{A}$ is the advection term, $\overline{O}$ is the orographic term, and $\overline{T}$ is the transient term. Mathematical expressions for each term are given below:

$$\overline{C}=-\frac{1}{g}\int_{p_0}^{300}\overline{q}(\nabla_h\cdot\overline{\mathbf{V}}_h)dp \tag{3.9}$$

$$\overline{A}=-\frac{1}{g}\int_{p_0}^{300}(\overline{\mathbf{V}}_h\cdot\nabla_h\overline{q})dp \tag{3.10}$$

$$\overline{T}\approx-\frac{1}{g}\nabla_h\cdot\left[\int_{p_0}^{300}\left(\overline{q\mathbf{V}_h}-\overline{q}\,\overline{\mathbf{V}}_h\right)dp\right] \tag{3.11}$$

$$\overline{O}=-\frac{1}{g}\overline{(q\omega)_s} \tag{3.12}$$

The convergence term (*C*) represents precipitation associated with horizontal wind convergence; the advection term (*A*) represents precipitation associated with the horizontal advection of moisture; and the transient term (*T*) represents precipitation associated with transient horizontal circulation. The integrations are from surface to 300 hPa to match the NCEP given level of specific humidity. The orographic term (*O*) represents the orographic

precipitation. Most of the structure in this term is determined by structure in the wind convergence field, not in the moisture field (Lenterss and Cook, 1995).

3.2.3 Analysis of wet spells and dry days

A wet day is defined here as one when the rainfall is equal or above 1 mm and a dry day is one when the rainfall is below that threshold. Wet spells are defined by consecutive wet days. In a study of the frequency of dry spells over southern Africa, Usman and Reason (2004) define dry spell as a pentad with less than 5mm of rainfall. Here, dry spells are not defined because over southern Mozambique prolonged dry days in dry years are recurrently observed. For example, if in a particular season no rain day with value above the threshold considered here is observed, that season would only have 1 dry spell according to the definition used for the wet spell (if similar definition was used for dry spells). On the other hand, if dry days were alternated with short periods of rain, we would have a high number of dry spells. To avoid this ambiguity, the annual frequency of dry days is analysed instead of dry spells.

Chapter Four

4.1 Cluster Analysis of daily OLR and Tropical Temperate Troughs

Cluster analysis applied to OLR data is used here to define tropical temperate trough (TTT) patterns over southern Africa and the South-West Indian Ocean. Fauchereau et al. (2008) have used a similar method to study convective activity and to define TTT over the same region, however their study focuses on South Africa, while the focus of the present study is the less studied Mozambique region. The OLR data used covers the period 1979-2003 during the austral summer rainfall season. The rainfall season is divided into two, the early season October – December (OND) and the late season January – March (JFM). The selection of these two periods is based on the significant intra-seasonal variability of TTT and rainfall over southern Africa. For example, in monthly analyses of TTT in the summer season, Todd and Washington (1999) have shown similarity between atmospheric patterns in early summer (November –December) but with important differences from the late summer (January-February). Also, since the study looks at relationships with SST and specifically ENSO and SIOD it makes more sense to stratify seasons as OND and JFM as these seasons correspond to certain phases of these modes (e.g. Reason et al., 2000; Hermes and Reason, 2005). Furthermore, the OND and JFM stratification is appropriate to distinguish the differences between rainfall variability in southern and Northern Mozambique.

4.1.1 Cluster analysis and EOFs

As explained in Chapter 3, EOFs applied to OLR data were used as the input for the cluster analysis. To explain 70% of the variance of OLR data, 50 PCs were retained for OND and 38 PCs for JFM. A value of 70% was chosen so as to isolate the main signal and get rid of noise. Note that Fauchereau et al. (2008) found that the results are not dependent on the percentage of variance retained, and indeed they used a lower value (51.1% of the variance) than the more

restrictive criterion used in this thesis. The cluster analyses were then applied to the resulting EOF data. For each season, nine different partitions were considered, starting from two clusters up to ten, and a classifiability index (Fig 4.1) was used to select the best partition. In OND, a partition of 3 clusters shows higher values of the classifiability index (Fig. 4.1a), so this is considered here as the best partition for OND. For JFM, the classifiability index (Fig. 4.1b) shows high values for a partition of two clusters (above 0.8); however, selecting only 2 clusters might discard potentially important results. Since the next highest values are for partitions of 3 to 5 clusters, with approximately the same value, it was decided to select a partition of five clusters. The clusters of interest in the present study are those related to TTT over southern Africa and SWIO, particularly linked to rainfall variability over Mozambique. Therefore spatial patterns of OLR and rainfall anomalies and also correlations between the annual frequencies of clusters and frequencies of wet spells and of dry days for rainfall stations in Mozambique are used in sections 4.1.2 and 4.2.1 to select the clusters for the present study.

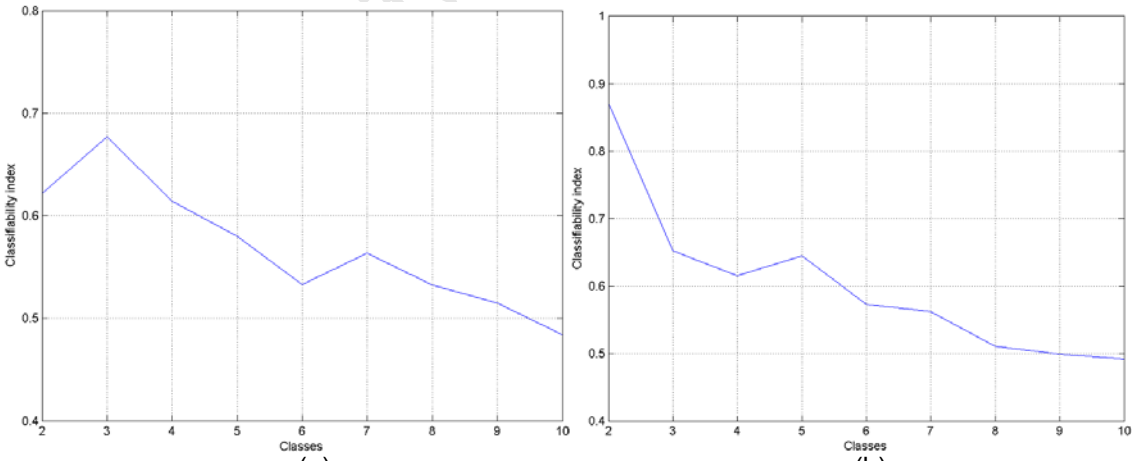

(a) (b)

Fig. 4.1 Classifiability index for the partitions in OND (a) and JFM (b).

4.1.2 Frequency of the clusters and their relationship

Figures 4.2 and 4.3 show the annual frequency of each cluster for OND and JFM, respectively. In OND (Fig.4.2), clusters 1 and 2 show some coherence in some El Niño years. For example in 1982, 1991, 1997, and 2002 El Niño years both clusters displayed low or no occurrence. However, cluster3 shows an opposite tendency, with high frequencies during El Niño years, and weak or no occurrence in non El Niño years. In JFM (Fig.4.3), cluster2 displays a more coherent association with El Niño, compared to other clusters. This cluster shows high frequency in most El Niño years and weak or no occurrence in non El Niño years. The relationship between the clusters and El Niño are further explored in section 4.3.1, using linear correlation between the annual frequencies of the clusters and Niño 3.4 index.

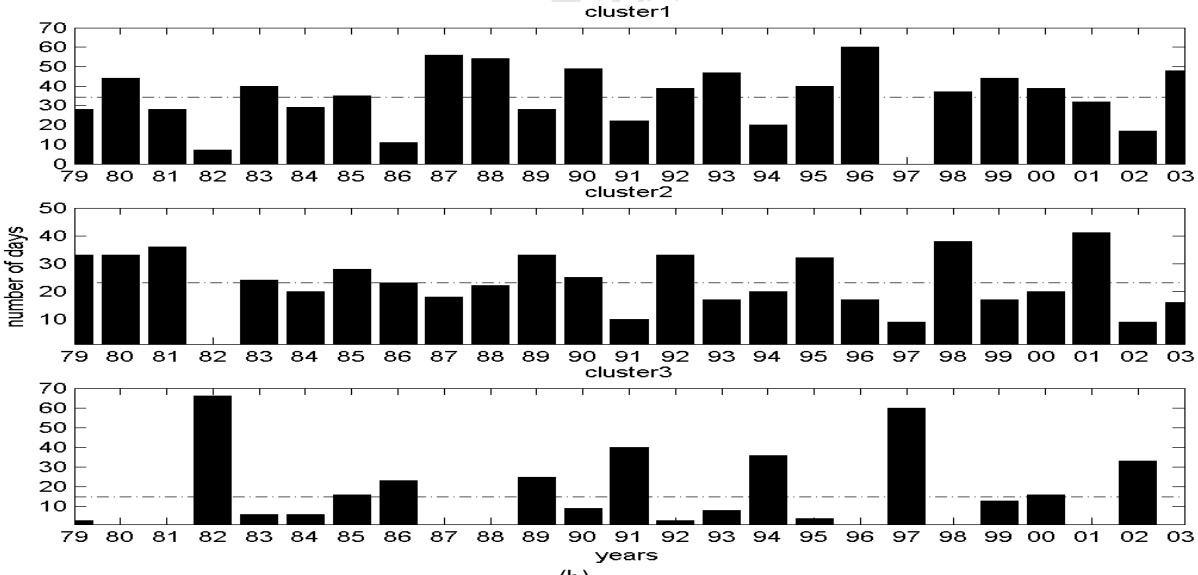

(b)

Fig. 4.2 Inter-annual frequency (number of days) of clusters for the selected partitions in OND.

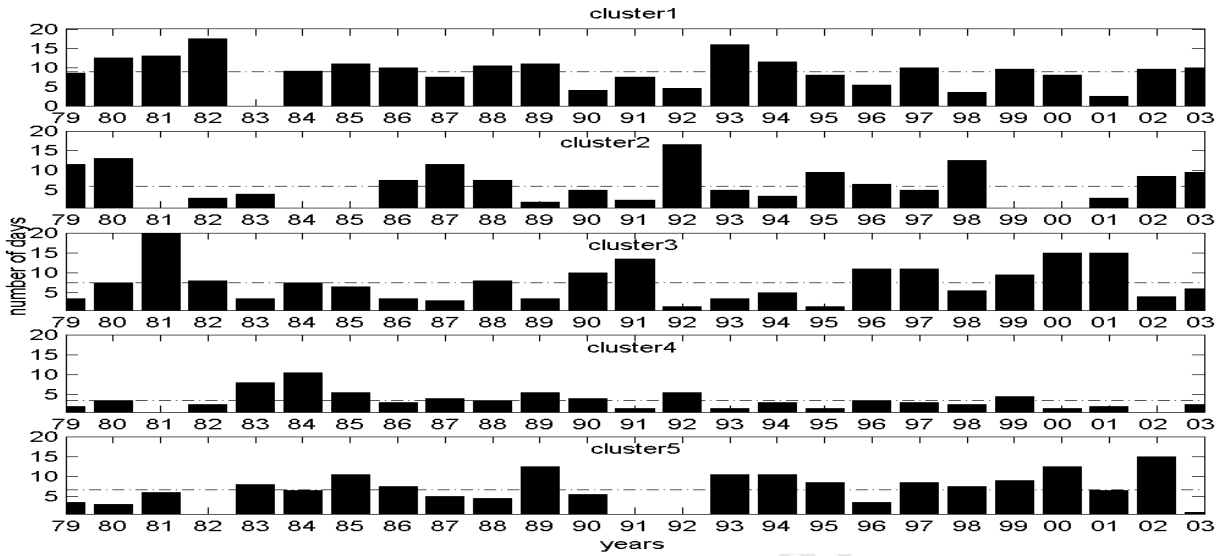

(b)

Fig. 4.3 Same as Fig.4.2 except for JFM

Correlations between the annual frequencies of the clusters (Figures 4.2 and 4.3) within the partitions for the 1979-2003 period were performed in order to explore possible inter-annual relationships. Table 4.1 shows the correlation coefficients. In OND, clusters 1 and 2 are strongly anti-correlated with cluster3, since both the correlation coefficients are negative and above 0.6 (absolute value). However, the correlation between clusters 1 and 2 is positive, but relatively weak. In JFM, cluster2 and cluster3 are significantly anti-correlated. Cluster2 exhibits also significant anti-correlation with cluster5. These correlations between the clusters are consistent with the goal of cluster analysis, i.e., to maximize the similarity within clusters and minimize the similarity between clusters (Wilks, 2006).

Table 4.1 Correlation coefficients between inter- annual frequencies of the clusters in OND (left) and JFM (right). Shaded numbers show correlations significant at p≤ 0.05

OND	Cluster2	Cluster3	JFM	Cluster2	Cluster3	Cluster4	Cluster5
Cluster1	0.28	**-0.80**	Cluster1	-0.21	0.01	-0.28	0.05
Cluster2		**-0.68**	Cluster2		**-0.57**	-0.14	**-0.38**
			Cluster3			-0.3	-0.01
			Cluster4				-0.05

4.2 Composites of OLR

The composites of OLR are based on daily indices obtained from cluster analysis. The anomalies are computed as the difference between the mean of the days when a particular cluster is observed and the rest of the period. The student's t test at 5% level is used to assess confidence level in the difference between the mean of the events represented in each cluster and the mean for the rest of the period. Monte Carlo Simulations (e.g. Von Storch and Zwiers, 2000) were applied in one of the clusters in OND and one in JFM; the results were similar with the Student's t test results. Because of the computing time and memory needed for Monte Carlo Simulations, for the rest of the clusters the Student's t test was used and only the results of this test are presented. A similar procedure was done by Cook (2001) for precipitation using Mann-Whitney rank-sum test.

Figure 4.4a shows the composite anomalies of OLR for the partitions considered in OND. Cluster1 exhibits a dipole pattern, with positive anomalies extending diagonally from central and north-eastern southern Africa towards the South-West Indian Ocean (SWIO). Negative anomalies prevail over south-western southern Africa extending towards the ocean area south of South Africa. Cluster2 exhibits a tripole pattern with negative anomalies extending from central southern Africa towards the SWIO. Positive anomalies parallel to the band of negative anomalies are observed over the tropical Indian Ocean and over the western part of southern Africa extending diagonally towards the Indian Ocean off the south coast of South Africa. Cluster1 and cluster2 show similar patterns, but with reversed signs. Cluster1 (cluster2) is associated with reduced (enhanced) convection over central and south-eastern southern Africa and enhanced (reduced) convection over the western and southern parts of southern Africa. Cluster3 exhibits a dipole pattern with negative anomalies extending from northern Mozambique and the western tropical Indian Ocean towards the

southeast. Positive anomalies are observed over the bulk of southern Africa and the mid-latitude SWIO.

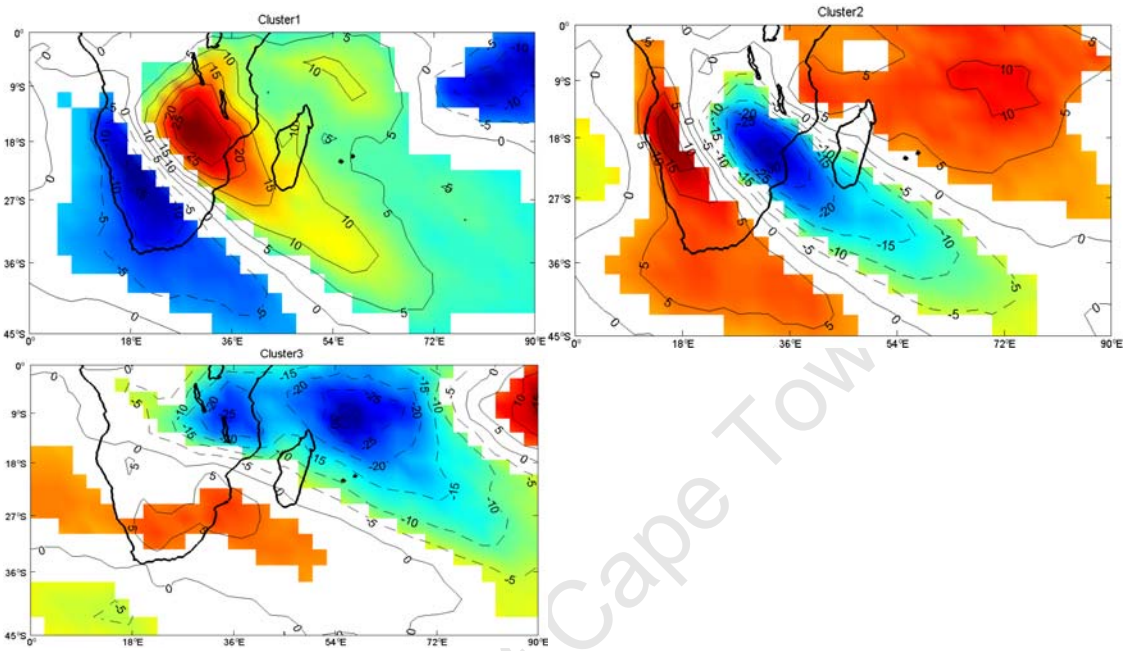

Fig.4.4a Composite of OLR (contour interval is 5 W/m^2) anomalies for OND clusters. Shaded areas are significant at 5%. Dashed (solid) contours denote negative (positive) values and represents more (less) convective cloud cover.

Figure 4.4b shows the composite anomalies of OLR for the partitions considered in JFM. Cluster1 exhibits negative anomalies over the western side of southern Africa and also in a diagonal band extending from eastern Madagascar towards the southeast. This cluster also exhibits two diagonal bands of positive anomalies, one extending from southern Mozambique towards the SWIO and another from Tanzania towards the eastern Indian Ocean. Cluster2 exhibits a dipole pattern with positive anomalies extending from southern Mozambique/Zimbabwe towards the central South Indian Ocean, a negative band extending south-eastward from the northern tip of Madagascar. Cluster3 also exhibits a dipole pattern with negative anomalies extending from central southern Africa, straddling south and central Mozambique towards the SWIO. Positive anomalies exist to the north and extend from Tanzania towards the

southeast Indian Ocean. The anomalies of cluster2 and cluster3 show opposing signs over southern Africa/SWIO, consistent with shifts in the position of cloud bands shown in Figure 2.5. Cluster2 suggests enhanced (reduced) convection over SWIO (southern Africa). The reverse is true for cluster3. Cluster4 exhibits positive anomalies over southern Africa and over the nearby South Indian and South Atlantic Oceans. The patterns of this cluster suggest significantly reduced convective activity over southern Africa. Cluster5 exhibits negative anomalies extending eastward from Tanzania across the equatorial South Indian Ocean. The spatial distribution of this pattern appears to be associated with the southernmost position of the ITCZ. This cluster also exhibits positive anomalies over the SWIO. Over southern Africa, the anomalies are weak.

The spatial patterns of negative OLR anomalies for cluster2 (OND) and cluster3 (JFM) are consistent with the position of cloud bands associated with the SICZ located over southeast southern Africa/SWIO (see e.g. Fig. 2.4 and Fig. 2.5 upper panel and Cook 2000). On the other hand, the spatial patterns of negative OLR anomalies for cluster3 (OND) and cluster2 (JFM) are also consistent with cloud bands associated with the SICZ, however shifted north-eastward, with the main axis located over the tropical and subtropical SWIO (see Fig. 2.5 lower panel and Cook 2001). The different positions of the negative anomalies of OLR observed in these four clusters are consistent with the mean position of SICZ during La Niña (cluster2 in OND and cluster3 in JFM) and El Niño (cluster3 in OND and cluster2 in JFM) as shown in Figure 2.5.

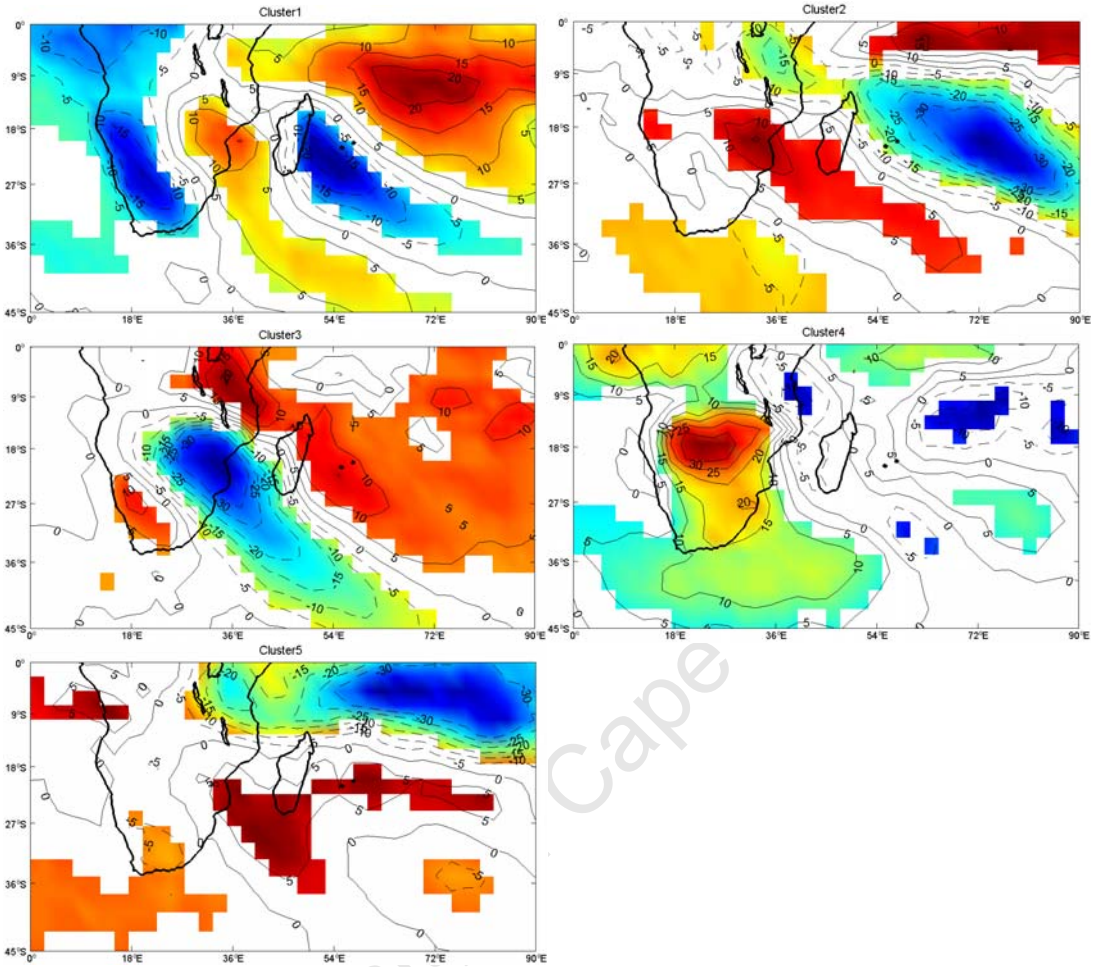

Fig.4.4b Same as Fig.4.4a except for JFM

4.3 Rainfall variability and anomalies and relationship with the clusters

In this section, the links between the inter-annual variability of rainfall and that of the clusters are analysed using monthly CRU2 rainfall data and 10 rainfall stations across Mozambique. The positions of the stations are depicted in Figure 3.1.

4.3.1 Composites of rainfall associated with each cluster

Composites of CRU2 rainfall data are presented as the difference between years with above average and years with below average occurrence for each cluster. The objective is to explore links between the annual frequency of the clusters and spatial and inter-annual patterns of rainfall variability over

southern Africa. To test the significance of the composites a similar procedure as for OLR was followed. Figures 4.5a and 4.5b show the anomalies associated with each cluster for OND and JFM respectively.

The rainfall patterns of cluster1 (OND) are negative and strong over northern Mozambique/Tanzania but weak over the central and southern parts of southern Africa (Fig. 4.5a). These anomalies of rainfall are consistent with the anomalies of OLR (Fig. 4.4a) for this cluster, however the positions of maxima values do not match. Negative anomalies of rainfall are stronger over northern Mozambique/Tanzania while positive anomalies of OLR show largest values over central Mozambique/Zimbabwe. These apparent contradictions may be associated with local effects which are not analysed here. On the other hand, the rainfall anomalies of clusters 2 and 3 (OND) display more consistent patterns with the anomalies of OLR. Cluster2 shows largest positive anomalies of rainfall over central Mozambique consistent with strong negative anomalies of OLR (Fig. 4.4a) there. Over southern Mozambique significant values (above 60 mm) are observed. The rainfall anomalies of cluster3 show a pattern opposite to that of cluster1. This cluster displays significant positive anomalies of rainfall over Tanzania, consistent with the significant negative anomalies of OLR (Fig. 4.4a) there. All three clusters show a dipole pattern of rainfall anomalies between the south-eastern and north-eastern regions of the domain. This dipole pattern in summer rainfall over southern Africa has been shown in a number of studies and it has been associated with the influence of ENSO on southern Africa rainfall (e.g. Jury, 1992; Nicholson and Kim, 1997; Cook, 2001).

The annual frequencies of the three clusters (OND) display significant correlations with ENSO at different lags (Table 4.2a). Correlations are negative with cluster1 and cluster2 and positive with cluster3. Note that composites of rainfall for annual frequency of clusters 1 and 2 show positive anomalies, while for cluster3 the anomalies of rainfall display opposite pattern (Fig. 4.5a). These correlations are consistent with a number of studies showing that El Niño (La Niña) is negatively (positively) correlated with rainfall over southeast southern

Africa (e.g. Nicholson and Kim, 1997; Rocha and Simmonds, 1997; Richard et al, 2000). While the correlations between annual frequencies of the three clusters and ENSO show significant values (Table 4.2a), the anomalies of rainfall over subtropical southern Africa do not show strong patterns in all the three clusters. However, cluster1 and cluster3 show strong anomalies over Tanzania (Fig. 4.5a left and right panels). Nicholson and Kim (1997) have shown significant and positive relationship between short rains (October – December) over equatorial East Africa. The strong correlations between Niño 3.4 index and rainfall over equatorial East Africa, particularly over Tanzania, shown by clusters 1 and 3 may indicate the potential of this index for prediction of the early season (OND) rains for this region. It is important to note that correlations are significant two months prior to the rain season (see Table 4.2a).

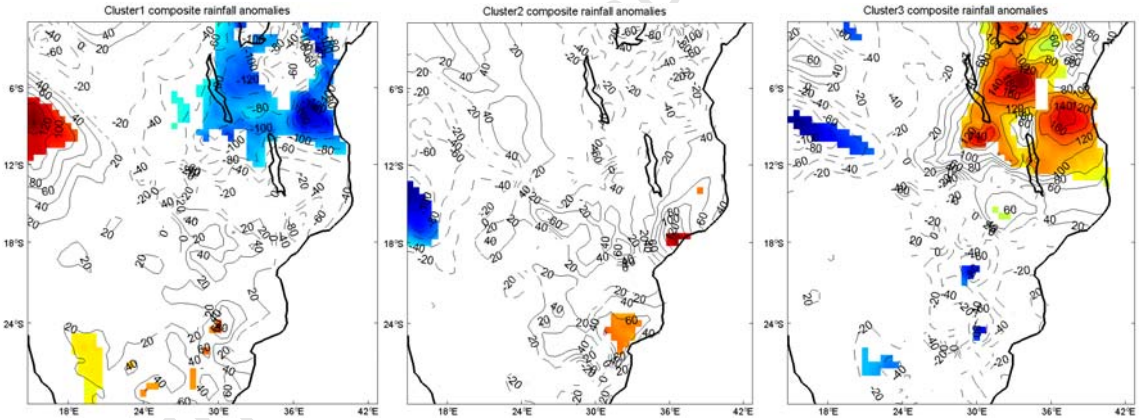

Fig.4.5a composites of rainfall anomalies (contour interval is 20 mm) based on the difference between years of above and below average occurrence of the OND clusters. Shaded areas are significant at 5% level. Dashed (solid) contours denote negative (positive) values.

Table 4.2a Lagged correlations between annual frequencies of OND clusters and Nino3.4 index from 12 to 0 lag. Numbers in bold show anomalies with p≤0.05

	OND	NDJ	DJF	JFM	FMA	MAM	AMJ	MJJ	JJA	JAS	ASO	SON	OND
Cl1	0.22	0.23	0.23	0.23	0.19	0.05	-0.19	-0.34	**-0.42**	**-0.47**	**-0.56**	**-0.61**	**-0.63**
Cl2	0.12	0.13	0.13	0.11	0.07	-0.04	-0.25	**-0.41**	**-0.52**	**-0.55**	**-0.57**	**-0.56**	**-0.55**
Cl3	-0.28	-0.28	-0.28	-0.27	-0.22	-0.05	0.25	**0.45**	**0.55**	**0.59**	**0.65**	**0.68**	**0.72**

In JFM (Fig. 4.5b) clusters 2 and 3 show the strongest patterns and they mirror each other, with opposite signs, consistent with the high anti-correlation between the two (see section 4.1.2). Cluster2 exhibits negative anomalies over central and southeast southern Africa and positive over the northeast. Cluster3 exhibits positive and significant anomalies over south and central Mozambique and central southern Africa, whereas over the northeast the anomalies are negative and weak. The patterns of these two clusters are also consistent with the patterns of OLR (Fig. 4.4b). Cluster1 shows positive anomalies of rainfall aligned horizontally from central southern Africa towards eastern central Mozambique, however the patterns are not significant. The rainfall patterns of cluster 4 are negative over the entire southern African African region, consistent with prevailing strong positive anomalies of OLR over the region, associated with this cluster. Cluster5 displays zonally oriented positive anomalies of rainfall over central southern Africa, between 12°S and 18°S. These anomalies of rainfall are located southward of the oceanic position of the ITCZ, inferred from the OLR anomalies (see Fig. 4.4b). However, this pattern of rainfall is not observed in the OLR anomalies over land, suggesting that it may result from other factors than convection.

Correlations between the annual frequencies of the clusters and the Niño 3.4 index (Table 4.2b), suggest that a strong relationship exists between the annual frequency of cluster2 and ENSO. Correlations are positive and significant from 8 months-lag (MJJ) to 0 month-lag (JFM). These strong correlations between cluster2 and the Niño 3.4 index, with significant lead time may indicate the importance of this index for seasonal prediction of JFM rainfall in eastern southern Africa during El Niño years. Cluster3 displays consistent negative correlations with Niño 3.4 index, but the correlations are only significant at 1 and 0 month-lag. Clusters 1 and 5 also display negative correlations at different lags, but in general weaker compared to clusters 2. Cluster4 displays weak correlations with Niño 3.4 index, although showing negative anomalies of rainfall

over southern Africa. However, not all droughts over southern Africa are associated with El Niño (e.g. Mulenga et al., 2003).

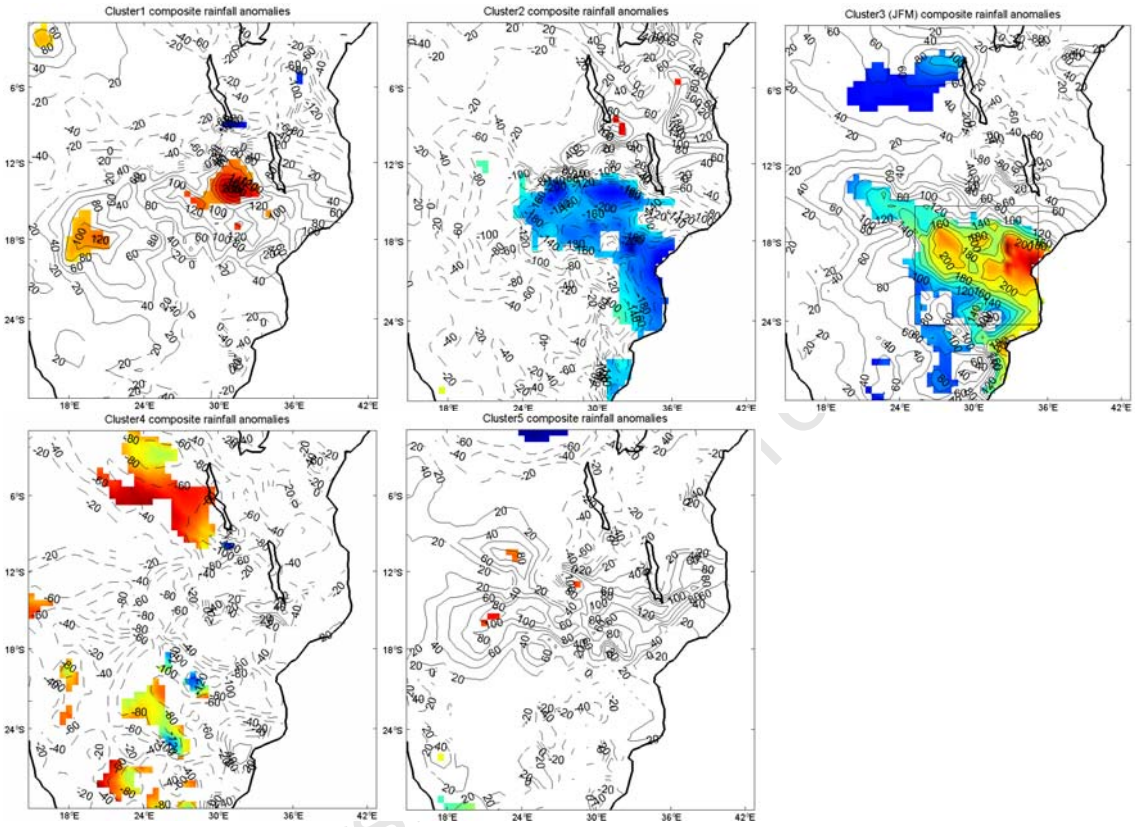

Fig.4.5b. Same as Fig.4.5a except for JFM

Table 4.2b Same as Table 4.2a except for JFM clusters

	JFM	FMA	MAM	AMJ	MJJ	JJA	JAS	ASO	SON	OND	NDJ	DJF	JFM
CI1	0.31	0.30	0.21	0.03	-0.14	-0.25	-0.28	-0.30	-0.29	-0.31	-0.33	-0.36	-0.39
CI2	-0.13	-0.11	-0.01	0.19	0.36	**0.49**	**0.53**	**0.56**	**0.59**	**0.62**	**0.65**	**0.66**	**0.67**
CI3	-0.15	-0.15	-0.18	-0.20	-0.21	-0.23	-0.26	-0.29	-0.32	-0.34	-0.37	**-0.41**	**-0.45**
CI4	0.36	0.33	0.27	0.19	0.09	0.02	0.01	0.00	-0.02	-0.04	-0.02	0.04	0.09
CI5	-0.06	-0.05	-0.08	-0.18	-0.25	0.18	-0.28	-0.32	-0.35	-0.38	**-0.40**	**-0.40**	-0.38

4.3.2 Relationship between clusters and the annual frequency of wet spells and of dry days over Mozambique

Links between inter-annual rainfall variability over Mozambique and cluster frequencies are further explored using correlations analyses between the clusters and the annual frequency of wet spells and dry days derived using data from the 10 rainfall stations. These relationships are explored in more detail in Chapter 6 for the selected clusters.

In OND (Table 4.3a), cluster2 shows positive correlations with the frequency of wet spells and negative correlations with the frequency of dry days for 3 stations over southern Mozambique. Given the spatial distribution of the stations (i.e. separated by large distances and oriented south-north), the correlations show that this cluster represents either a propagating or a large scale system. The correlations are also consistent with the spatial patterns of composite anomalies of rainfall shown in Fig. 4.5a, i.e., high frequency of cluster2 is associated with positive anomalies of rainfall over southern Mozambique. The other two clusters show some isolated correlations but without any clear spatial pattern.

Table 4.3a Correlations between inter-annual frequencies of wet spells and of dry days with OND clusters. Bolded numbers show correlations significant at p≤ 0.05

Cluster number		St1	St2	St3	St4	St5	St6	St7	St8	St9	St10
Cl1	wet	**0.47**	0.03	0.00	-0.20	0.13	-0.19	0.12	**-0.39**	-0.23	**-0.45**
	dry	0.00	-0.11	-0.04	-0.09	0.02	0.14	-0.18	**0.41**	**0.46**	-0.03
Cl2	wet	0.32	**0.60**	**0.49**	0.27	0.34	0.08	-0.02	-0.24	-0.07	-0.06
	dry	-0.38	**-0.45**	**-0.52**	0.01	-0.13	**-0.50**	-0.34	**0.39**	0.00	0.06
Cl3	wet	**-0.40**	-0.28	-0.22	-0.03	-0.18	0.13	0.00	**0.50**	0.14	0.37
	dry	0.10	0.24	0.28	0.06	0.13	0.14	0.23	**-0.53**	-0.26	-0.03

In JFM, clusters 2 and 3 show strong correlations with stations over southern and central Mozambique (Table 4.3b). Cluster2 is negatively (positively)

correlated with the annual frequency of wet spells (dry days). Cluster3 is positively (negatively) correlated with the annual frequency of wet spells (dry days). The correlations in JFM are more robust than in OND, likewise the composite anomaly patterns of clusters 2 and 3 in JFM are the most robust in all analysed clusters. The possible reasons for the differences in strength of the patterns between the early and late summers are explored in the analysis of the circulation patterns associated with each selected cluster.

Table 4.3b Same as Table4.3a except for JFM

Cluster number		St1	St2	St3	St4	St5	St6	St7	St8	St9	St10
Cl1	wet	-0.10	-0.02	0.38	0.00	-0.05	0.11	0.24	-0.20	-0.01	-0.13
	dry	0.09	0.11	-0.19	0.11	-0.05	-0.05	0.06	-0.19	-0.06	0.07
Cl2	wet	**-0.45**	**-0.48**	**-0.64**	-0.35	-0.38	-0.30	**-0.57**	-0.15	-0.13	0.39
	dry	**0.55**	**0.41**	**0.67**	-0.01	0.06	0.28	0.21	0.02	0.23	0.27
Cl3	wet	**0.47**	**0.53**	**0.51**	0.15	0.30	0.11	**0.53**	0.03	-0.07	**-0.44**
	dry	**-0.66**	**-0.59**	**-0.55**	-0.20	-0.02	-0.06	-0.27	0.06	-0.12	-0.11
Cl4	wet	0.10	0.01	-0.01	0.10	0.04	0.04	-0.12	-0.03	-0.08	0.02
	dry	-0.01	0.18	-0.09	0.15	0.00	0.25	0.05	0.16	0.30	0.07
Cl5	wet	0.33	0.19	0.11	0.26	**0.42**	0.30	-0.07	0.28	0.09	-0.05
	dry	-0.21	-0.33	-0.15	0.10	-0.13	-0.35	-0.16	-0.06	-0.27	**-0.42**

4.4 Cluster selection

Cluster analysis, composites of OLR and rainfall and also correlations between rainfall stations and cluster frequencies have shown that the patterns of cluster2 in OND and cluster3 in JFM are representative of TTT over southern Africa and are also linked to wet conditions over southern and central Mozambique. The spatial distributions over land of negative anomalies of OLR of these two clusters are consistent with the position of largest loadings of PC1 pattern of Rocha and Simmonds (1997) applied to summer (November-March) rainfall station data. The same patterns of OLR are also consistent with the first

PCA of Janowiak (1988) applied to African rainfall for the December – March period, which accounts for 14,5 per cent of variance. On the other hand, the patterns for cluster2 in JFM are linked to convective activity over the South Indian Ocean and with dry conditions over the bulk of southern Africa. The anomaly pattern of rainfall for cluster2 (see 4.5b upper middle panel) is also consistent with the two above mentioned clusters in terms of spatial distribution. Note also the dipole pattern of rainfall anomalies between southern/central Mozambique and northern Mozambique and Tanzania displayed in all three clusters (see Fig. 4.5a and 4.5b). Cook (2000) suggests that this dipole pattern results from the movement of the SICZ. It is important also to note that the rainfall patterns of cluster2 and cluster3 (JFM) are similar, but with reversed signs.

All three clusters discussed in this section have shown significant correlations with ENSO at different lags and also have shown significant relationship with rainfall variability over southern Africa in general; therefore they are selected for further analyses. The dates of observation for each selected cluster are shown in Table1 (Appendix A).

4.5 Atmospheric patterns associated with each selected cluster

Here the anomalies and mean circulation patterns associated with each cluster are analysed. The patterns associated with wet conditions (cluster2 (OND) and cluster3 (JFM) over southern Africa are first analysed in Section 4.5.1. In Section 4.5.2, the atmospheric patterns characteristic of cluster2 (JFM), are analysed. This cluster is associated with convective activity located over the South Indian Ocean and dry conditions over southern Africa.

4.5.1 Cluster 2 (OND) and Cluster3 (JFM)

Cluster2 (OND) and cluster3 (JFM) are analysed together as both are associated with wet conditions over southern Africa and, as indicated before,

their OLR patterns are reminiscent of cloud bands associated with the SICZ over southern Africa.

4.5.1.1 Geopotential height anomalies

The anomalies of geopotential height of cluster2 (OND) and cluster3 (JFM) display trough type anomalies (henceforth we refer to these anomalies as troughs) consistent with the TTT or SICZ over southern Africa and SWIO. In the early summer season (OND), the troughs display a wavenumber-4 pattern over the Southern Hemisphere (Fig.4.6a). The patterns of this cluster are consistent with the second and third EOFs of Ghil and Mo (1991) performed in the 500 hPa geopotential for the SH winter in the intra-seasonal band. These authors suggested that the 2 EOFs explain 5.1% ± 0.8% and 4.8% ±0.8% of the total variance respectively and are not well separated statistically. They also suggested that the 2 EOFs represent an eastward travelling planetary wave. The pattern of the 4 troughs is also consistent with the pattern of semi-stationary or slowly moving cloud bands over the Southern Hemisphere (see Fig. 11.25 in Tyson and Preston-Whyte, 2000).

Over southern Africa, the trough is well developed to the southeast of Madagascar, and it is observed throughout the troposphere (see Fig.1 in the the Appendix B). Over the continent a near surface ridge type anomaly (henceforth referred to as a ridge) is observed (see Fig.1a in Appendix B), however at the 700 hPa level the trough is well depicted and strengthens with height (Fig.1 in the Appendix B). This apparent westward tilting suggests a baroclinic system (Gill, 1982), and has been reported as typical of the Southern Hemisphere westerly waves (see e.g. Tyson and Preston-Whyte, 2000). A significant ridge at higher latitudes over the South Atlantic Ocean with maxima values south of southern Africa is also observed. This pattern suggests ridging anticyclones, which are characteristic of temperate disturbances that produce rainfall over southern Africa (see e.g. Mason and Jury, 1997). Over the tropical South Indian Ocean,

significant positive anomalies of geopotential height are observed near the surface with negative anomalies at upper levels (Fig.1 in the Appendix B). This pattern of geopotential height is associated with local low level anticyclonic and upper level cyclonic circulation anomalies (see Fig. 2 in the Appendix B).

In the late summer (JFM), the 500 geopotential height anomalies show a wavenumber-3 pattern (Fig.4.6b). This pattern is found in both intra-seasonal and inter-annual analyses of South Hemisphere variability (e.g. Kidson, 1988; Kidson, 1991; Cai and Watterson, 2002). Troughs are observed over southern Africa-SWIO, south of Australia and over southern South America. The ridges over the three subtropical ocean basins show stronger anomalies compared to the troughs. Over the SWIO/southern Africa, the ridge is shifted north-westward. Ridging of the South Atlantic anticyclone south of the continent is apparent. The trough over southern Africa shows a slight southward tilting and at upper levels, a ridge is observed over the position of the low level trough (see Fig. 3 in the Appendix B). As mentioned in Chapter2, the presence of a trough at the surface and a ridge aloft creates ideal conditions for the development of upward vertical motion. The patterns over northeast Madagascar and northwest Australia suggest an active Walker Cell over the South Indian Ocean, with its ascending branch on the eastern side and descending on the western side. A descending branch over northern Madagascar also contributes to the strengthening of the north-western region of the South Indian anticyclone, which in turn leads to strong low level easterly anomalies (see Fig. 4 in the Appendix B).

4.5.1.2 Vertical Integrated moisture fluxes

Composite anomalies of integrated moisture fluxes (equations 4.3 and 4.4) of cluster2 (OND) and cluster3 (JFM) are analysed here. As indicated before, the levels for the specific humidity in the NCEP reanalysis are between 1000 to 300 hPa, therefore the integration here is considered for the same levels.

Figures 4.7 and 4.8 show the fluxes for cluster2 (OND) and cluster3 (JFM) respectively.

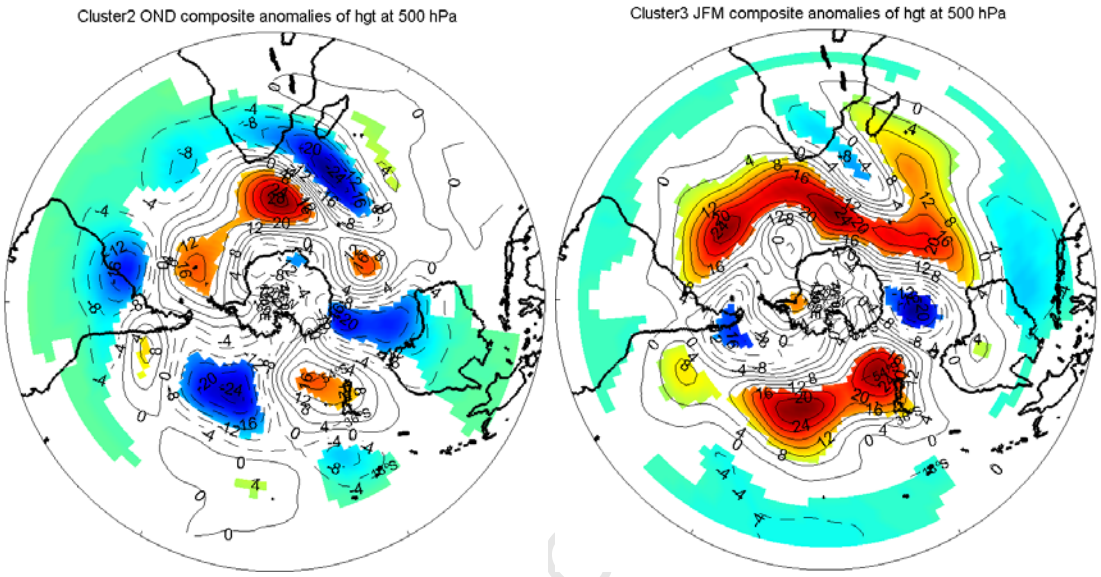

(a) (b)

Fig.4.6 Composites of geopotential height anomalies at 500hPa associated with (a) cluster2 (OND), and (b) cluster3 (JFM). Contour interval is 4m. Shaded areas are significant at 5% level.

The anomalous fluxes associated with cluster2 (Fig. 4.7) displays a pattern defined by the position of the trough south of Madagascar. South (north) of the trough, onshore (offshore) anomalies are observed. The onshore fluxes over South Africa may explain positive anomalies of rainfall observed south of the position of the convective activity associated with the TTT (compare Fig. 4.5a middle panel and Fig. 4.4a upper right panel), and appear to be associated with the ridging anticyclone south to southeast of South Africa. Significant offshore anomalies of moisture fluxes are observed over central Mozambique, in the same region where maximum convective activity (as suggested by the anomalies of OLR) is observed. These apparent offshore moisture fluxes might be associated with significant mid and upper level offshore wind anomalies (see Fig.2 in the Appendix B). At low levels onshore southerly wind anomalies from

the Mozambique Channel are observed (Fig.2a in Appendix B), apparently linked to the ridging anticyclone between the Atlantic and Indian Oceans. Southerly low level winds may contribute to the moisture convergence over central Mozambique. Furthermore, the anomalies of integrated moisture fluxes suggest a weakening of the export of Indian Ocean moisture to Namibia and the South Atlantic Ocean, and hence the relative convergence over central Mozambique.

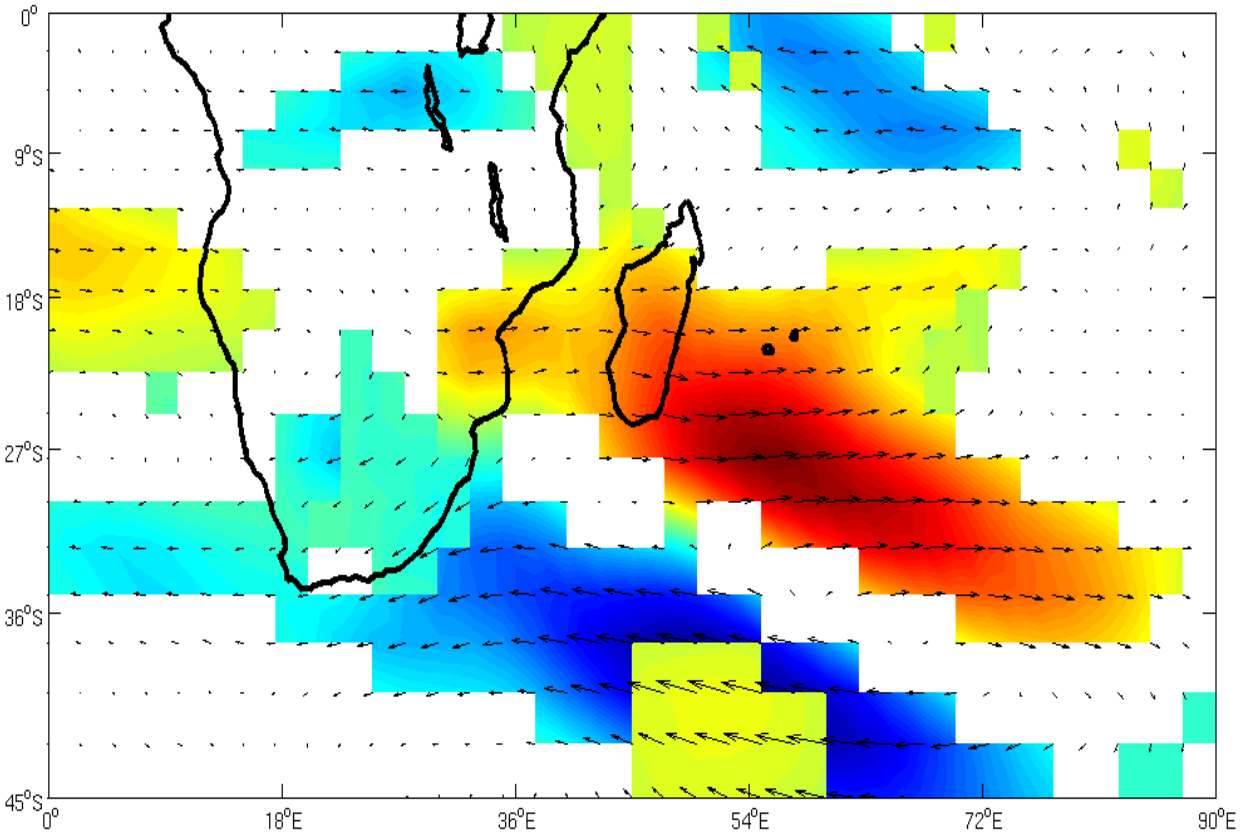

Fig.4.7 Composite anomalies of vertical integrated (1000-300 hPa) moisture fluxes ($g.Kg^{-1}ms^{-1}$ with arrows scaled at 1 unit/degree latitude) associated with cluster2 (OND). A Shaded regions show anomalies significant at 5% level.

The anomalies of moisture fluxes associated with cluster3 (JFM) are dominated by anomalous anticyclonic circulation over the South Indian Ocean (Fig. 4.8), consistent with the patterns of geopotential height for this cluster. Over the tropical South Indian Ocean, strong eastward moisture fluxes associated with anomalous easterly flow (see Fig. 4 in the Appendix B) are observed. Over the

southern section of the South Indian Ocean anticyclone, significant south-eastward moisture fluxes are observed. These fluxes converge over the position of the trough (see Fig. 4.6b) south to southeast of Madagascar. Over South Africa, westward anomalies of moisture fluxes, linked to the cyclonic circulation to the southeast of Madagascar, are observed. These westward fluxes of moisture may contribute to the positive anomalies of rainfall observed over the southernmost part of the eastern southern Africa (see Fig. 4.5b upper right panel).

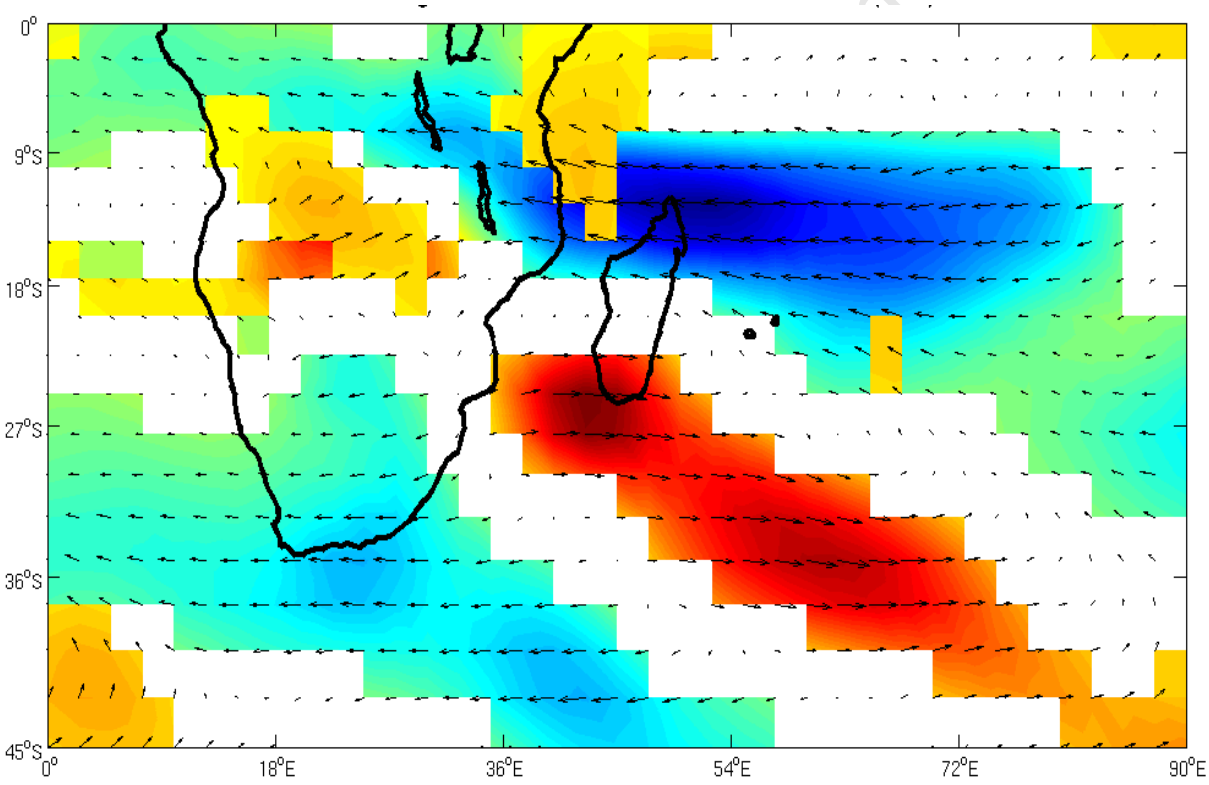

Fig.4.8 Same as Fig.4.7 except for cluster3 in JFM

4.5.1.3 Role of moisture convergence in producing rainfall

The different terms that contribute to the convergence of moisture associated with the two clusters are analysed here (equations 3.9-3.12). Figures 4.9 and 4.10 show the plots for each term in OND and JFM respectively, together with plots of precipitation (CMAP). Positive values of convergence (C), advection

(A), transients (T) and orography (O) do not necessarily represent realized precipitation amounts, only the contribution toward the total precipitation. Since a term can be offset to a large degree by another term of opposite sign, it is possible to have a term whose value is large and positive in a region where there is little or no precipitation (Lenterss and Cook, 1995).

Largest values of precipitation are associated with the convergence term (Fig.4.9b and Fig.4.10b) for both clusters. The maxima are observed over the tropical South Indian Ocean linked to the ITCZ position and consistent with maxima in precipitation on CMAP plots (Fig. 4.9a and Fig.4.10a). Rainfall over western southern Africa, particularly over Angola and central parts of South Africa, appears to significantly contributed by the convergent term in both cluster2 (OND) and cluster3 (JFM). The maxima in precipitation observed over Angola may be linked to a deep Angolan low, however these maxima are not observed in the CMAP plots. The convergent term shows also a diagonal band of precipitation stretching from Madagascar to the southeast in both clusters (Fig. 4.9a and Fig.4.10a). A similar band is also observed in the plots of CMAP rainfall (Fig.4.9a, Fig.4.10a). In OND the band of precipitation is truncated from the mainland and it shows maximum values over Madagascar. Note also a similar maximum in precipitation over Madagascar in the plot of CMAP data. In JFM the band is not truncated (as in OND), but it shows a circular pattern of precipitation over Mozambique Channel/eastern Madagascar.

The advection term (Fig.4.9c) linked to cluster2 (OND) displays a diagonal band of precipitation extending from the central southern Africa to the southeast over the mid-latitude SWIO. This pattern is not observed in the CMAP plot (Fig.4.9a), particularly the oceanic extension off the southeast of South Africa. A similar pattern associated with cluster3 (JFM) is observed, over central southern Africa, but the oceanic extension off the southeast of South Africa is absent (Fig.4.9c). Ridging to the south of South Africa (see Fig. 4.6) might be responsible for these patterns of precipitation. In both clusters, diagonal bands of precipitation extend from southeast Madagascar to the southeast Indian Ocean

(Fig. 4.9c and Fig. 4.10c). These diagonal bands appear to be linked to moisture advection on the southern margins of the Indian Ocean anticyclone (see Fig. 2a and Fig. 4a in the Appendix B).

The transient term for cluster2 (OND) displays a pattern similar to that of the advection term over subtropical southern Africa and southwest Indian Ocean, off South Africa. Like the case of the advection term, the extension off the southeast coast of South Africa appears to be associated with ridging Atlantic anticyclone. Over the SWIO, elongated bands of precipitation extending from southeast Madagascar towards the southeast are observed in both cluster2 (Fig. 4.9d) and cluster3 (Fig. 4.10d). These bands appear to be linked to the troughs observed in the same regions (Fig. 4.6). Over the continent, the precipitation associated with the transient term, extends in a diagonal band from the southwest to the southeast, for both cluster2 (Fig 4.9d) and cluster3 (Fig. 10d). These bands of precipitation might be linked either to westerly waves to the south (through ridging near the surface) or easterly waves to the north (associated with easterlies flow to the northern and western margins of the South Indian anticyclone), or interactions between both.

The orographic term shows high values of precipitation in the eastern coast of southern Africa for both cluster2 (Fig. 4.9e) and cluster3 (Fig. 4.10e). These high values of precipitation on the eastern coast appear to be associated with strong onshore winds, which are in turn forced by shifts or strengthening of the western margins of the South Indian Anticyclone. Anticyclonic ridging may also contribute to the high values observed in the eastern coast of South Africa and southern Mozambique (see Fig. 1 and Fig. 3 in the Appendix B).

The terms contributing to moisture convergence, analysed here, may fairly explain the structure of precipitation in the oceanic extension of the SICZ (depicted from the CMAP data). For example, for cluster2 (OND) the diagonal band of precipitation observed in the rainfall composite (Fig. 4.9a) is also observed in the terms representing convergence (Fig. 4.9b), advection (Fig. 4.9c)

and transients (Fig. 4.9d). This result suggests that all these three terms contribute to the diagonal extension of precipitation off the southeast coast of Madagascar. The same is true for cluster3 (JFM). However the structure of precipitation overland, associated with the SICZ is not clear in these terms.

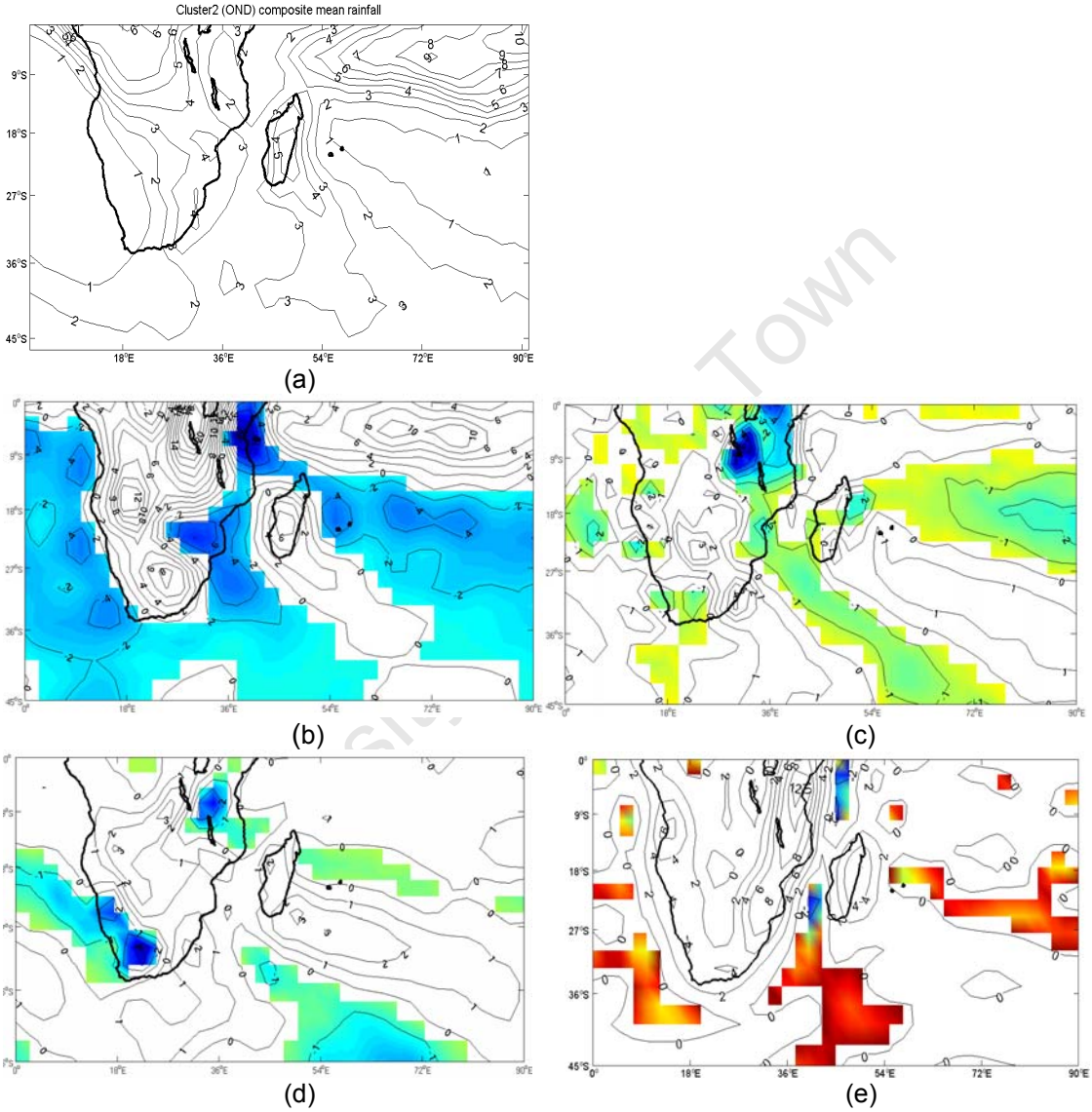

Fig.4.9 OND plots of (a) CMAP precipitation (b)Convergence term, (c) advection term, (d) transient, (e) orographic term. Shading indicates negative values. Contour interval is 1mm/day for plots a, c and d and is 2 mm/day for plots b and e.

For example, the convergence term (the term associated with the highest values of precipitation here) show high values of precipitation (Fig. 4.9b and Fig.4.10b) to the west of subtropical southern Africa, while plots of CMAP data show the

highest values to the east (over central Mozambique) in both clusters (Fig. 4.9a and Fig.4.10a). Only the orographic term shows high values of precipitation on the eastern coast of southern Africa, but it cannot explain the diagonal structure over the central southern Africa depicted in the composites of CMAP precipitation. The analyses in this section suggest that the structure of precipitation associated with the SICZ overland is complex and is not well captured in the equations for the moisture convergence analysed here

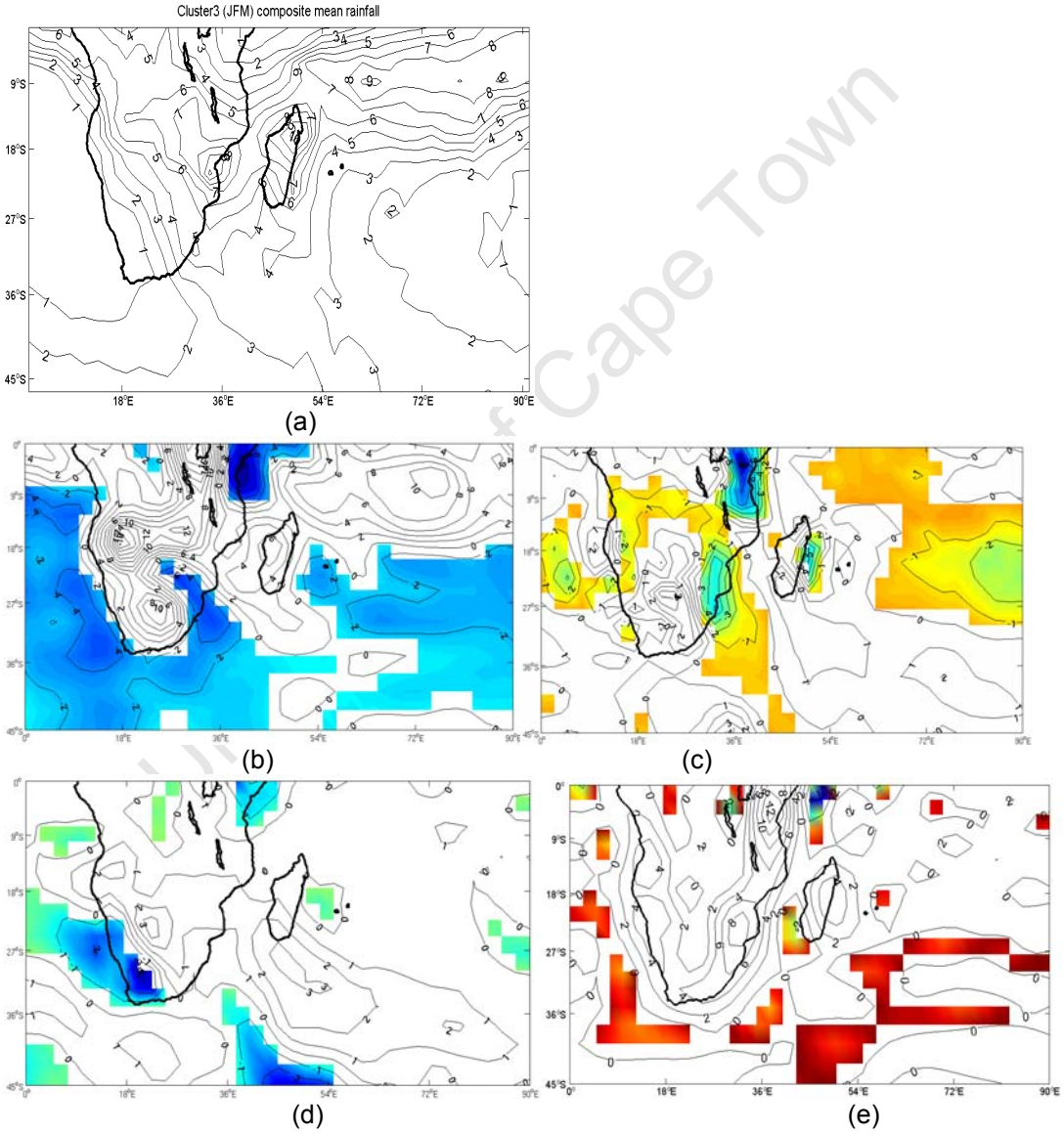

Fig.4.10 Same as 4.9 except for JFM

4.5.2 Cluster2 (JFM)

In this section, geopotetial height anomalies and vertical integrated moisture fluxes for cluster2 are analysed. As indicated before, this cluster is associated with dry conditions over the bulk of southern Africa.

4.5.2.1 Geopotential height anomalies

Composite of geopotential height anomalies at 500 hPa of cluster2 (JFM) shows two significant troughs over the subtropical South Indian and Pacific Oceans (Fig.4.11). Over the South Atlantic Ocean, a significant trough is observed near the Antartica. Over the Southern Hemisphere tropical belt, positive anomalies prevail. These patterns are similar with the anomalies of geopotential height shown in Cook (2001), derived from a General Circulation Model, and with idealized warming in the eastern Pacific typical of ENSO (see Figure 3 in Cook, 2001). The ENSO type anomalies are also consistent with strong positive correlations observed between this cluster and Niño 3.4 index (Table 4.2b). Near the surface, the trough is confined to the northeast of Madagascar and at the upper level, a ridge is observed overlaying it, while a reversed pattern is observed over western Australia (see Fig. 5 in the Appendix B). Similar to cluster3 (JFM), the circulation patterns of cluster2 suggest an active Walker Cell over the tropical South Indian Ocean, but with the ascending branch over eastern Madagascar and descending over western Australia. This circulation pattern is consistent with the Walker Cell circulation during El Niño (see Fig. 2.6).

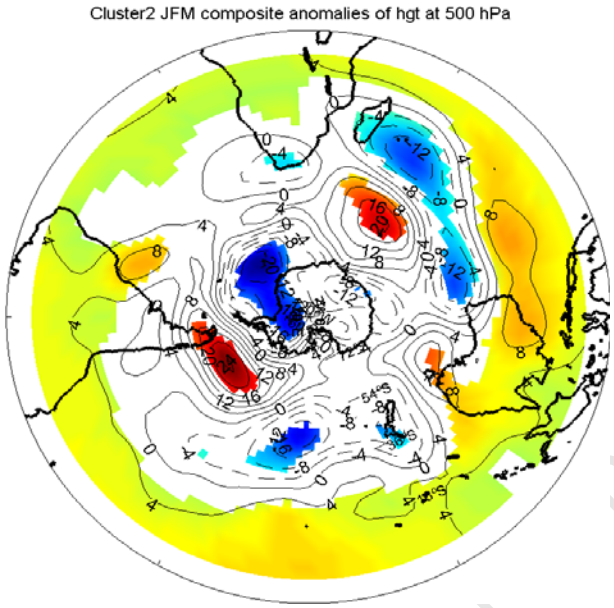

Fig.4.11 Same as Fig.4.6 except for cluster2 in JFM

4.5.2.2 Vertical integrated moisture fluxes

The vertical integrated moisture fluxes for cluster2 display cyclonic anomalies over the South Indian Ocean (Fig.4.12), consistent with the trough shown in Figure 4.11. Over the tropical South Indian Ocean, significant westerly anomalies prevail, with strongest values over the northeast of Madagascar. These westward moisture flux anomalies indicate weakening of the onshore moisture fluxes from the tropical South Indian Ocean, thus contributing to the observed reduced precipitation over southern Africa, associated with cluster2 (Fig. 4.5 upper middle panel). The convergence of moisture observed over the tropical South Indian Ocean, may also contribute to the trough eastern of Madagascar (see Fig. 4.11), which suggest an eastward shift of the SICZ. Over southern equatorial Africa, westerly moisture fluxes from the equatorial Atlantic are observed. These anomalies of moisture fluxes may be associated with the positive anomalies of rainfall observed over Tanzania and northern Mozambique (see Fig. 4.5b middle upper panel). Some studies have shown significant correlation between rainfall over this region and moisture fluxes from the tropical Atlantic (e.g. Mapande and Reason, 2005; Vigaud et al., 2007). Over the

subtropical southern Africa, and mid-latitudes south of southern Africa the patterns of moisture fluxes are weak.

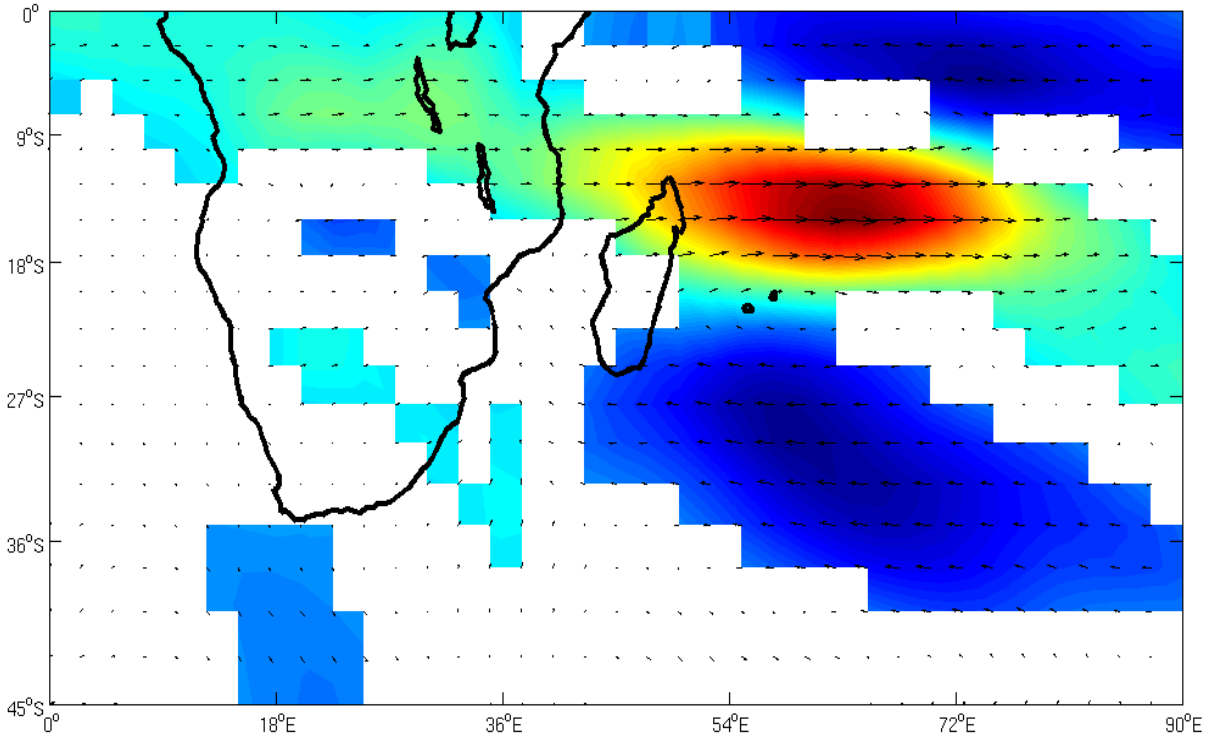

Fig.4.12 Same as Fig.4.7 except for cluster2 (JFM)

4.6 Summary

In this chapter, the clusters of interest in the present study were selected. Cluster2 in OND and cluster3 in JFM both representing the TTT positioned over southern Africa/SWIO and associated with wet conditions over the bulk of southern Africa, particularly over central and southern Mozambique, were analysed. Cluster2 (JFM) is associated with significant dry conditions over the bulk of southern Africa, mainly over south and central Mozambique, therefore was also selected.

The atmospheric patterns analysed here show that cluster2 (OND) and cluster3 (JFM) are associated with Southern Hemisphere wavenumber 3-4 with

trough/ridge pattern. Geopotential anomalies for cluster2 (OND) are dominated by wavenumber-4 pattern with troughs over the southeast southern Africa and South America, south of Australia and eastern South Pacific. These troughs strengthen with height throughout the troposphere. Geopotential anomalies for cluster3 (JFM) are dominated by a wavenumber-3 pattern, with troughs over the southern parts of the continents and ridges over the three Southern Hemisphere ocean basins. Unlike cluster2 (OND), the troughs associated with cluster3 (JFM) weaken with height. Over southern Africa, an upper level ridge overlays the low level trough associated with cluster3 (JFM).

Anticyclonic ridging, to the south of southern Africa, appears to be the mechanism by which the mid-latitude westerly waves affect the circulation over southern Africa associated with both cluster2 (OND) and cluster3 (JFM). Over tropical and subtropical regions, westward shift or strengthening of the northwest margins of the South Indian anticyclone appears to play the most significant role. Westward shift or strengthening of the northwest margins of the South Indian anticyclone results in strengthening of the onshore easterly winds and moisture fluxes from the tropical Indian Ocean. This mechanism is stronger for cluster3 (JFM) as compared to cluster2 (OND), apparently because of the influence of the Walker Cell in the late summer, as suggested by the anomalies of geopotential. Interactions between the circulations in the westerlies, associated with ridging and the easterlies on the western margins of the South Indian Anticyclone, may trigger or sustain the oceanic extension of the SICZ. These interactions are particularly apparent in the circulation associated with cluster3 (JFM). Strong onshore moisture fluxes associated with strong South Indian anticyclone, may explain the significant positive anomalies of rainfall over southern Africa associated with this cluster.

Atmospheric patterns associated with cluster2 (JFM) are basically limited to the tropical region. The mid-latitude patterns are in general weak. This cluster displays a significant trough over the South Indian Ocean, east of Madagascar, with northeast monsoons and subtropical Indian Ocean easterly winds

converging towards the position of the trough. The patterns of this cluster also suggest an active Walker Cell over the South Indian Ocean, with ascending branch over eastern Madagascar and a descending branch over western Australia. Low level convergence over the western side of the tropical South Indian Ocean, contributes to weakening of the easterly winds over the northern sector of the South Indian Ocean high. Weakening of the easterly winds and convergence of the northeast monsoon over eastern Madagascar, all contribute to dry conditions over southern Africa.

Inter-annual patterns of all these three clusters are analysed in the next chapter.

Chapter Five

5. Inter-annual variability of the clusters and relationship with ENSO and SIOD

In this chapter, the inter-annual variability of the clusters selected in Chapter 4 are studied using composites, correlation and regression analyses. The years used for the composites of each cluster are shown in Table 5.1. For cluster2 (OND) 10 years with above average annual frequency (see Fig. 4.2 middle panel) were selected. For cluster2 and cluster3 in JFM 8 years with above average frequency (see Fig. 4.3 second and third panel respectively) were selected. The main objective here is to explore links between the inter-annual variability of these clusters and the two principal modes of climate variability which impact on rainfall over southern Africa. These two modes are ENSO, and the South Indian Ocean subtropical dipole. Previous studies (e.g. Rocha and Simmonds, 1997; Reason, 2001, 2002; Washington and Preston, 2006) on relationships between southern Africa rainfall and SST over Indian Ocean have not explored these relationships in the particular context of TTT or the SICZ. We believe that exploring SICZ variability may give more insight into the physical mechanisms associated with southern Africa rainfall variability and their relationships with the large scale climate modes.

The first aspect we explore in this chapter is how much the selected clusters influence the atmospheric circulation patterns over southern Africa/SWIO for those years in which these clusters display a high frequency. This is done by comparing the composite anomalies of geopotential height associated with years of high frequency with the composite anomalies of events for each cluster (analysed in Chapter 4). Similarity in patterns may indicate the influence of a particular cluster on the inter-annual variability of geopotential height, and hence in the prevailing general circulation. Furthermore, linear regression is used to isolate patterns associated with ENSO in order to explore if other modes that may be independent of ENSO, have significant influence on the circulation variability. Note that linear regression will not isolate non-linear ENSO

interactions with other modes. Following Washington and Preston (2006), the linear influence of ENSO is removed by regressing the annual frequency of the variables against the annual frequency of the Niño 3.4 index, and then these regression values are subtracted from the raw data. The Niño 3.4 index is selected because previous studies have shown significant correlation between this index and rainfall over southern Africa (e.g. Goddard and Graham, 1999).

Table 5.1 Years used in the composites of the annual frequencies of the clusters

	Cluster2 (OND)	Cluster2 (JFM)	Cluster3 (JFM)
Years	1979,1980,1981,1985,1989 1990,1992,1995,1998,2001	1979,1980,1987,1992, 1995,1998,2002,2003	1981,1990,1991,1996, 1997,1999, 2000,2001

5.1 Composite anomalies of geopotential height and wind

The geopotential anomalies for cluster2 (OND) are weaker compared to anomalies in the composite of individual events shown in the previous chapter. This may indicate that other patterns significantly influence the composite of geopotential height for the years that cluster2 exhibits high frequency. As indicated in Chapter 4, cluster2 (OND) is dominated by mid-latitude westerly systems. Perturbations in the westerlies have a high degree of variability (e.g. Tyson and Preston-Whyte, 2000), and that may weaken the composites based on the annual frequency of the cluster2. However, over southern Africa, a weak trough extending from western South Africa towards the SWIO is observed. North of this trough, a ridge prevails (Fig5.1a). These anomalies are consistent with the anomalies in the composite events (Fig. 4.6a), i.e., a trough over subtropical southern Africa and a ridge to the north. Over the Southern Hemisphere as a whole, a wavenumber-3 pattern is apparent, with the ridges over the subtropical and mid latitudes of the three ocean basins. The ridges over the South Pacific and South Indian basins display significant anomalies over their western sides, while over the South Atlantic, the ridge displays significant

anomalies over its eastern side. The ridge over the tropical SWIO is associated with onshore moisture anomalies over northern and central Mozambique (see Fig. 8 in the Appendix C). Troughs are also observed south of Australia and South America. These patterns are observed throughout the troposphere (see Fig.4 in the Appendix C) and are consistent with the Southern Annular Mode (e.g. Thompson and Wallace, 2000) in which geopotential anomalies of opposite sign are observed between the Antarctica and the mid-latitudes around 45°S.

Composite anomalies associated with the annual frequency of cluster3 (JFM) display strong patterns (Fig.5.1b) consistent with the anomalies in the composite of events for this cluster. The anomalies are also consistent with a wavenumber-3 pattern; however over the South Pacific, the anomalies show two centres with significant values over both the eastern and western sides. Negative anomalies are observed in the subtropical and tropical belts over the Pacific, eastern Indian Ocean and South America. These patterns have been linked to La Niña (e.g. Reason et al., 2000). Over central and western southern Africa, a significant low, not well depicted in the composite of events, is observed. The low is observed near the surface, but it displays the strongest values at 700 hPa level, and at upper levels it is absent (see Fig.5 in the Appendix C). This pattern suggests a deep Angola low, the source region of the TTT over southern Africa (e.g. Reason et al., 2006a), and it has been associated with positive anomalies of rainfall over southern Africa (e.g. Reason and Jagadheesha, 2005). However, the core region of the low is located to the west of the maxima rainfall anomalies (compare Fig 4.5b upper right panel and Fig. 5.1b), suggesting that it is not only the air mass uplift over southern Africa that contributes to the observed anomalies of rainfall. Low level convergence of winds and of moisture over eastern southern Africa associated with a stronger South Indian Ocean anticyclone and with a deep Angola low may also play an important role (see e.g. Fig. 5.2 and Fig. 10 in the Appendix C).

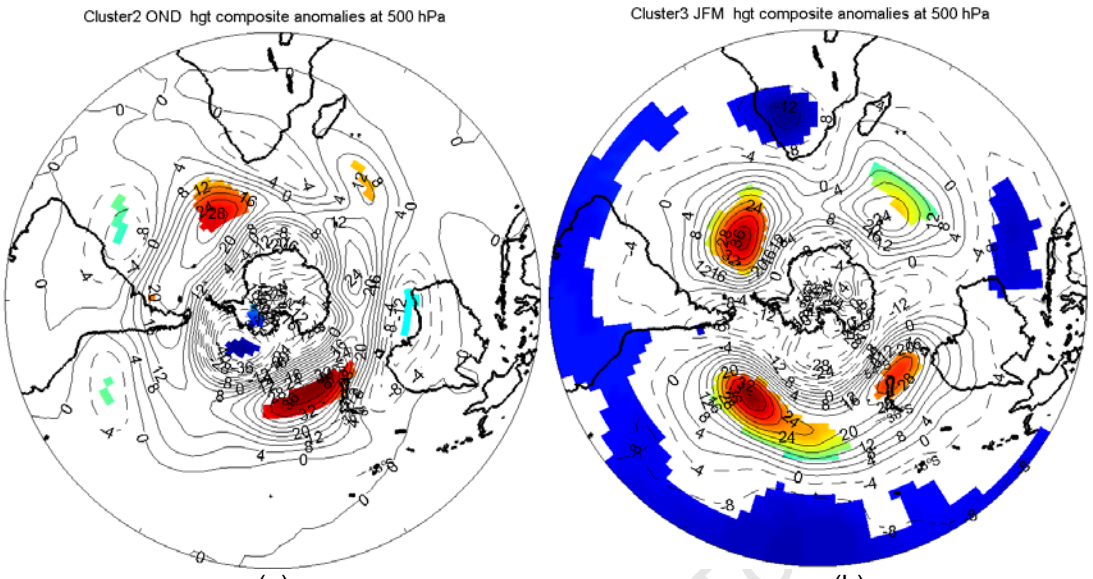

(a) (b)

Fig.5.1 Composites of geopotential height (contour interval is 4 m) anomalies at 500 hPa for the annual frequencies of (a) cluster2 (OND) and (b) cluster3 (JFM). Shaded areas show values significant at 5% level.

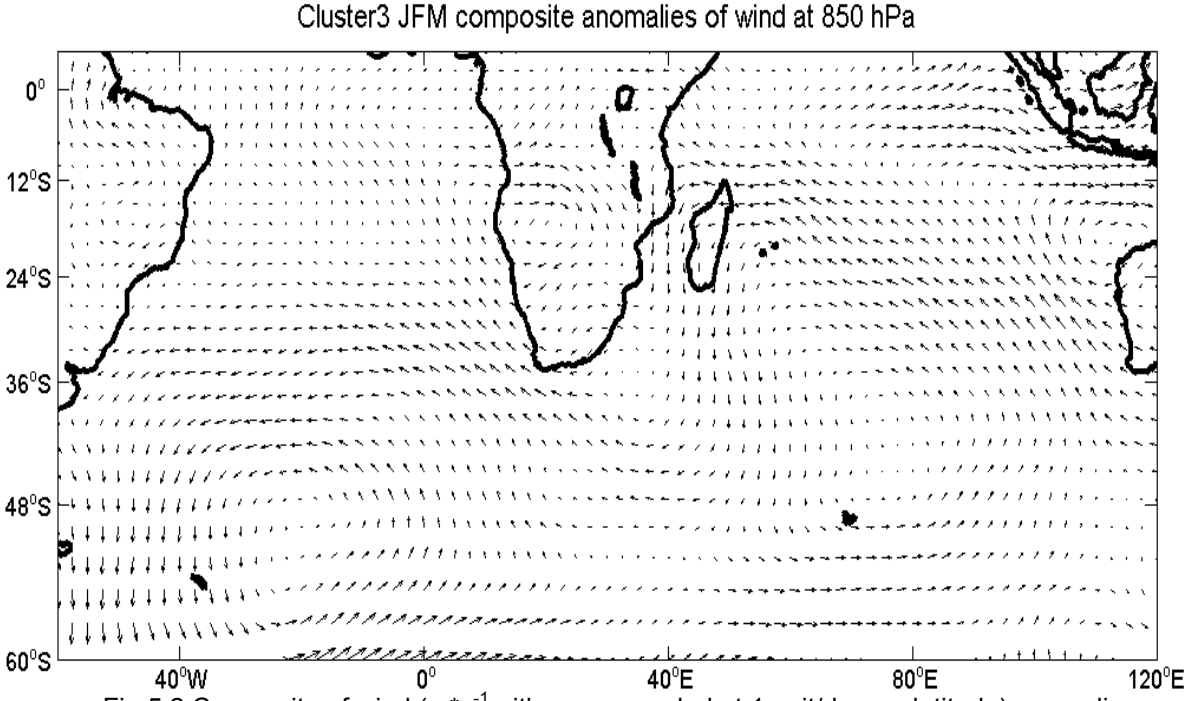

Fig.5.2 Composite of wind ($m*s^{-1}$ with arrows scaled at 1 unit/degree latitude) anomalies at 850 hPa associated with annual frequency of cluster3 (JFM)

The composites of geopotential height anomalies for cluster2 (JFM) are dominated by zonally oriented pattern of positive anomalies over the entire

tropical and subtropical belts (Fig.5.3). These anomalies are consistent with those of the composite of the events (Fig.4.11) and also in general consistent with El Niño patterns (see e.g. Reason et al. 2000). However, the trough over the central South Indian Ocean observed in the composite of events is shallow and weaker in the composites annual frequency of cluster2. Moreover, the Walker Cell type anomalies over tropical Indian Ocean observed in the composite of events are not apparent in the composites of the annual frequency of cluster2 (compare Fig. 5 and Fig. 11 in the Appendixes B and C respectively). On the other hand, the anomalies of geopotential height over southern Africa are stronger in the composite of annual frequency of occurrence of cluster2 as compared to the composite of events. At 700 hPa, a closed ridge is observed (Fig.6 in the Appendix C) over southern Africa. These differences between the patterns in the composite of events and in the composite of annual frequency of cluster2 may suggest that different forcing mechanisms are involved in the annual composites. Also, it appears from the comparison between Figure 4.11 and Figure 5.3 that cluster2 captures mostly aspects of the atmospheric circulation associated with ENSO over the ocean. Note that El Niño has been associated with positive anomalies of pressure throughout the troposphere over southern Africa (e.g. Lindesay, 1988b; Richard et al., 2000; Mulenga et al., 2003). Thus, the composites of the geopotential height for the annual frequency of cluster2 may show patterns over southern Africa that in some years may occur simultaneously with those over the Ocean, but not captured due to limitations of the statistical method.

Composites of wind anomalies at 850 hPa show convergence over tropical South Indian Ocean (apparently associated with the position of the SICZ there) and divergence over southern Africa (Fig.5.4). Low level convergence over the northeast of Madagascar may represent weakening of the South Indian Ocean trade winds, and consequently weaken the moisture fluxes from tropical Indian Ocean to southern Africa. Increased subsidence (associated with a low level ridge over southern Africa) and reduced influx of moisture contributes to the

negative anomalies of rainfall over central and eastern southern Africa. On the other hand, onshore winds and moisture from the Mozambique Channel and convergent northeast monsoons from the equatorial Indian Ocean may contribute to the positive anomalies of rainfall over northern Mozambique/Tanzania (see Fig 4.5b upper central panel).

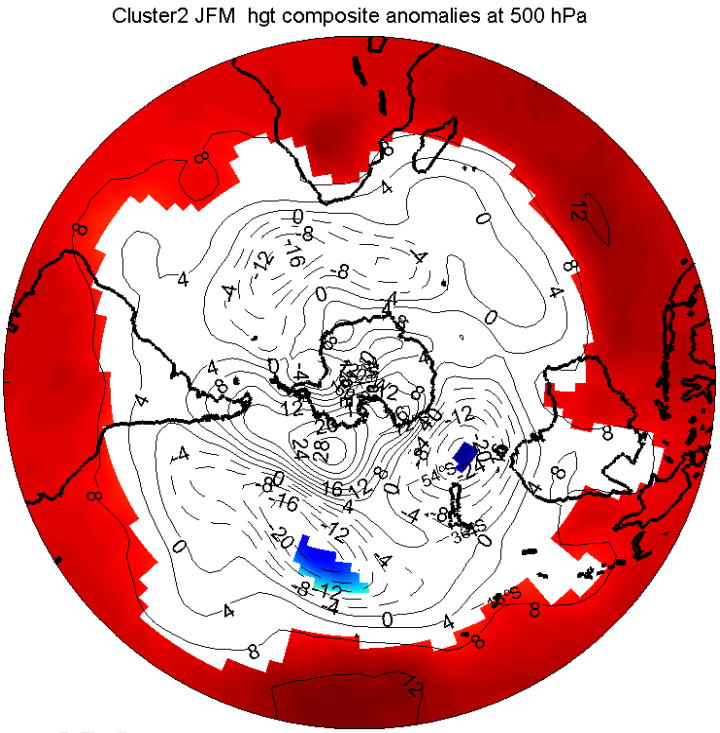

Fig. 5.3 Same as Fig. 5.1 except for cluster2 (JFM).

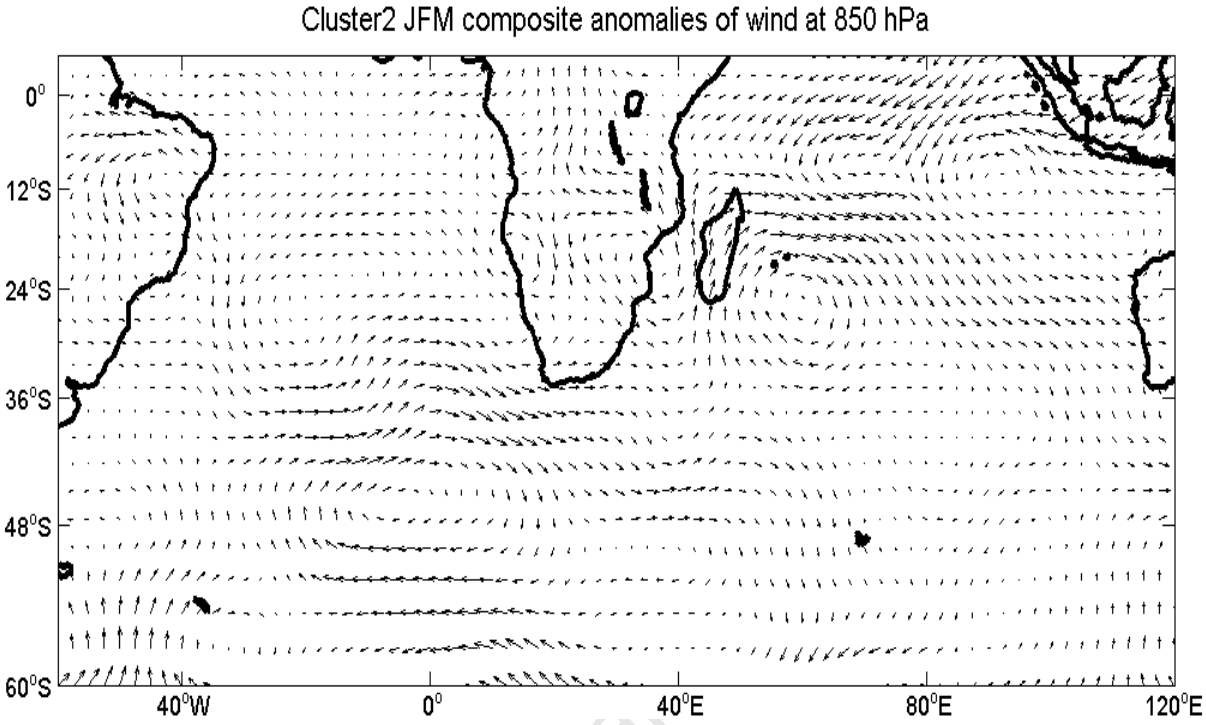

Fig. 5.4 Same as Fig. 5.2 except for cluster2 (JFM).

5.2 Relationship between clusters and ENSO

ENSO is the dominant global climate mode and it has been shown to play a significant role in summer rainfall variability over southern Africa (e.g. Lindesay, 1988a; Mason and Jury, 1997; Reason et al., 2000). The objective here is to explore links between ENSO and the inter-annual variability of the clusters selected in Chapter 4. Correlations between the Niño 3.4 region anomaly index and the annual frequency of each cluster were also analysed. Correlation coefficients are shown in Table 4.2 (Chapter 4). All the three clusters analysed in this chapter displayed significant correlations with ENSO at different lags (with Niño 3.4 index leading). Here we try to isolate atmospheric patterns, either associated with or independent of ENSO, using regression analyses, as explained above (section 5). This is done in order to identify the atmospheric mechanisms and also SST patterns that are linked with or independent of ENSO. Although more sophisticated approaches (e.g. Enfield and Mestas-Nuñez, 1999;

Mestas-Nuñez and Enfield, 2001) have been applied to try to remove the ENSO influence, no method is without drawbacks. In this thesis we use a simple linear method.

5.2.1 Circulation patterns independent and linked to ENSO

Figures 5.5 show the geopotential anomalies at 500 hPa for cluster2 (OND) and cluster3 (JFM) after removing the influence of ENSO.

The patterns for cluster2 (Fig. 5.5a) in OND do not show significant changes from Figure 5.1a, however the geopotential height anomalies become weaker over the SWIO on the northern and western sides of the South Indian anticyclone. This may represent a weakening of the easterly winds as the gradient is also reduced resulting in reduction of moisture fluxes to southern Africa over the SWIO.

Significant changes are observed with cluster3 in JFM after removing the influence of ENSO (compare Figure 5.5b with Figure 5.1b). For example, negative anomalies over the tropical belt and the low pressure cell over southern Africa weaken significantly (Fig. 5.5b). This is consistent with studies mentioned above showing that these patterns are linked to La Niña. However, the wavenumber-3 -4 structure with the centre over the three ocean basins remains robust and the anomalies are strengthened on the northern and western sides of the cells at the low and mid troposphere (see Fig. 13 in the Appendix C).

The two clusters (clusters2-OND and cluster3-JFM) show a positive phase of the Southern Annular Mode pattern (stronger for cluster2 than cluster3) in conjunction to the wavenumber-3 -4 structure (Thompson and Wallace, 2000).

The anomalies in the South Indian anticyclone for cluster3 (after removing the linear influence of ENSO) are stronger near the surface over the northwest side and decrease with height, while at the centre of the anticyclone, the anomalies increase with height (see Fig. 13 in the Appendix C). Strengthening the northward and westward sections of the South Indian Ocean anticyclone

would contribute to stronger easterly winds and increased moisture fluxes towards southern Africa. This mechanism has been pointed out to be important for supplying moisture to the subtropical convergence zones (e.g. Kodama, 1999), such as the SICZ of interest here.

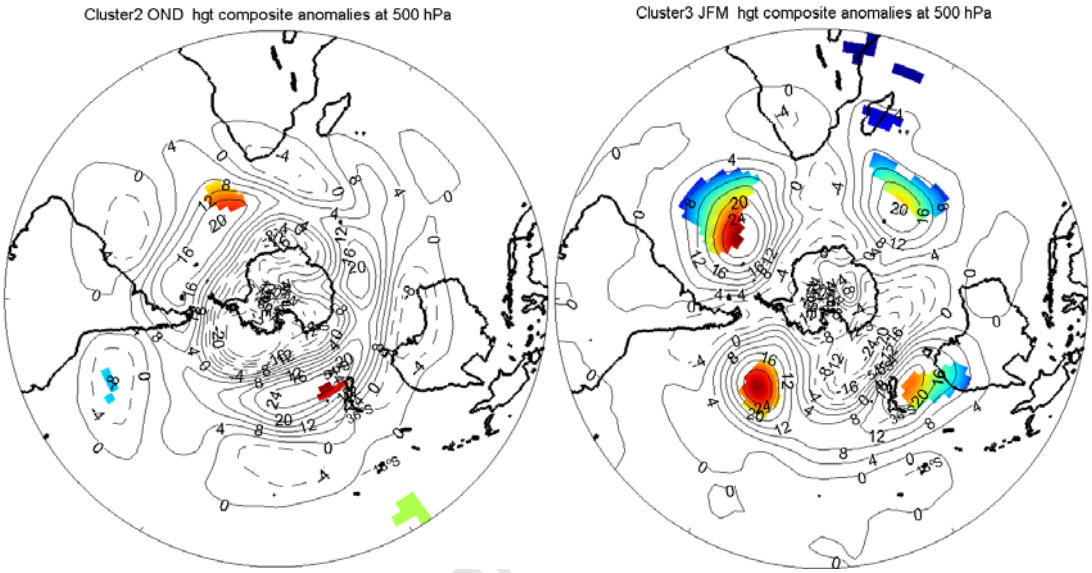

(a) (b)

Fig. 5.5 Same as Fig. 5.1 except after removing the linear influence of ENSO.

For cluster2 (JFM), no significant patterns are observed after removing the influence of ENSO particularly over the tropical and subtropical regions. This suggests that the patterns of cluster2 (Fig.5.3) are strongly linked to ENSO.

The influence of ENSO on southern Africa rainfall has been attributed to shifts in the position of the Walker Cell accompanied by shifts in the location of the main axis of cloud bands associated with TTT in the Indian Ocean/southern Africa/Atlantic Ocean sectors (see Fig.2.5 from Tyson and Preston-Whyte 2000). To explore this, we composite the zonal and vertical flow related to ENSO (data regressed against Niño 3.4 index), averaged over the band 10°S-15°S for JFM clusters. Only JFM clusters are considered because the patterns of cluster2 (OND) appear to be linked more to subtropical and temperate systems.

Composites with raw (without isolating the influence of ENSO) data are also displayed for comparison. Figures 5.6 and 5.7 show the plots for cluster3 and cluster2 respectively.

The patterns of cluster3 display upward motion over southern African longitudes and downward over the SWIO sector in both plots. These patterns are consistent with enhancement of the ascending branch of the Walker type cell over southern Africa and the descending branch over SWIO associated with La Niña years. The upward motion is stronger when raw data is considered (Fig.5.6a), while when La Niña is considered alone, the upward motion becomes weaker (Fig.5.6b). The explanation for this may lie in the strengthening of the continental convergence associated with a stronger South Indian anticyclone, which as shown above, is independent of ENSO signal. Some studies suggest that upward motion in the subtropical convergence zones is maintained by diabatic heating (e.g. Kodama, 1999; Cook, 2000). In the case of the SICZ advection of moist warm air from subtropical and tropical Indian Ocean may contribute significantly to diabatic heating and upward motion.

Cluster2 shows a reversed circulation compared to cluster3, i.e. downward motion over southern African longitudes and upward over the SWIO sector, which is also consistent with the shift in position of the Walker Cell. Anomalies over the continent are stronger when raw data is considered (Fig.5.7a), and weaker when the influence of ENSO is isolated (Fig.5.7b). The explanation for this is less clear, but appears to be linked to the enhancement of low level divergence over the continent associated with stronger negative geopotential height anomalies over the South Indian Ocean when raw data are used.

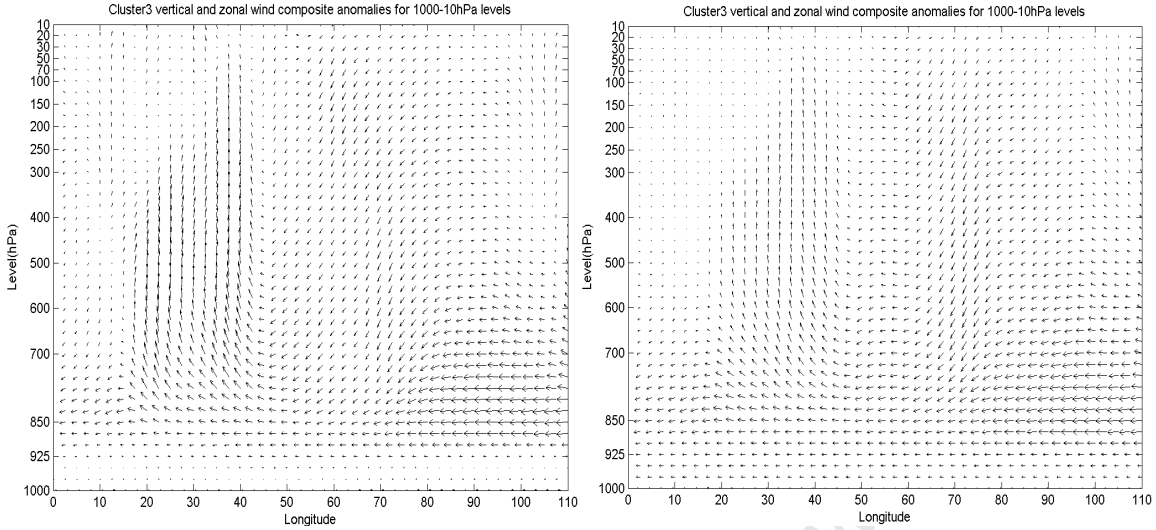

(a) (b)

Fig.5.6 Composite anomalies of zonal (m*s-1) and vertical (Pa*s-1) motion for cluster3 raw data (a) and La Niña isolated patterns (b). Arrows are scaled at 1 unit/degree latitude.

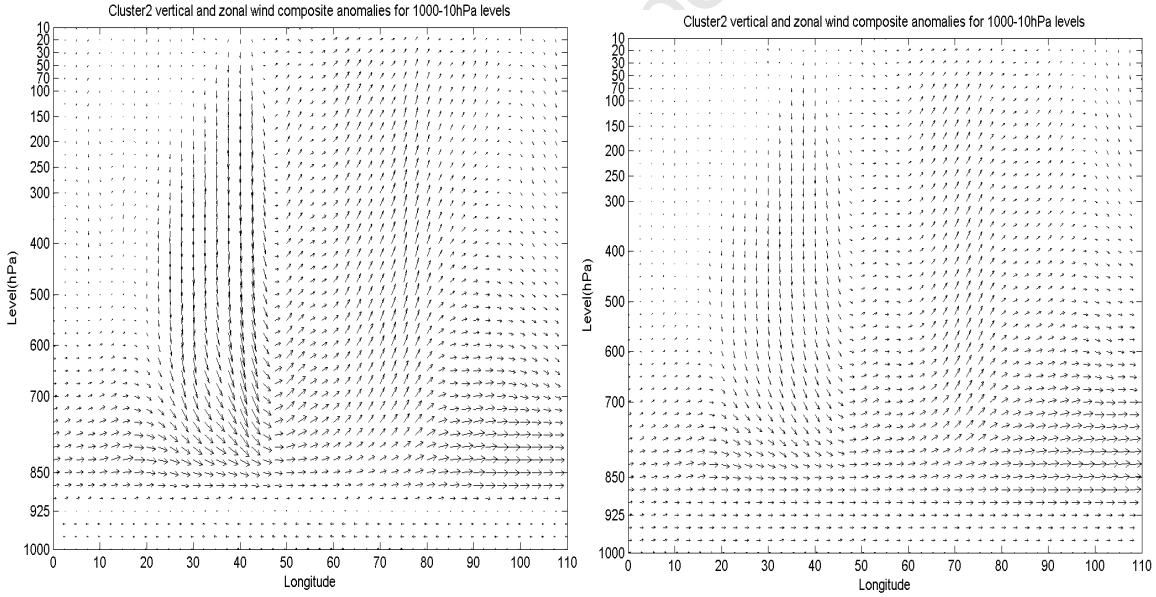

(a) (b)

Fig.5.7 Same as Fig. 5.6 except for cluster2 (JFM) raw data (a) and El Niño (b).

5.3 Relationship between inter-annual frequency of clusters and SST and links with ENSO

Relationships between rainfall over southern Africa and SST over the Indian and Atlantic Oceans have been documented in a number of studies (e.g. Walker,

1989; Rocha and Simmonds, 1997; Reason and Mulenga, 1999; Reason, 2002; Washington and Preston, 2006). As shown in these studies, relationships are stronger with Indian Ocean patterns, either linked to or independent of ENSO. Based on composite analyses, we explore which patterns are associated with the clusters analysed here, and what mechanisms are involved in forcing rainfall in the SICZ. To isolate patterns linked to ENSO, the same procedure as for the atmospheric circulation is followed. First, the Indian Ocean SSTs are regressed against the annual frequency of Niño 3.4 index, afterwards the regression values are subtracted from the raw data.

5.3.1 Composites of SST of clusters associated with wet conditions over southern Africa

SSTs linked to cluster2 (OND) show patterns of warm anomalies over the SWIO, south to southeast of Madagascar, and south of around 30°S over the South Atlantic and cool anomalies over subtropical and tropical South Indian and Atlantic Oceans. These patterns are observed at 0 and 1 month lag with SST leading (Fig. 5.8a shows anomalies at 0-month lag). They are consistent with the positive SIOD in which negative anomalies are observed over the eastern side and positive anomalies over the western side of the South Indian Ocean (Behera, and Yamagata, 2001; Reason, 2001). They are also consistent with La Niña associated SST patterns characterised by cool anomalies over central tropical and subtropical Indian Ocean (Reason et al., 2000). Both patterns have been associated with positive anomalies of rainfall over southern Africa (e.g. Reason and Mulenga, 1999; Reason, 2002; Washington and Preston, 2006). At 2 months lag (Fig. 5.8b), the warm anomalies weaken significantly in both basins. Over the South Indian Ocean, warm anomalies vanish completely at 3 months lag (July-September; Fig. 5.8c), but the cool pattern persists at up to 4 months lag, however it is not statistically significant. When the influence of ENSO is removed, no significant changes are observed.

Composite anomalies of SST linked to cluster3 in JFM (Fig.5.9a) display similar patterns to cluster2 in OND. However, the warm patterns in cluster3 are more robust over both the SWIO and South Atlantic. Also when lagged composites are considered, the patterns of anomalies described above persist up to 4-months lag (SON), although weakening from 2-months lag. Some modelling studies have suggested that both warm anomalies (e.g. Reason and Mulenga, 1999; Reason, 2002) and cool anomalies (Washington and Preston, 2006) over SWIO force the anomalies of rainfall over southern Africa. These links are explored in section 5.4.

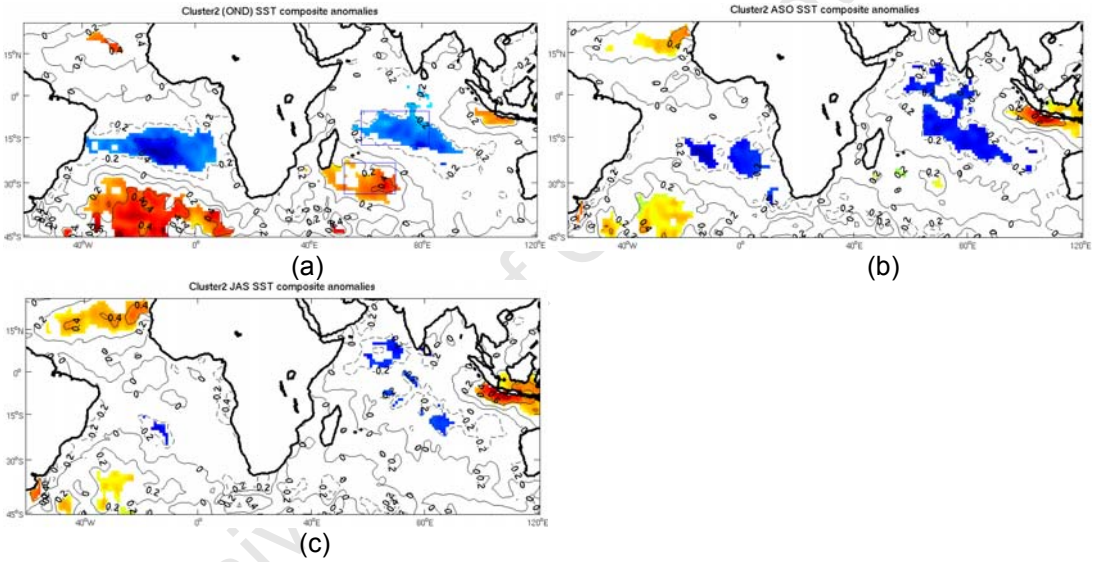

Fig.5.8 Composite anomalies of SST associated with the annual frequency of cluster2 (OND) at 0 lag (a); 2 months-lag (b) and 3 months-lag (c). Contour interval is 0.2 °C. Shaded areas are significant at 5% level. Boxes show the averaged areas for the SST index used in the correlations (see text).

When the influence of ENSO is removed by linear regression (Fig5.9b), the positive pattern over the SWIO south of Madagascar remains robust and positive anomalies over the Mozambique Channel become stronger. Note that SST in this region has been shown to correlate positively with eastern South Africa summer rainfall (Reason and Mulenga, 1999). Different from composites of cluster2 (OND), the negative pattern over central subtropical Indian Ocean weakens significantly after removing the influence of ENSO. However, in

composites of two extreme wet years (1974 and 1976) for JFM, Washington and Preston (2006) found a similar pattern to persist even after regressing away the Southern Oscillation index. In the South Atlantic, both positive and negative anomalies weaken slightly.

The SIOD pattern observed in both composites of cluster2 (OND) cluster3 (JFM) is discussed in Faucheareau et al. (2003) and Hermes and Reason (2005). These studies suggest that this SST mode and a similar one in the South Atlantic Ocean are mainly forced by large scale atmospheric circulation associated with Southern Hemisphere planetary waves (wavenumber-3 -4 patterns). Hermes and Reason (2005) indicate that the anomalies in the warm pole are stronger in JFM for both Indian and Atlantic dipole modes. Note here that the warm poles in both basins are stronger in JFM (Fig. 5.9a) as compared to OND (Fig.5.8a).

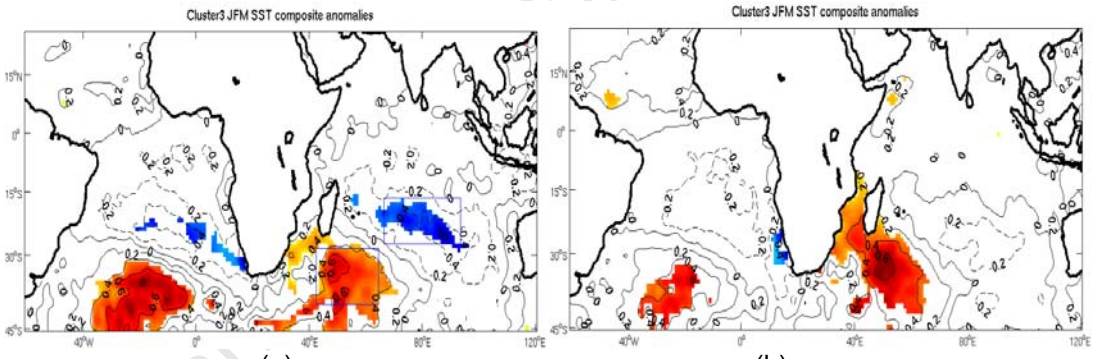

(a) (b)

Fig.5.9 Same as Fig. 5.8a except for cluster3 (JFM) at 0 month-lag (a) and at 0-lag but with the linear influence of ENSO removed (b).

5.3.2 Composites of SST of the cluster associated with dry conditions over southern Africa

In this section, SST patterns associated with cluster2 are analysed following the same method as previously. The patterns of cluster2 show warm and significant anomalies over the tropical and subtropical South Indian Ocean and cool anomalies over the SWIO and mid-latitudes in the South Atlantic (Fig.5.10a). Lagged composites (with SST leading) display persistent warm

anomalies over the subtropical Indian Ocean for periods longer than three month lag. Figure 5.10b shows the composite anomalies at 3 months lag (OND anomalies). This pattern is consistent with the negative SIOD in which positive anomalies are observed over the eastern side and negative over western side of the South Indian Ocean. However, the warm pole is stronger while the cool pole does not show significant patterns. The pattern is also consistent with El Niño associated anomalies in which warm SST anomalies are observed over the bulk of the tropical and subtropical Indian Ocean (Reason et al., 2000; Mo, 2000). As already indicated, both SST patterns have been associated with dry conditions over subtropical southern Africa (e.g. Jury et al., 1996; Reason, 2002). At 0-month lag, when the influence of ENSO is removed, the anomalies become insignificant in both the Indian and Atlantic Oceans. However at 3-month lag, a negative SIOD is still apparent (Fig. 5.10c).

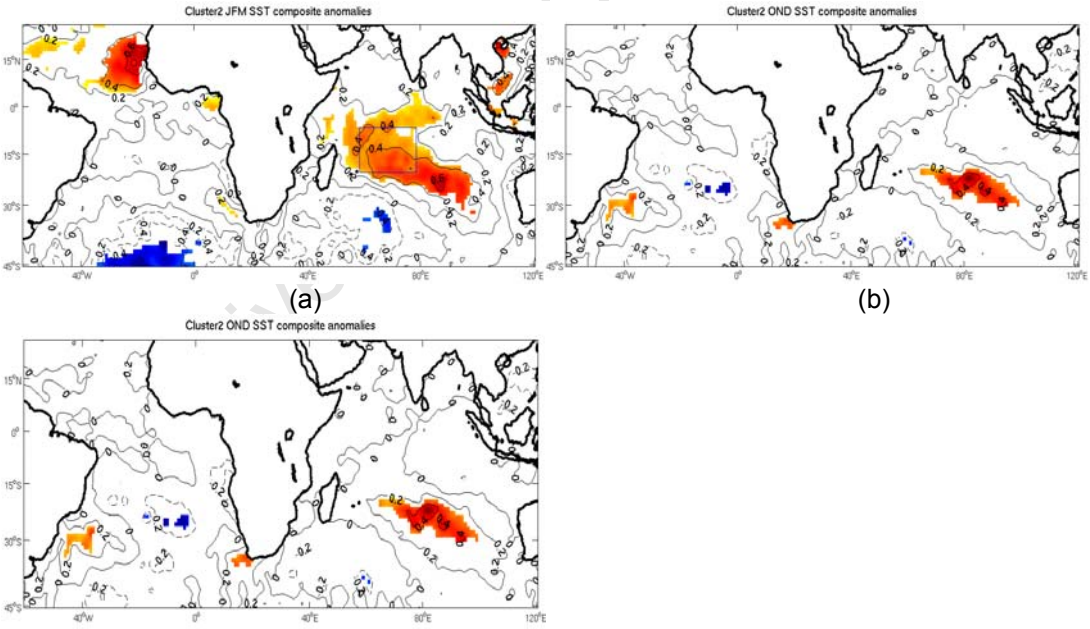

(a) (b)

(c)

Fig.5.10 Same as Fig. 5.8a except for cluster2 (JFM) at 0-lag (a) at 3-months lag (b) and for 3-months lag with the linear influence of ENSO removed(c).

5.4 Relationship between convective activity and rainfall over southern Africa with SST patterns over Indian Ocean

Here we analyse the relationships between the patterns of SST over the Indian Ocean and the annual frequencies of cluster2 (OND) and cluster3 (JFM). The aim is to explore which patterns of SST show statistically significant relationships with convective activity and rainfall over southern Africa, with specific relevance to Mozambique. This is done by examination of correlations between time series of SST versus OLR and rainfall averaged over eastern southern Africa. The region considered over land is shown in Figure 4.5b, upper right panel. Note that all the three clusters discussed here display the strongest patterns of both rainfall and OLR over that region. The averaged boxes for SST anomalies are shown in Figures 5.8a, 5.9a and 5.10a. OLR and rainfall are fixed in time while SSTs are considered for different seasons.

Correlations of annual frequency of cluster2 (OND) with SST are in general weak, except between the cool pole and rainfall at 1 and 0-month lag (Table 5.2). Cool anomalies over the tropical SWIO linked or independent of ENSO have been shown to force positive anomalies of rainfall over the bulk of southern Africa (see e.g. Washington and Preston, 2006).

Table 5.2 Correlations of time series of SST (warm and cold poles) with annual frequencies of OLR and rainfall associated with cluster2 (OND). Bold number indicate values significant at p<0.05

Season (SST)	OLR/warm		OLR/cool		Rainfall/warm		Rainfall/cool	
	r	p	r	p	r	p	r	p
JJA	-0.18	0.4	0.11	0.61	0.14	0.5	-0.07	0.75
JAS	-0.05	0.82	0.15	0.47	0.04	0.83	-0.14	0.49
ASO	-0.07	0.75	0.12	0.57	0.1	0.6	-0.21	0.31
SON	0.07	0.75	0.16	0.45	0.12	0.58	-0.35	0.09
OND	-0.04	0.86	0.30	0.14	0.16	0.45	**-0.47**	0.02

For cluster3 (JFM), the warm pole displays strong and significant correlations (at p<0.05) from 2-months lag (NDJ) with both OLR and rainfall

(Table 5.3). When the lag is increased, the correlations weaken significantly and at 4-months lag no correlations are observed. The warm pole over the subtropical SWIO has been shown to force positive anomalies of rainfall over subtropical southern Africa (e.g. Reason, 2002). Correlations with the cool pole for cluster3 (JFM) are observed at all lags considered here, however, they are not stable. For example, at 4-months lag (SON) correlations are significant (at p≤0.1), and they weaken between 3 and 2-months lag, at 1-month lag the correlations become again significant (at p≤0.1), and they display strongest values at 0-month lag (significant at p≤0.05). The reason for these changes in the significance of correlation is not clear. However, similar behaviour is observed in the composites of ENSO related rainfall in Nicholson and Kim (1997), for similar regions (Fig. 3 regions 7 and 9 – these regions are basically confined to central and southern Mozambique) as that considered for the time series of rainfall and OLR used to correlate with SST here. For example in region 9 (which covers central and southern Mozambique) the rainfall response to ENSO forcing is strong between October and November, it weakens between December and January and it strengthen again between February and April (see Fig. 4 in Nicholson and Kim, 1997). This result may indicate that the correlations observed here, between rainfall/OLR and the SST anomalies in the Indian Ocean are linked to La Niña forcing.

Table 5.3 Correlations of time series of SST (warm and cold poles) with the annual frequencies of OLR and rainfall associated with cluster3 (JFM). Bold number indicate values significant at p<0.05

Season (SST)	OLR/warm		OLR/cool		Rainfall/warm		Rainfall/cool	
	r	p	r	p	r	p	r	p
SON	0.0	0.98	0.34	0.1	0.0	0.99	-0.38	0.06
OND	-0.28	0.18	0.25	0.23	0.25	0.22	-0.31	0.14
NDJ	**-0.52**	0.01	0.26	0.22	**0.48**	0.02	-0.29	0.15
DJF	**-0.53**	0.006	0.37	0.07	**0.47**	0.02	-0.37	0.07
JFM	**-0.51**	0.01	**0.41**	0.04	**0.43**	0.03	**-0.40**	0.05

For cluster2 (JFM) only warm anomalies are considered because cool anomalies are in general weak (see Fig. 5.10a). Correlations of SST with the annual frequency of rainfall are negative and with the annual frequency of OLR are positive, and consistent increase of the correlation coefficients, as the lag decreases, is observed for both rainfall and OLR (Table 5.4). The strongest correlations are observed at 1 and 0-month lag (significant at $p<0.05$). At 2-months lag, the correlations weaken, but significant (at $p<0.1$) values are observed for both OLR and rainfall. Correlations are still observed at 3 and 4-months lags, but in general they are weak.

Table 5.4 Correlations of time series of SST (warm pole) with the annual frequencies of OLR and rainfall associated with cluster2 (JFM). Bold number indicate values significant at $p<0.05$

Season (SST)	OLR/warm		Rainfall/warm	
	r	p	r	p
SON	0.28	0.18	-0.27	0.18
OND	0.3	0.14	-0.31	0.13
NDJ	0.37	0.07	-0.38	0.06
DJF	**0.43**	0.03	**-0.44**	0.03
JFM	**0.42**	0.04	**-0.47**	0.02

5.5 Relationship between SST patterns over Indian Ocean and latent heat fluxes

In this section, latent heat fluxes from NCEP reanalysis are composited in order to explore possible physical mechanisms linking SST over the South Indian Ocean and atmospheric circulation associated with the anomalies of rainfall analysed above. Figure 5.11 shows the composite anomalies for the three clusters.

The composite of cluster2 (OND) shows significant and positive anomalies of net latent heat flux over the tropical SWIO, to the northeast of Madagascar (Fig. 5.11a). In the same region, negative anomalies of SST are observed (see

Fig. 5.8a). Low level anticyclonic wind anomalies over the same region (see Fig. 2a in the Appendix B) appear to be responsible for positive anomalies of latent heat flux. Easterly winds are enhanced over the equatorial and tropical South Indian Ocean, thus apparently contributing to the significant evaporation and cooling over that region. Over the warm pole, southeast of Madagascar, anomalies are weak suggesting that fluxes of latent heat do not play a significant role in the observed anomalies of SST.

The composite of cluster3 (JFM) shows strong positive anomalies over the southeast Indian Ocean, off Australia and also over the tropical SWIO, east of Madagascar (Fig. 5.11b). These anomalies are consistent with strong easterly anomalies of wind over the same regions (see Fig. 5.2) and suggest that increase in latent heat flux play a role in the cool pole of SST associated with cluster3 (see Fig. 5.9a). Over the Agulhas region and on the western coast of South Africa, significant positive anomalies in the net latent heat fluxes, are also observed. SST anomalies in the Agulhas region are weak, but in the western coast of South Africa negative anomalies prevail (see Fig. 5.9). Divergent flow on the western side of the trough located to the southwest of Madagascar (over the Agulhas region) and the strengthening of the south-easterlies on the western coast of South Africa (see Fig. 5.2) may be responsible for the positive anomalies of net latent heat fluxes observed over these regions. Strong positive anomalies of latent heat fluxes are also observed in central southern Africa, apparently linked to a surplus of moisture over the region. Over the warm pole in the SWIO, the anomalies of net latent heat flux are in general weak and with mixed sign. Positive (negative) anomalies are observed over the western (eastern) side of the SST pole. Negative anomalies of latent heat flux, indicate that the ocean is gaining heat, and this suggests atmospheric forcing of the SST pole (see e.g. Zhang and McPhaden, 1995; Hermes and Reason, 2005).

The composite of net latent heat flux for cluster2 (JFM) shows positive anomalies over the tropical Indian Ocean and over the SWIO (Fig. 5.11 c). These anomalies are located in regions of positive anomalies of SST (see Fig. 5.10a).

However, over the region with maximum positive anomalies of SST, southeast of Madagascar, the anomalies of net latent heat flux are weak. Note that over these anomalies of SST, a trough is observed (see 4.11 and Fig. 5 in the Appendix B). A strip of negative anomalies of net latent heat flux is observed, extending westward from the eastern South Indian Ocean, off Australia. These anomalies are consistent with the weakening of the easterly winds there, as suggested by the westerly anomalies of wind (see Fig. 5.4) associated with cluster2.

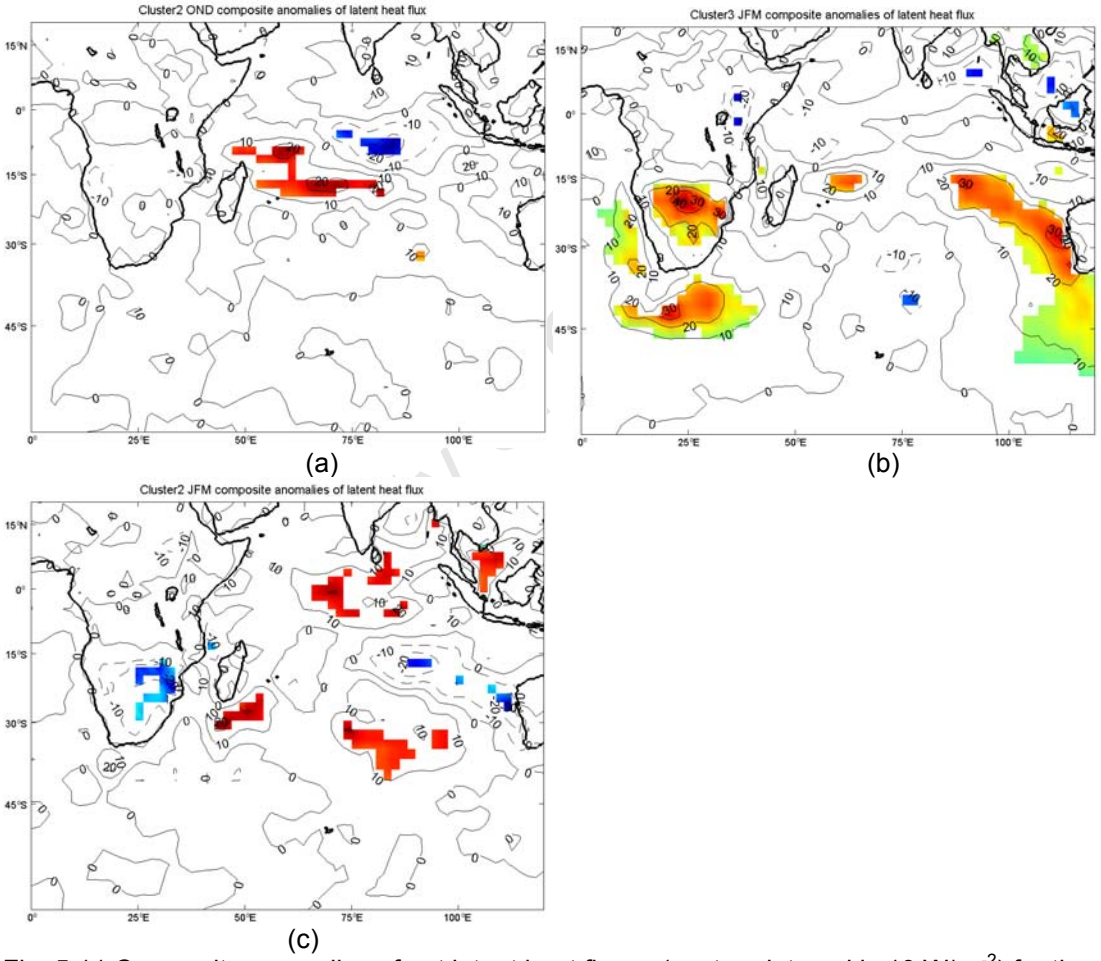

Fig. 5.11 Composite anomalies of net latent heat fluxes (contour interval is 10 W*m^{-2}) for the annual frequency of cluster2 in OND (a), cluster3 in JFM (b) and cluster2 in JFM (c). Positive values indicate upward fluxes.

5.6 Summary

In this Chapter, we analysed the inter-annual variability of the clusters and their atmospheric circulation, links with ENSO and SST over the Indian Ocean.

Composites of geopotential height for years when cluster2 (OND) displays a high frequency suggest that both anticyclonic ridging between the Atlantic and Indian Ocean south of South Africa and South Indian Ocean Anticyclone anomalies play an important role in the early summer (OND) atmospheric circulation associated with the TTT. Positive rainfall anomalies over central Mozambique (shown in Fig.4.5a middle panel) appear to be associated with strengthened anticyclonic circulation, north of Madagascar that contributes to low level moisture fluxes towards north and central Mozambique (see Fig.8 in the Appendix C). The interaction between the onshore fluxes on the eastern margins of the ridging anticyclone and a ridge over tropical southern Africa (see Fig. 7b in the Appendix C) appears to enhance the moisture fluxes towards subtropical southern Africa (shown in Fig. 8 in the Appendix C), that apparently contributes to the observed anomalies of rainfall over southern Mozambique (see Fig.4.5a middle panel).

Correlation between the annual frequency of cluster2 (OND) and the Niño 3.4 index, shows significant and negative coefficients at different time lags (from 5-month lag to 0-month lag). It appears from the analyses of the geopotential height that links between the inter-annual variability of the TTT over southern Africa and ENSO are associated with anomalous longitudinal and latitudinal shifts and also the strength of the South Indian Ocean anticyclone. During La Niña years, the South Indian Ocean is shifted or stretched north-westward. These shifts contribute to stronger divergence to the north over the tropical western Indian Ocean and tropical eastern Africa, which in turn supports the moisture convergence over the subtropical southern Africa/SWIO. This result may also explain some dipole patterns of summer rainfall between northeast and

south over southern Africa shown in a number of studies (e.g. Jury, 1992; Todd and Washington, 1999; Cook, 2000).

Composites of geopotential height for years when cluster3 (JFM) displays high frequency show that this cluster has strong influence on the annual variability of the circulation of the late summer (JFM). The circulation mechanisms associated with this cluster involve both La Niña and mid-latitude waves. La Niña's influence is associated with enhancement of low pressure over southern Africa (i.e. stronger than average continental heat low), which in turn contributes to stronger convergence and uplift over the subcontinent. Also, it appears that La Niña is associated with enhancement of the pressure gradient between subtropical and tropical South Indian Ocean. The mid-latitude waves appear to be associated with two important mechanisms displayed in Figure 5.5b (see also Fig. 13 in the Appendix C), both favouring the convergence and development of cloud bands over southern Africa, namely:

1. The strengthening of the easterly winds over the northern and western margins of the South Indian Ocean anticyclone, consequently strengthening the convergence of moisture towards southern Africa.
2. The presence of a trough extending from southern Africa towards the polar region.

These results are consistent with the strong correlations between an atmospheric index (BMI) of Rocha and Simmonds (1997) and rainfall over south eastern Africa, mentioned in Chapter 2. As indicated above, they suggest that the BMI index is indicative of the changes in pressure over the SWIO and changes in the position of the mid-latitude trough over the mid-latitudes. Both the mid-latitude trough and anomalies in the South Indian Ocean anticyclone are shown here, apparently linked to the Southern Hemisphere wavenumber-3 or -4 pattern (see Fig. 5.5b and Fig. 9 in the Appendix C). The results are also consistent with the schematic representation of the cloud bands during wet conditions shown in Figure 2.6 from Tyson and Preston-Whyte (2000), which are the main rain

producing systems over southern and central Mozambique (e.g. Washington and Todd, 1999).

In the composite of cluster3 events, a circulation anomaly reminiscent of a Walker type cell was observed suggesting in some La Niña years forcing mechanisms associated with these anomalies may be important on causing low level divergence over the regions to the north of Madagascar. Although not apparent in the composites of annual frequency, anticylonic ridging to the south of South Africa between the Atlantic and Indian Oceans, was well depicted in the composite of events, suggesting that it may also play some role in strengthening the SICZ in some years, particularly the oceanic extension.

The SST anomalies in the above described atmospheric circulation patterns appear to play some role when the anomalies are located over the tropical regions, particularly in the late summer (JFM). At mid-latitudes, the role of SST in forcing the atmospheric circulation patterns analysed here is not clear. Composites of SST over the Indian Ocean associated with the two clusters display significant anomalies reminiscent of positive SIOD and La Niña patterns, which have indeed been associated with increased rainfall over southern Africa (e.g. Rocha and Simmonds, 1997, Reason and Mulenga, 1999; Reason, 2001 and 2002; Jury et al., 2004). Also, correlations between time series of SST averaged over boxes representing warm and cool poles with time series of rainfall and OLR averaged over land area show significant values, particularly with cluster3 (JFM). Note that, both Fauchereau et al. (2003) and Hermes and Reason (2005) studies argue that the SST dipole patterns are mainly responding to atmospheric forcing rather than forcing the atmosphere.

The links between the positive SIOD and rainfall associated with SICZ, discussed above, may be a result of both responding to the same atmospheric forcing. The analyses presented here suggest this scenario. For example, Cai and Watterson (2002) argue that the 500 hPa modes can be generated by atmospheric internal dynamics alone, and that ocean dynamics, air-sea interactions, and ENSO forcing are not essential to generate them. In the

analyses above, these modes appear to play important roles in the inter-annual variability of the SICZ. As already indicated above, a wavenumber-3 or -4 pattern apparently superimposed on the Southern Annular Mode appear to be responsible for the observed positive anomalies of geopotential height in the South Indian Ocean anticyclone and also for the position of the mid-latitude trough.

A westward shift (relative to its mean summer position) and strengthening of the South Indian anticyclone results in significant convergence of moisture over southern Africa, which is the apparent primary forcing of the SICZ over southern Africa. As indicated above, some studies have also suggested these mechanisms as responsible for the generation and strengthening of the subtropical convergence zones over the Southern Hemisphere (e.g. Lenterss and Cook, 1995; Kodama, 1999; Cook, 2000). Southern Hemisphere planetary waves (wavenumber-3 or 4 pattern), have also been implicated in the generation of the SIOD (e.g. Fauchereau et al. 2003, Hermes and Reason, 2005). Hermes and Reason (2005) argue that latent heat fluxes, upwelling and Ekman heat transport, that results from changes in the tropical easterlies and mid latitudes westerlies (which are in turn manifest of changes in the South Indian Ocean anticyclone) all contribute to the observed SST anomalies associated with the SIOD. Furthermore, they suggest that the changes in the South Indian Ocean anticyclone result from modulation of the wavenumber-3 or 4 in the Southern Hemisphere atmospheric circulation.

It appears from the results of the studies (e.g. Fauchereau et al. 2003; Hermes and Reason, 2005) mentioned here and the results in this thesis, that the Southern Hemisphere planetary waves play an important role on forcing both the SICZ and the SIOD. That could be the main reason for the significant statistical relationship observed between some patterns of SST and rainfall over southern Africa, particularly the warm SST anomaly over the subtropical SWIO. The conceptual model shown in Figure 5.12 from Tyson and Preston-Whyte (2000) also suggests that both the SICZ and the anomalies of SST (particularly

warm anomalies over subtropical SWIO) are forced by shifts in the longitudinal position of the South Indian anticyclone. This figure suggests that when the South Indian anticyclone is shifted westward cool (warm) anomalies are observed over north (southeast) of Madagascar in the SWIO. Simultaneously, it shows significant inshore moisture fluxes and cloud bands typical of SICZ. The geopotential height anomalies, moisture fluxes and SST for cluster3 all agree with this conceptual model.

As already pointed out, some modelling studies (e.g. Rocha and Simmonds, 1997; Reason, 2002; Washington and Preston, 2006) have suggested physical links between the TTT and associated rainfall anomalies over southern Africa and the SST anomalies over the South Indian Ocean. Most of these studies argue that the SST force the TTT and hence anomalies of rainfall over southern Africa.

For example, Reason (2002) suggests that warm anomalies south of Madagascar force negative anomalies of surface pressure and near surface cyclonic wind anomalies. The analyses here suggest that the presence of the SICZ there results from moisture convergence on the southwest margin of the South Indian anticyclone and some contribution from the mid-latitudes. Composites of latent heat fluxes show weak anomalies that are in general negative (Fig. 5.11 a, b) over the warm pole southeast of Madagascar, where the mid-latitude trough associated with the SICZ is located. This suggests weak air sea interaction there, and negative anomalies of latent heat flux, may indicate atmospheric forcing the SST anomalies as also suggested in other studies (e.g. Fauchereau et al. 2003, Hermes and Reason, 2005).

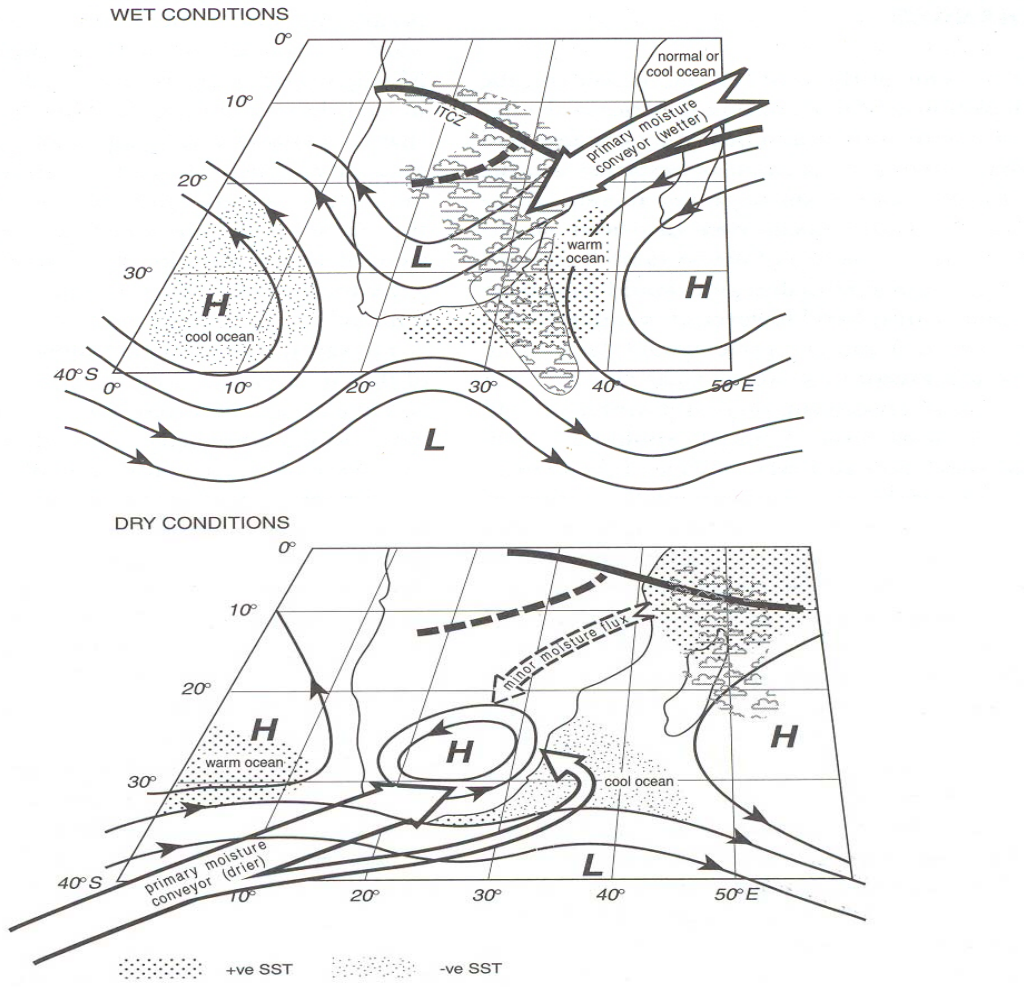

Fig. 5.12 A conceptual model to illustrate changing circulation controls, SST, moisture transport conveyors and location of tropical convection in extended wet and dry spells over southern Africa (From Tyson and Preston-Whyte, 2000).

Another example, suggesting SST forcing for the TTT over southern Africa is given in Washington and Preston (2006). They argue that cool anomalies in the Mascarene plateau region induce anomalous anticyclonic circulation which in turn drives an anomalous low-level easterly moisture flux into eastern southern Africa. The anomalies of atmospheric circulation, moisture fluxes, SST and latent heat fluxes for cluster2 in OND seems to be in agreement with their results. An anticyclonic anomaly is observed over the cool pole northeast of Madagascar (see Fig.2a in the Appendix B) over the position of the cool pole. Positive

anomalies of net latent heat fluxes there, suggest SST forcing of the low level anticyclonic anomalies, which result in low level onshore moisture fluxes (Fig. 8 in the Appendix C). However, an upper level cyclonic anomaly is observed overlying the low level anticyclone (Fig. 2c in the Appendix B). This upper level cyclonic anomaly appears to be linked to an upper level anticyclone anomaly, centred over the Saudi Arabia/Somalia region. Upper level convergence may force the low level divergence through subsidence (see e.g. Cook, 2001). The observed positive anomalies in latent heat flux may result from stronger than normal winds, which in turn may cool the SST, through evaporation and mixing (e.g. Hermes and Reason, 2005). As indicated in Chapter 2, an upwelling region has been identified over the tropical South Indian Ocean resulting from negative curl between the south-easterly trades and equatorial westerlies (Xie et al., 2002; Hermes and Reason, 2008). The strengthening of the south-easterly trades would enhance the negative curl and hence the upwelling and shallow thermocline north to northeast of Madagascar and contribute to the SST cooling.

The SST patterns for cluster3 (JFM) are similar to those for cluster2 (OND) but they are more robust. Time series of both warm and cool poles in the South Indian Ocean displayed stronger correlations with the annual frequency of anomalies of rainfall and OLR at different time lags. Over the cool pole north of Madagascar, the anomalies of atmospheric circulation and of latent heat for cluster3 (JFM) are similar to those for cluster2 (OND), however the onshore south - easterly anomalies and moisture fluxes are stronger for the JFM cluster. The difference in the strength of the easterly anomalies and moisture fluxes appear to be associated with the fact that in the early summer (OND), strong anomalies are associated with Southern Hemisphere mid-latitude westerly waves while, in the late summer (JFM), strong anomalies are associated with the anticyclones over the three oceanic basins. This result is consistent with studies showing that in the early summer westerly waves play a more important role for rainfall over southern Africa, while in the late summer easterly waves play the most important role (e.g. Tyson and Preston-Whyte 2000). Over the warm pole,

southeast of Madagascar, anomalies of latent heat fluxes suggest weak interactions between the SST and overlying atmospheric circulation. Further west, over the Agulhas Current region, positive latent heat fluxes suggest enhanced evaporation, apparently linked to onshore wind forced by the ridging anticyclones.

Significant anomalies of geopotential height associated with cluster2 are confined to tropical regions consistent with strong links between this cluster and ENSO. The eastward shift of the SICZ is not apparent in the composites of annual frequency of cluster2 (Fig. 5.3) as suggested in Figure 2.5 (lower panel). However, in the composite of events of cluster2, a diagonal trough was observed across South Indian Ocean (see Fig. 4.11), apparently not linked to middle and high latitude circulation. This trough appears to be forced by the position of maxima in SST (Fig. 5.9) east of Madagascar, and the convergence of the southward monsoon towards those warmer SST (see Fig. 6 and Fig.12 in the Appendixes B and C respectively). The forcing mechanisms discussed here are consistent with the Lindzen and Nigam (1987) model (see equations 5.1 and 5.2 below). They argue that over tropical regions in a well mixed boundary layer, atmospheric temperature gradients will reflect SST gradients, and thus, pressure gradients. The mathematical expression of the Lindzen and Nigam (1987) model is given below after some simplifications (from Von Storch and Navarra, 1999, after Neelin, 1989):

$$ku - fv + \frac{\partial \Phi}{\partial x} = 0 \qquad (5.1)$$

$$kv + fu + \frac{\partial \Phi}{\partial y} = 0 \qquad (5.2)$$

where: Φ is the geopotential; k is a coefficient of surface resistance representing friction; f is the Coriolis parameter and u and v are zonal and meridional components of velocity respectively.

The presence of a trough over the position of maximum SST anomalies (compare Fig. 5.10 and Fig. 4.11) appears to be associated with convergence of winds and also the latitudinal change of Coriolis parameter (see e.g. Fig. 6a,b in the Appendix B). Anomalies of latent heat flux at the position of the trough are positive, but weak, suggesting a modest role of evaporation in the generation or maintenance of the trough. The weakening of the trough in the annual composites of cluster2 may suggest that, only in cases of strong ENSO events is the trough present.

The analyses in this chapter suggest that the main mechanisms controlling significant wet conditions over southern Africa, particularly those associated with SICZ are apparently associated with the Southern Hemisphere planetary waves (wavenumber-3 and 4) and La Niña. SST anomalies over the Indian Ocean are also forced by the same mechanisms and their contribution to the rainfall over southern Africa, particularly associated with SICZ seems to be modest. On the other hand, dry conditions appear to be strongly linked to El Niño, particularly in the late summer (JFM). The forcing appears to be through modulation of SST over the Indian Ocean which in turn forces the convergence of the northeast monsoons to the east of Madagascar and also weakens the subtropical easterly flow. These two air masses are important sources of moisture to southern Africa during late summer (JFM) season.

Chapter Six

6. Inter-annual variability of wet spells and dry days

The aim in this chapter is to explore the relationship between the clusters and inter-annual frequency of wet spells and dry days over Mozambique. Here we use daily rainfall data for the period 1962-2004 late rain season (JFM) from 10 stations in Mozambique covering the whole of the country (see Fig. 3.1). Because of the small number of stations available with little or no missing data, it was not plausible to do any regionalization; therefore the analyses are done for each individual station. Four stations (stations number 4, 5, 6 and 10) have a few years with missing data, however given the length of the observations (44 years) the final results may not be highly affected. A wet day is defined as one when the rainfall is equal or above 1 mm and dry day as one when the rainfall is below that threshold (e.g. Usman and Reason, 2004). Wet spells are defined by consecutive wet days. However, dry spells are not defined because over southern Mozambique prolonged dry days in dry years are often observed. For example, if in a particular season no rain day with value above the threshold considered here is observed, that season would only have 1 dry spell according to definition used for the wet spell (if similar definition was used for dry spells). This definition would be misleading, as high number of dry spells are expected during dry years (see e.g. Usman and Reason, 2004).

6.1 Wet spells and dry days characteristics, variability, anomalies and links with ENSO

The three stations over southern Mozambique (stations 1-3) and over western central Mozambique (station 6) show the lowest (highest) number of rain (dry) days (Table 6.1). The three south stations also show a low number of wet spells. The wet spells are more prolonged in the central and northern stations as compared to the southern stations (Table6.2). For example, the annual average

of wet spells lasting for 4 days is below 1 (and is close to 0 for 6 days) in the three southernmost stations, but above 1 in all northernmost stations.

Table6.1 Mean (1962-2004) Mean number of wet days, wet spells and dry days for each station (JFM)

	St1	St2	St3	St4	St5	St6	St7	St8	St9	St10
Rain days	23.1	26.9	27.9	34.7	36.7	38.3	26.1	42.6	53	35.5
Wet spells	13.5	13.5	13.5	12.9	13.7	14.7	13.0	18.0	17.8	15.9
Dry days	67.3	63.5	62.3	59.7	55.0	53.6	64.4	47.5	37.3	56.9

Figure6.1 shows the annual mean of the total amount of rainfall accumulated for different lengths of wet spells. For all stations, the shorter wet spells are the most frequent; however, the most significant percentage of the total annual amount of rainfall is associated with the longer wet spells. Only three stations (namely St1, St8 and St10) show mean annual rainfall equal or above 100mm, for wet spells lasting for one day, while the others exhibit lower values. These stations show a higher number of wet spells lasting for only one day (Table 6.2). The interest in this study is the wet spells associated with the more predictable large scale weather systems, particularly that associated with clusters analysed in previous chapters, hence only wet spells lasting for more than one day are considered below. However, here we consider smaller time length of wet spells as compared with the time length of the clusters, because the analyses are for individual stations, which may only capture a smaller (as compared with gridded data) period of the full time length of a propagating system. In the southern and central stations, an average of 3 wet spells with duration of 2 days are observed per year in each JFM season (Table 6.2) which is reasonable approach for the annual average of observation for cluster3 (see Fig. 4.3 and Table1 in the Appendix A), which is associated with wet conditions over the bulk of southern Africa.

Table6.2 Mean (1962-2004) number of wet spells per length (days) for each station (JFM)

Duration of wet spells (days)	St1	St2	St3	St4	St5	St6	St7	St8	St9	St10
1	8.0	6.8	6.8	6.3	6.0	6.1	7.0	7.9	6.3	8.7
2	3.4	3.9	3.4	2.8	3.2	3.3	2.8	4.0	4.1	3.7
3	1.2	1.5	1.5	1.7	2.0	2.3	1.8	2.8	2.4	1.8
4	0.4	0.6	0.8	1.3	0.8	1.3	0.7	1.4	1.5	1.1
5	0.3	0.5	0.6	0.5	0.7	0.9	0.3	0.7	1.0	0.5
6	0.0	0.2	0.2	0.4	0.3	0.3	0.2	0.4	0.7	0.3

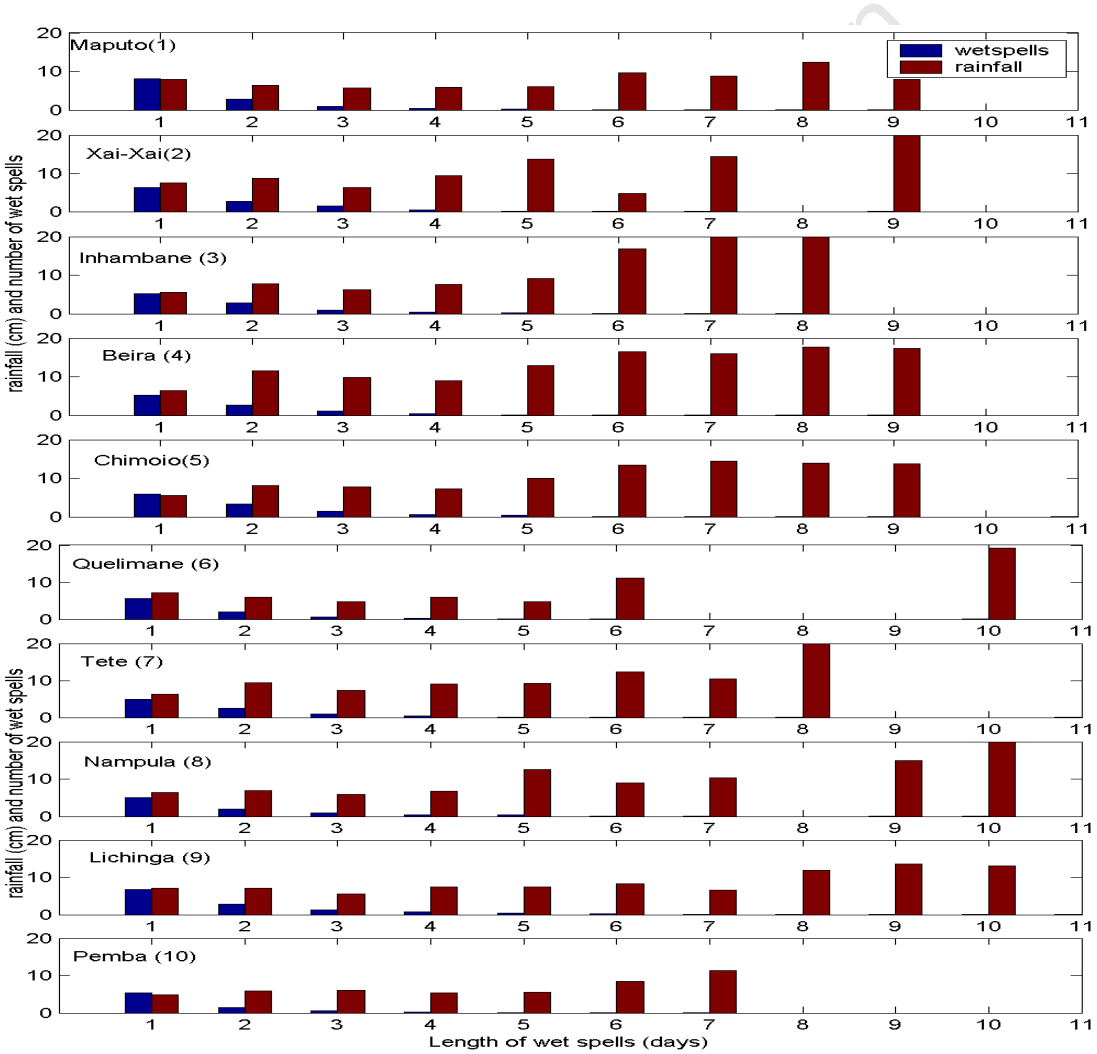

Fig. 6.1 Seasonal (JFM) mean number of wet spells for different lengths (in days) and associated mean rainfall (cm) accumulated for each length of wet spell (JFM) for the period 1962-2004.

Table 6.3 shows the correlations between anomalies of the annual frequencies of wet spells and dry days and the annual total rainfall. Both the frequencies of dry days and of wet spells exhibit significant correlations with the rainfall anomalies. Correlations are higher with the frequency of dry days than with the frequency of wet spells, because we only consider wet spells greater than one day. On the other hand, correlations between frequency of wet spells and annual rainfall anomalies are in general higher for stations over southern and central Mozambique than for stations over the northern and eastern central parts of the country. This result suggests that the number of wet spells is more important for defining anomalies of seasonal rainfall (in terms of total recorded rainfall) over southern and central regions than over northern regions.

Table6.3 Correlations of the annual frequencies of wet spells (2 or more days) and dry days and with the inter-annual anomalies of rainfall. All correlations coefficients are significant at p≤0.01

	St1	St2	St3	St4	St5	St6	St7	St8	St9	St10
Wet spells	**0.70**	**0.61**	**0.72**	**0.64**	**0.44**	**0.47**	**0.66**	**0.39**	**0.48**	**0.43**
Dry days	**-0.69**	**-0.70**	**-0.81**	**-0.70**	**-0.84**	**-0.78**	**-0.77**	**-0.70**	**-0.75**	**-0.73**

However, with the exception of the northeast station (station 10), all the other stations display a coherent correlation signal between the Niño 3.4 index and the annual frequency of wet spells and with inter-annual frequency of dry days (Table 6.4). The correlations are positive with inter-annual frequency of wet spells and negative with inter-annual frequency of dry days. Maximum coefficients of correlation are observed with the stations over southern Mozambique (stations 1-3) and St7 over central Mozambique. St5 and St9 over central and northern Mozambique display significant correlation only with the annual frequency of dry days.

The correlations here suggest that links between rainfall and ENSO over Mozambique for both El Niño and La Niña events are stronger over the southern part. This is consistent the correlations between the annual frequencies of

cluster2 and cluster3 with the Niño 3.4 index (shown in Chapter5). St4 and St6 over central Mozambique display weak correlations with ENSO for the annual frequencies of both wet and dry spells. Both stations are located over coastal region (see Fig. 2.1). St4 is located in the region where both cluster2 and cluster3 display the strongest anomalies of OLR (Fig. 4.4b) and rainfall (4.5b). However correlations between the annual frequency of wet spells and of dry days with the annual frequency of these two clusters show weak values (see Table 4.3b). On the other hand, the two stations are located in the region displaying the maximum annual precipitation over Mozambique (see Fig. 1.2). Thus, the apparent reason for the weak correlations between the annual frequencies of wet spells and dry days in these stations with ENSO and with clusters 2 and 3 may be associated with the different atmospheric systems influencing rainfall on the region where they are located. The maximum southward penetration of the ITCZ in austral summer is around the position of the two stations (see e.g. Waliser and Gautier, 1993). The region is also under influence of the SICZ as suggested from composites of OLR for cluster3 (Fig. 4.4b) and the cloud bands shown in Fig 2.5. Also the two stations are located in the region of preferred tropical cyclones and storm landfall (see e.g. Kuleshov et al., 2008).

Table 6.4. Correlation of the annual frequencies of wet spells (2 or more days) and of dry days with Niño 3.4 index for JFM. Bold numbers indicate correlations significant at p≤0.01

	St1	St2	St3	St4	St5	St6	St7	St8	St9	St10
Wet	**-0.38**	**-0.43**	**-0.45**	-0.11	-0.21	-0.15	**-0.55**	-0.24	-0.23	0.26
Dry	**0.38**	**0.48**	**0.46**	0.12	**0.42**	0.17	**0.67**	0.19	**0.54**	-0.25

The opposite signs in correlations for station10 are in agreement with the dipole anomaly pattern in rainfall between the north-eastern and south-eastern parts of southern Africa in the inter-annual variability of rainfall reported in a number of studies (e.g. Jury, 1992; Todd and Washington, 1999; Cook, 2000). Although significant correlations are observed between Niño 3.4 and the three

southernmost stations, a time series of wet spells (Fig.6.2) shows that a high frequency of wet spells is not necessarily linked to strong La Niña years. For example, years of highest frequency of wet spells (1972, 1978, 1999 and 2000) do not always coincide with strong La Niña years, since only 1999 and 2000 were La Niña. On the other hand, years classified as strong La Niña (1974, 1976, 1989) do not all show a high frequency of wet spells and one (1989) displays a below average frequency. However, station7 displays consistent above average frequency of wet spells during La Niña years. Strong El Niño years show a generally consistent high frequency of dry days (see Fig.6.3) for all stations with significant correlations with Niño 3.4 index (examples are 1973, 1983, 1992 and 1998). This suggests that over Mozambique, the El Niño signal is more consistent than is the La Niña one. As shown in Fig. 6.1, the total annual rainfall for late summer (JFM) in most of the stations analysed here is highly associated with longer time spells. Stronger correlations between ENSO and the annual frequencies of wet spells may imply stronger correlations between ENSO and the total annual rainfall.

Lagged correlations between annual frequencies of wet spells and dry days (Fig. 6.4) with the Niño 3.4 index show distinct patterns for southern, central and northern Mozambique.

For southern Mozambique, correlations between the Niño 3.4 index and annual frequency of dry days (wet spells) in the three stations (1-3) show a consistent pattern of positive (negative) correlations (Fig. 6.4 upper panel), from 9 months lag (AMJ). The correlations increase as the lags decrease and maxima values are observed from 7 months lag (JJA) and maintain about the same values up to 0 month lag (JFM).

In central Mozambique (Fig. 6.4 middle panel), station 7 displays a pattern of correlation similar to that of the three southern stations (1-3), however both frequencies of wet spells and of dry days show strongest correlations with the Niño 3.4 index in station 7. The other three stations in the central Mozambique, show in general weak correlations, however from 6 months lag (JAS) the

correlations with the Niño 3.4 index are also consistently positive (negative) with the annual frequency of dry days (wet spells).

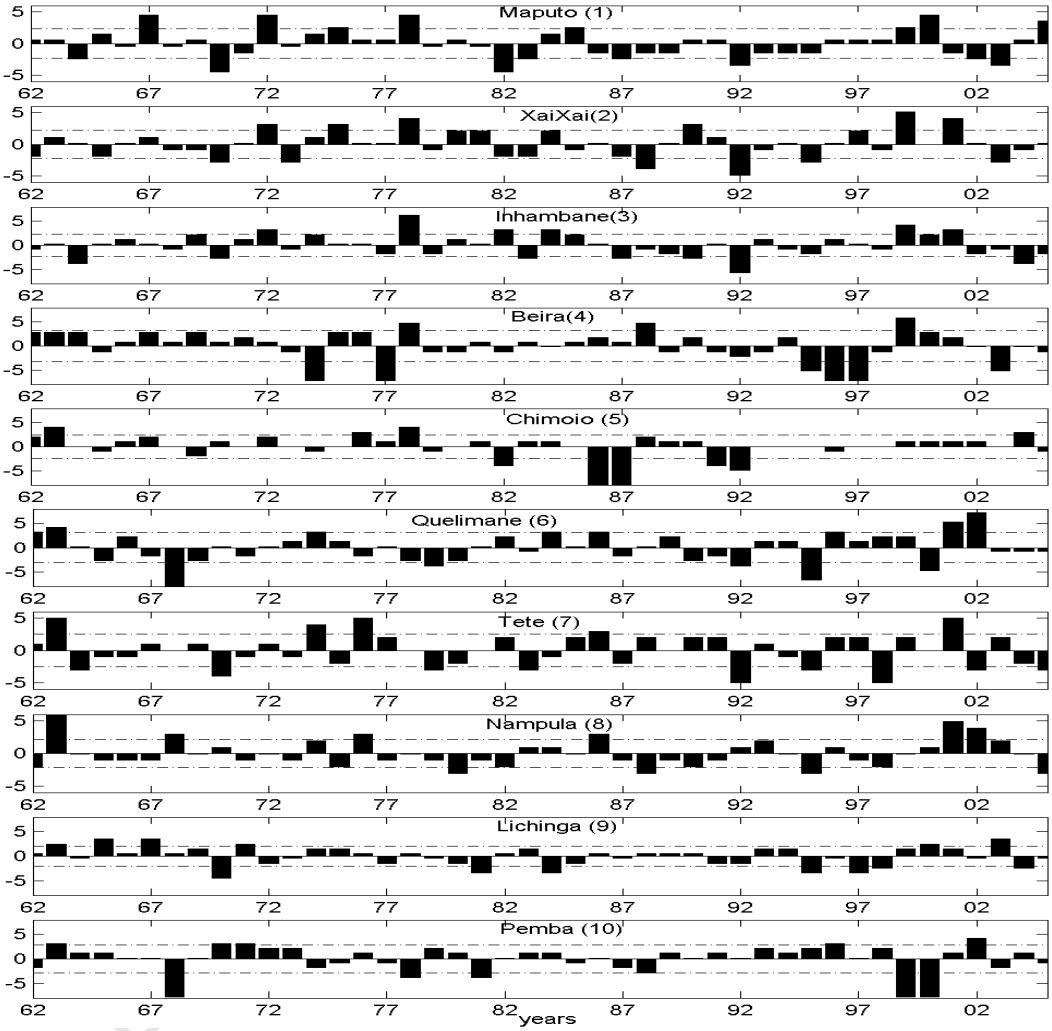

Fig. 6.2 The bars show inter-annual anomalies of number of wet spells (only wet spells lasting for more than one day are considered) and the dashed lines the standard deviations in each station.

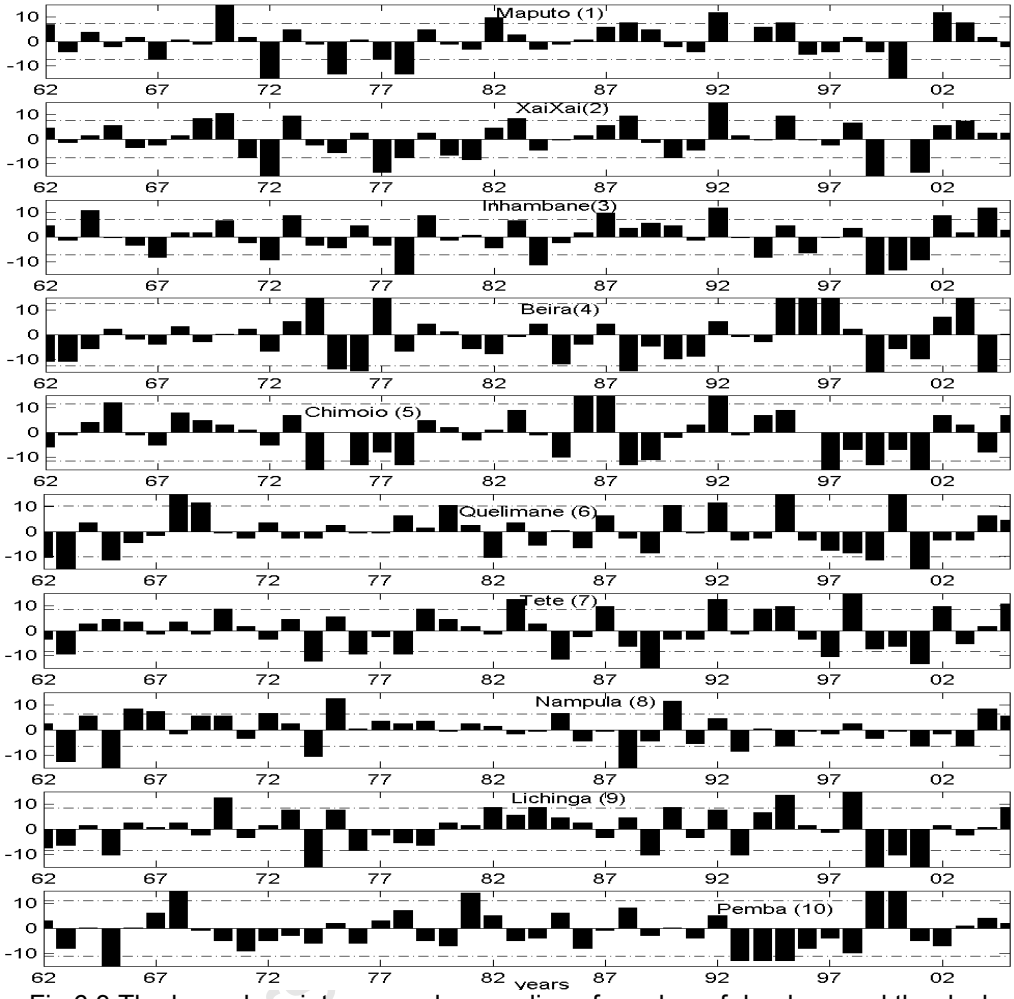

Fig.6.3 The bars show inter-annual anomalies of number of dry days and the dashed lines the standard deviations in each station.

In northern Mozambique the sign of correlations between the Niño 3.4 index and the annual frequency of dry days and wet spells is mixed (Fig. 6.4 lower panel). Stations 8 and 9 show the same sign of correlations as the southern and central stations, i.e., positive (negative) for annual frequency of dry days (wet spells). However, only station 9 displays significant positive correlations (values above 0.4 from 9 months lag), and only for the annual frequency of dry days. Station 10 displays a pattern of correlation with the Niño 3.4 index opposite to the other nine stations, i.e., positive (negative) with the annual frequencies of wet spells (dry days). However, station 9 which is located at about the same latitude does not display the same pattern of correlation. This

opposite response of rainfall to ENSO forcing for stations at about the same latitude over northern Mozambique, may result from circulation anomalies unfavourable (favourable) to rainfall in the interior (coastal) regions in the northern Mozambique (as suggested in Fig. 12 in Appendix C, for cluster2 which characterises anomaly circulations during El Niño).

During El Niño years, the northeast monsoons are diverted to the central South Indian Ocean and over southern Africa an anticyclonic circulation prevails (Fig. 12 in the Appendix C). These circulation anomalies are apparently favourable for rainfall over the coastal regions of the northeast southern Africa, because of the convergence occurring there between the moist and warm northeast monsoons and the southeast winds from the Mozambique Channel. However, weaker northeast monsoons and weaker easterly winds may not transport enough moisture to the interior regions. These results may possibly explain the opposite signs of correlations shown for station 9 and 10 and also the dipole anomalies of precipitation between northeast (north about 12° S) and the rest of southern Africa (Fig. 4.5b upper middle panel).

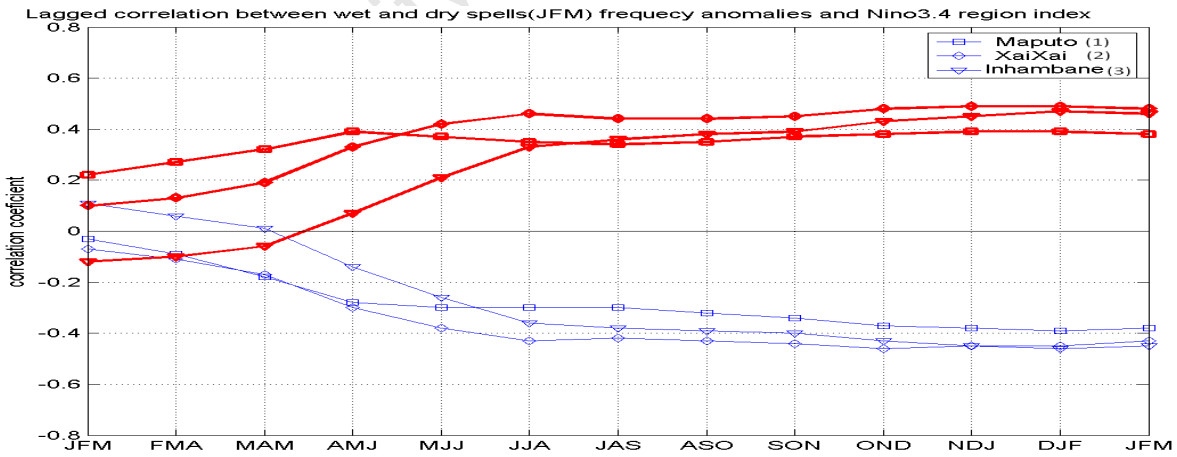

Fig.6.4 Correlations between wet spells and dry days with Niño 3.4 index, for south stations. Heavy line refers to correlation with dry days and light to wet spells.

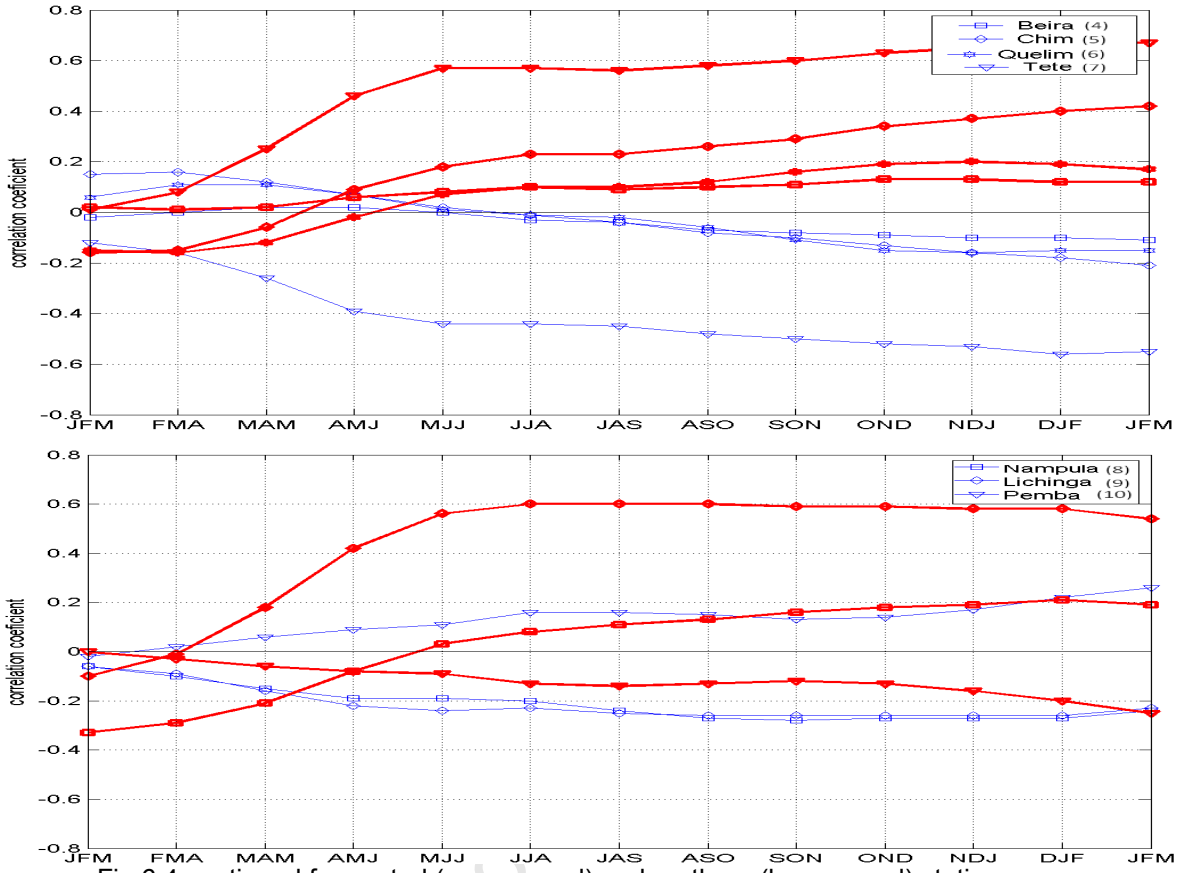

Fig.6.4 continued for central (upper panel) and northern (lower panel) stations.

Running correlations (with 10 years window) were performed to explore the stability of the correlations during the period of the analyses. The three southern stations (1-3) and one in central Mozambique (St7) show a consistent pattern of positive correlation with dry spells and negative with wet spells (Fig.6.5). However, there is a clear trend with increasing values of the coefficient of correlation for both wet and dry spells with maximum values observed in the mid 1990s. In the 1970s, a minimum in correlations is observed with some stations showing no correlation. Moreover, correlations with station 7 remain above absolute 0.4. From the mid 1990s, a decreasing tendency is also observed. However, in general the correlations between annual frequencies of wet spells and of dry days with Niño 3.4 in the four station (1-3 and 7) are consistent with the increase in sensitivity of the southern Africa rainfall to ENSO related circulation anomalies after 1970, suggested by Richard et al. (2000). The

central and northern stations show cyclical patterns with some stations changing phases for both dry and wet spells (see Fig.1in the Appendix D).

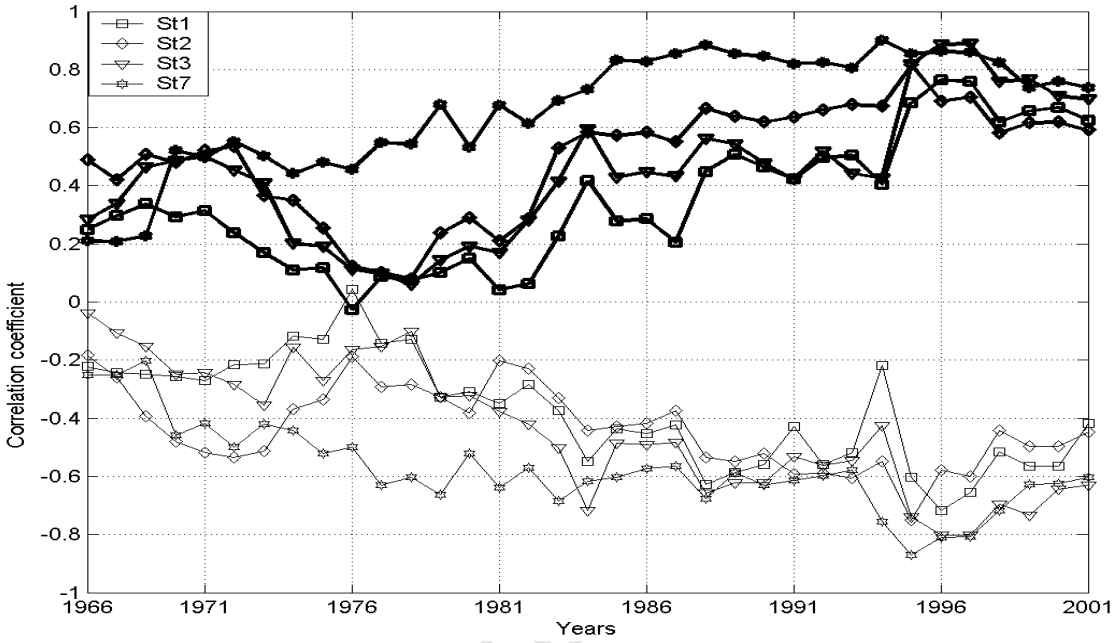

Fig. 6.5 Running correlation (10 years window) between wet (light lines) and dry (heavy lines) with Niño 3.4 index, for the period 1962-2004.

6.2 Convective activity associated with wet spells.

Composites of OLR are used here to study convective activity associated with the above analysed wet spells. The anomalies are calculated as the differences between years with above average occurrence of wet spells and with below average occurrence.

Diagonal bands of negative anomalies reminiscent of TTT over southern Africa are observed in the composites of stations for the southern and central Mozambique (stations 1-7). Over the tropical and south-eastern Indian Ocean, the anomalies are positive suggesting enhanced subsidence (Fig. 6.6). This result is consistent with the analyses in previous chapters indicating that strengthening of the high pressure cell over the South Indian Ocean is associated with wet conditions over much of southern Africa. OLR anomalies in the stations over northern Mozambique (stations 8-10) are weaker, however

negative anomalies are observed over northern Mozambique implying wetter conditions there.

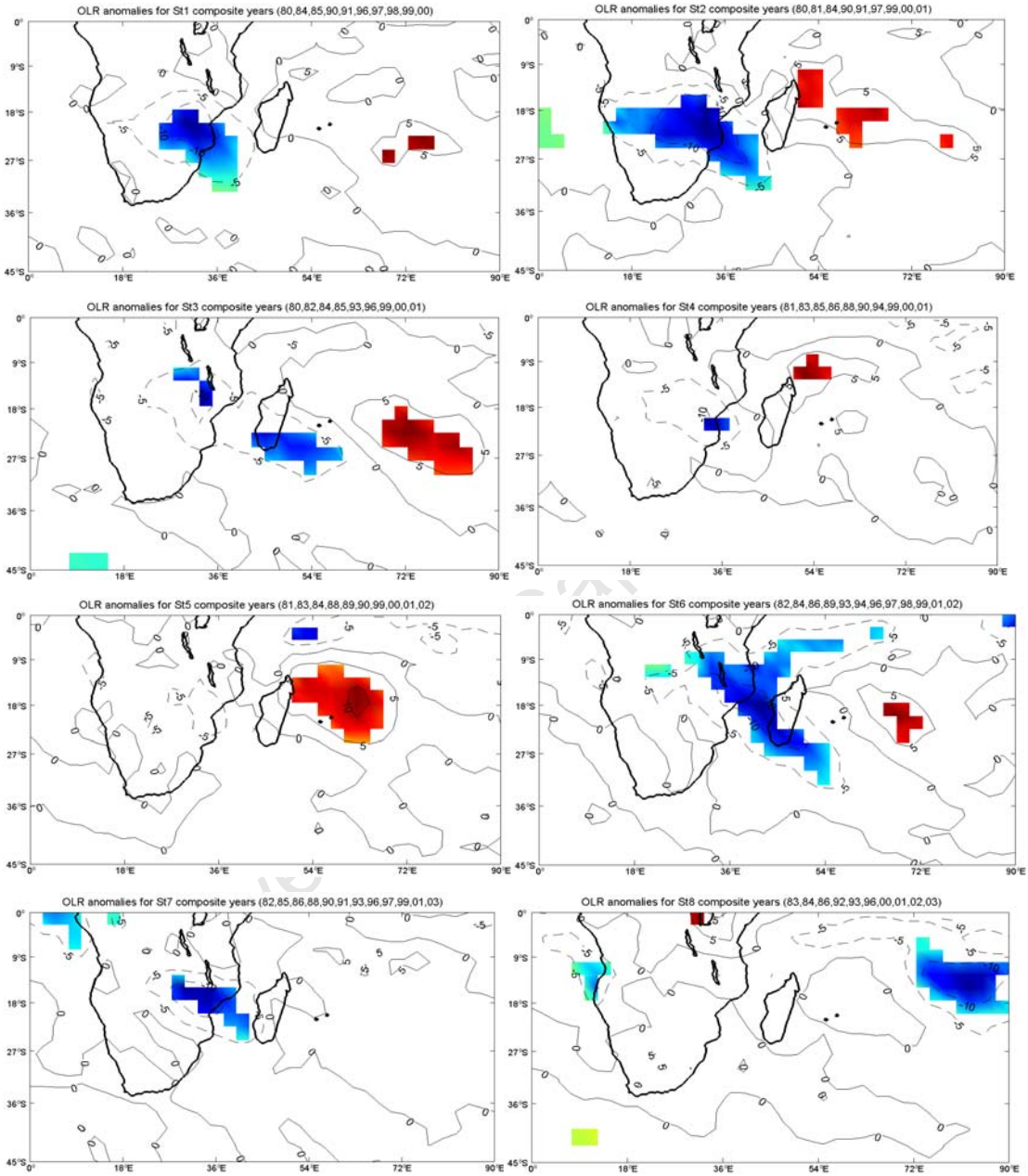

Fig.6.6 Composite anomalies of OLR (contour interval is 5 W/m2) associated with high frequency of wet spells on individual stations over Mozambique. Shaded areas are significant at 5% Student's t test. Dashed lines indicate negative values.

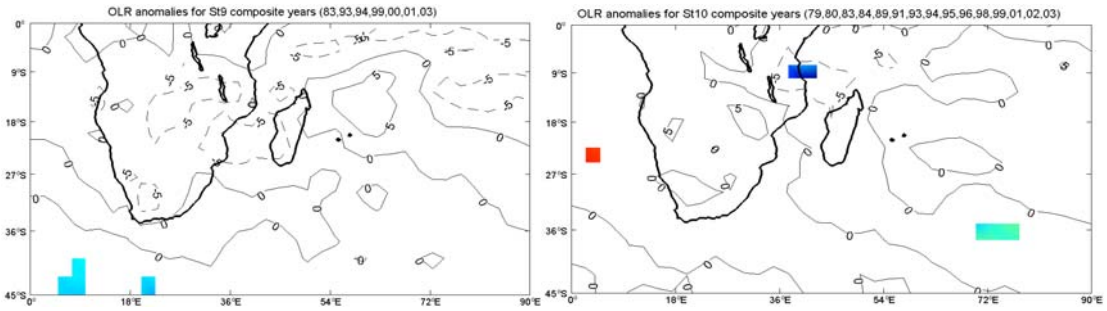

Fig. 6.6 continued

6.3 Relationship between clusters, inter-annual frequency of wet spells, dry days and Indian Ocean SST

In Chapter 4, correlations between the cluster frequencies and the frequencies of wet spells or of dry days were computed. The two clusters analysed in JFM displayed strong correlations with stations over southern Mozambique (stations 1-3) and also station 7 over central Mozambique (Table 4.3b). The aim here is to explore links between SST anomalies and the annual frequencies of wet spells and of dry days and compare the patterns with those obtained with the cluster analysis. The composites here are computed as the difference between years with equal or above and the years with below the standard deviation (See Fig.6.2 and 6.3) occurrence of wet spells or dry days. The composites analysed here involve relatively long time series (1962-2004), so this would give more confidence to the results obtained with the clusters and also shed light on the physics behind the frequency of wet spells and dry days over particularly southern Mozambique and their relationship with SST over the South Indian Ocean.

Composites of SST for the annual frequency of wet spells display consistent patterns, for three stations over the south (stations 1-3) and one over central Mozambique (station 7). The patterns are characterised by negative anomalies in the tropical South Indian Ocean, typical of La Niña (see e.g. Reason et al, 2000) and positive in the subtropics and mid-latitudes of the South Indian Ocean (Fig. 6.7). These patterns are in general consistent with composite

patterns of cluster3, particularly stations 2, 3 and 7. Composite for station7 shows stronger negative anomalies, which can be explained by the strong correlation between the annual frequency of wet spells and Niño 3.4 index in this station. Note that, different from other stations, all the years in which the frequency of wet spells are above the standard deviation, are La Niña. The other six stations analysed here did not display coherent patterns.

When composites are computed after regressing SST against the Niño 3.4 index, all the stations display weaker patterns, however for some stations the patterns are consistent with the positive SIOD (i.e. positive anomalies over the SWIO and negative over the eastern South Indian Ocean). This pattern is particularly observed with station7, however if composites are considered for a smaller period (1979-2004, same period as with cluster3) a similar pattern is depicted in composites for station2 (see Fig.6.8). Hermes and Reason (2005) have shown an increase in frequency of the positive SIOD in the 1990s as compared to the rest of the period (1948-1999) of their analyses. This increase in the number of positive SIOD events in the 1990s may explain why the SST dipole pattern is observed when composites of SST associated with wet spells in St2 are restricted to the period 1979-2005 and is absent when the period 1962-2004 is considered. Note that Hermes and Reason (2005) associate the increase in number of the positive SIOD events in the 1990 with the tendency of the AAO to become more positive in phase after 1980s as shown in some studies (e.g. Mo, 2000; Thompson and Wallace, 2000).

As for the wet spells, the three southern stations (Sts 1-3) and St7, display consistent patterns in years with high frequency of dry days. The patterns are characterised by warm anomalies over the North and subtropical South Indian Ocean (Fig.6.9), typical of El Niño years (Reason et al., 2000). Compared to the SST anomalies associated with wet spells, composite anomalies of annual frequency of dry days are more robust. These anomalies are consistent with the pattern of cluster2 (see Fig. 5.8a), and also consistent with SST anomalies typical of El Niño (e.g. Jury et al., 1996; Reason et al., 2000).

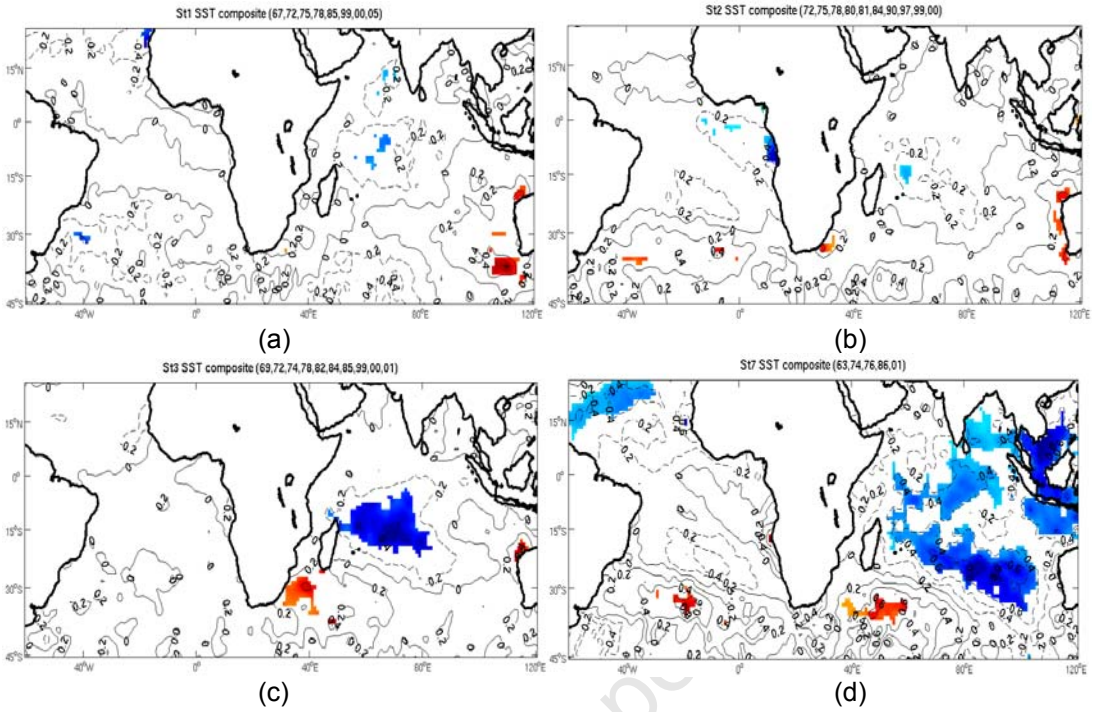

(a) (b)

(c) (d)

Fig.6.7 Composites of SST for the annual frequencies of wet spells in station 1 (a), station 2 (b), station 3 (c) and station 7 (d). Contour interval is 0.2° C. Shaded areas are significant at 5%.

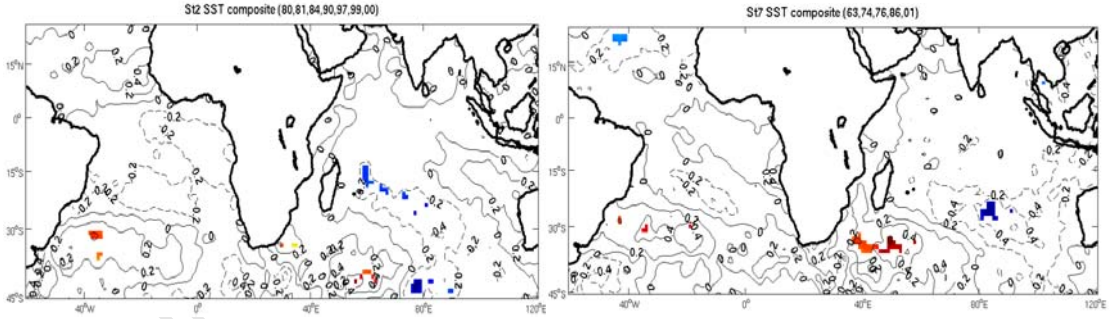

(a) (b)

Fig.6.8 Same as Fig.6.7 except for stations 2 (a) and station 7 (b) with ENSO signal linearly removed. For station2 (a) the period considered is 1979-2004.

The spatial distribution of the most significant positive anomalies shown in Figure 6.9, (mainly Stations 2, 3 and 7) are consistent with the position of the trough associated with cluster 2 (see Fig. 4.11), particularly the diagonally oriented strip east of Madagascar. As indicated in Chapter 5, the trough appears to be mainly linked to the convergence of the northeast monsoons over this diagonally oriented anomaly of SST located east of Madagascar thus contributing

for the dry conditions over southern Africa. On the other hand, a zonally oriented maximum of positive anomalies in the equatorial South Indian Ocean is apparent in the composite of the stations mentioned. In the composites of cluster2 similar zonally oriented positive SST anomaly is observed in the equatorial South Indian Ocean, although weaker (see Fig. 5.8a). When the SSTs are regressed against the Niño3.4 index, the composites display insignificant anomalies.

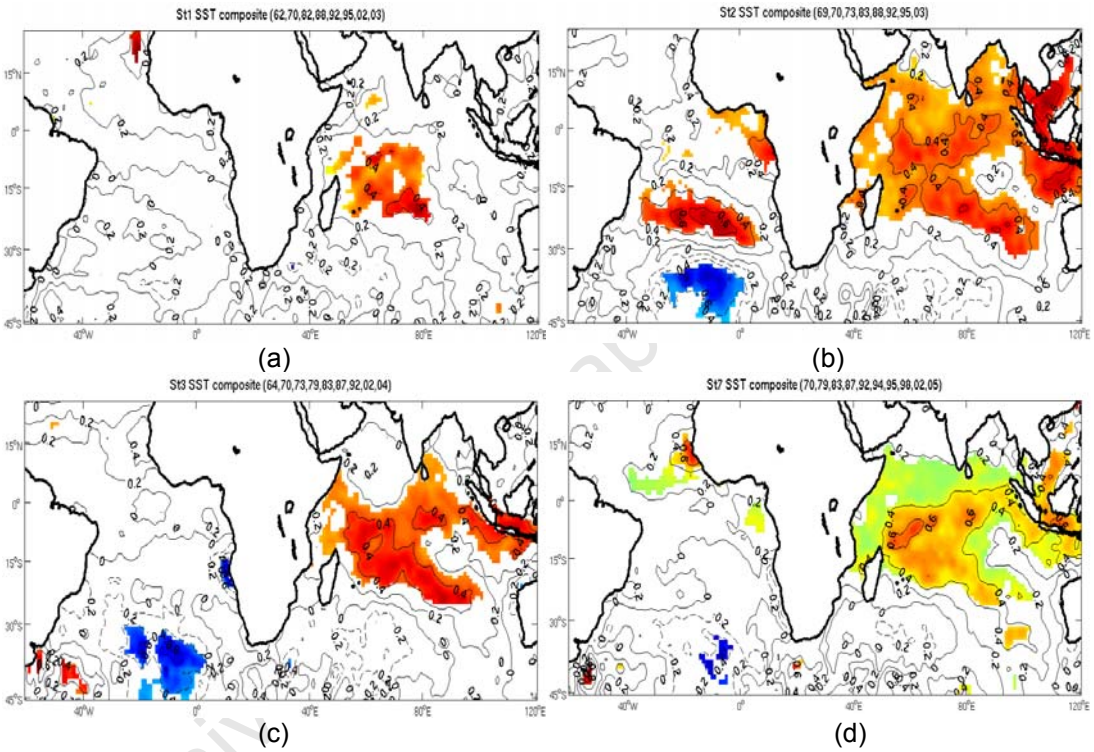

Fig.6.9 Same as Fig.6.7 except for annual frequency of dry days.

6.4 Summary

The annual frequency of wet spells and of dry days reveals strong inter-annual variability coherence in the stations over southern Mozambique (stations 1-3) but also with the station7 in central eastern Mozambique. Correlations of these frequencies with the Niño3.4 index and composites of OLR and SST also display coherent patterns for these stations. OLR patterns associated with wet spells are reminiscent of tropical-temperate cloud bands (see Fig. 2.4) and are

also consistent with the patterns of OLR composites of cluster3. This result suggests that these tropical-temperate cloud bands are indeed the main rain producing systems over southern and central Mozambique.

The atmospheric mechanisms forcing cluster3 may also explain the dipole pattern in the inter-annual rainfall variability over southern Africa, and also observed in composites of OLR and the correlations between the frequencies of wet spells and of dry days, performed here. These mechanisms are associated with enhancement of wind and moisture divergence over tropical SWIO and the northeast of southern Africa and convergence over central and subtropical eastern southern Africa. Strong low level divergence to the north of Madagascar is important for strengthening the convergence of moisture towards the central and southern regions of southern Africa. While this increases the likelihood of wet conditions over these regions it decreases it over the northeast of southern Africa. Also, strong wind divergence over the tropical South Indian Ocean will cool the SST, by evaporation and possibly other mechanisms not analysed here such as mixing, wind forced upwelling (e.g. Hermes and Reason, 2005, 2008).

Composites of SST anomalies in the Indian Ocean associated with the annual frequency of wet spells over stations in the south and central Mozambique (Sts 1-3 and St. 7) are consistent with composite of SST anomalies for annual frequency of cluster3. They all display anomalies consistent with La Niña patterns, i.e., cooling in the tropical Indian Ocean (e.g. Reason et al., 2000) and with the positive SIOD (e.g. Behera and Yamagata, 2001; Reason, 2001), i.e., negative (positive) anomalies in the southeast (western, south of Madagascar) of the South Indian Ocean.

Dry conditions tend to display a more coherent pattern both temporally and spatially over southern and central Mozambique, particularly if the dry conditions are associated with El Niño. The composite of SST anomalies associated with annual frequency of dry days in the stations over southern (St 1-3) and St7 over central Mozambique are consistent with SST anomalies associated annual frequency of cluster2. The patterns are characterised by

warming in the tropical Indian Ocean typical of El Niño (e.g. Reason et al., 2000; Mo, 2000).

Station7 in the central western Mozambique displays the strongest correlations both for annual frequencies of wet spells and of dry days with Niño 3.4 index. Composites of SST anomalies associated with annual frequency of wet spells and of dry days in this station also display the strongest patterns. The apparent strong links between this station and ENSO may be associated with its position (see Fig. 3.1 for the location of the stations) in the region where easterly winds and moisture fluxes from the tropical Indian Ocean converge with winds and moisture associated with the Angolan low (see Fig. 4.8 and also Fig. 4 in the Appendix B). Modulation of the strength of the Angola low has been indicated as the mechanism by which the ENSO signal affects rainfall over southern Africa (e.g. Reason and Jagadheesha, 2005). Composites of geopotential height anomalies associated with years of high frequency of cluster3 (Fig. 5.1b and Fig. 5.3b) also suggest a modulation of the Angola low as being an important mechanism by which ENSO affects rainfall in southern Africa.

Stations in the eastern central Mozambique (stations 4 and 6) display weak links with ENSO, and the SST anomalies associated with annual frequencies of wet spells and of dry days at these two stations are weak. However, the maximum value of rainfall in Mozambique is observed in the region where the two stations are located. This weak relationship between these stations and ENSO appears to be linked to the different systems that contribute to the rainfall over the central Mozambique, namely, the ITCZ, cloud bands associated with TTT, tropical cyclones and storms which have different forcing mechanisms (see e.g. Reason et al. 2006a; Kuleshov et al., 2008), some of these systems are partially independent of ENSO.

Over northern Mozambique, composites of OLR and SST associated with high frequencies of wet spells and of dry days are in general weak. Correlations between annual frequency of wet spells and of dry days with Niño 3.4 in St10 on the northeast Mozambique, display opposite sign compared to other nine

stations, i.e., positive (negative) correlations with the annual frequency of dry days (wet spells). This correlation sign is consistent with the dipole pattern of rainfall between northeast and central southeast southern Africa discussed in a number of studies (e.g. Jury, 1992; Washington and Todd, 1999; Cook, 2000).

Chapter Seven:

7. Summary and conclusions

Statistical analyses have been used in the past to explore the relationships between SST in the Indian Ocean and rainfall over southern Africa. Some patterns of SST in the South Indian Ocean, either associated with or independent of ENSO, have been found to correlate significantly with rainfall over southern Africa (e.g. Rocha and Simmonds, 1997; Reason and Mulenga, 1999, Reason, 2001). General circulation models, forced with these patterns of SST, have been used to try to understand the physical mechanisms explaining the correlations (e.g. Rocha and Simmonds, 1997; Reason, 2002; Washington and Preston, 2006). However, feedbacks between the atmosphere and the SST limit the ability of the GCMs to determine if it is the atmospheric forcing or if it is the SST forcing that influences the rainfall the most. Also, rainfall over southern Africa is associated with a multitude of atmospheric systems (e.g. Reason et al. 2006a), which may not be well represented in the GCMs. The aim in this thesis has been to identify, based on convective activity, the tropical temperate troughs (TTT - the main summer rain producing systems over subtropical southern Africa), which collectively form the South Indian Convergence Zone, and to explore the large scale atmospheric and SST patterns linked to this atmospheric system. The main interest here was to understand the physical mechanisms explaining the relationships between rainfall over southern Africa (with particular emphasis on Mozambique) and SST in the South Indian Ocean.

Before summarising the main results of this thesis, it is useful to first review the results of previous work that has shown what SST and circulation patterns are associated with positive anomalies of rainfall over southern Africa.

- Modulation of the South Indian Anticyclone, such that it is strengthened over its northern and western margins (resulting in stronger than average wind and moisture fluxes towards the subcontinent) is one important atmospheric mechanism forcing the SICZ to be preferentially

located over southern Africa/SWIO. This mechanism has been previously shown to be important for setting up and strengthening the SICZ over southern Africa/SWIO (e.g. Todd and Washington, 1999; Cook, 2000). However, some aspects not discussed before and observed here, are highlighted:

- Southern Hemisphere planetary waves (wavenumber-3 or -4) were observed to modulate the South Indian anticyclone. This modulation has been previously isolated as important in the evolution of the subtropical South Indian Ocean SST dipole mode (e.g. Fauchereau et al., 2003; Hermes and Reason, 2005). However, this thesis is the first study to isolate its importance in the inter-annual variability of the TTT.

- Seasonality was observed in the modulation of the South Indian anticyclone. In the early (OND) summer the South Indian anticyclone was not significantly strengthened as compared to the late (JFM) summer. As result, the easterly winds were observed to be more important for strengthening the SICZ in the late rather than the early summer.

- La Niña was observed to strengthen the northern and western margins of the South Indian anticyclone in the early (OND) summer. In the late (JFM) summer the influence of La Niña over the South Indian Ocean was through enhancement of the pressure gradient between the tropical and subtropical regions.

Composites of SST, associated with positive anomalies of rainfall over southeast southern Africa, displayed patterns reminiscent of the positive subtropical Indian Ocean dipole (e.g. Behera and Yamagata, 2001), and also

patterns typical of La Niña, i.e. cooling over the subtropical and tropical Indian Ocean (Reason et al., 2000), for both OND and JFM seasons.

To explore the statistical relationships between these patterns of SST and rainfall over southern Africa, time series averaged over the regions with the largest anomalies of SST (shown in Fig. 5.8 and Fig. 5.9) and rainfall/OLR were used. The cool anomalies in the central subtropical Indian Ocean could be either linked to ENSO or to the positive SIOD; however the warm anomalies south of Madagascar have only been associated with the positive SIOD. The time series of rainfall and OLR used in the correlations cover mostly central and southern Mozambique (region shown in Fig. 4.5b upper right panel). The observed correlations are detailed below:

1. Correlations between rainfall/OLR and cool SST anomalies over central South Indian Ocean.
    - In OND, the correlations were significant only with rainfall (negative) and only at 1month and at 0 month lag.
    - In JFM, the correlations were significant with both OLR and rainfall. With OLR, the correlations were positive and significant at 4 months lag. They weakened between 3 and 2 months lag and were again significant between 1 and 0 month lag. With rainfall, the correlations were negative, but with about the same magnitude and tendency as with the OLR.
2. Correlations between rainfall/OLR and warm anomalies in the SWIO, south of Madagascar.
    - In OND, no significant correlations were observed.
    - In JFM, the correlations were significant with both OLR (negative) and rainfall (positive) from 2 months lag. The correlations were stronger than with the cool anomalies in the central South Indian Ocean.

Atmospheric circulation anomalies, and associated latent heat flux anomalies over the South West Indian Ocean, were found in this thesis to be important for generating the anomalies of rainfall over south and central parts of Mozambique.

Increased net latent heat fluxes and low level easterly anomalies of wind were observed over the cool anomalies of SST in the tropical and subtropical South Indian Ocean. These increased latent heat fluxes suggest that the ocean is losing more heat through evaporation, forced by strong easterly winds, and hence cooling.

The relationship between rainfall over south and central Mozambique and the warm SST pole over the SWIO, south of Madagascar, is less clear. Only weak anomalies in the latent heat flux occurred over the warm SST pole, suggesting weak air sea interactions in this region. However, the study by Hermes and Reason (2005) may give some explanation for the relationship between rainfall and this warm SST anomaly. Their study has shown that strengthening of the easterlies over the South Indian Ocean contributes to the warming in the warm pole south of Madagascar due to Ekman heat transport. The same study has indicated that strengthening of the South Equatorial Current (forced by stronger easterlies) results in a significant increase (about 20%) in westward transport of heat in the upper ocean (upper 100m), which contributes to the warm pole south of Madagascar via the East Madagascar and Agulhas Current. Therefore the strengthening of the easterlies winds over the South Indian Ocean will impact on both the warm pole south of Madagascar and rainfall over southern and central Mozambique, which may explain the significant correlations between the two.

The analyses of the SST, associated with the positive SIOD and with the SICZ mainly positioned over central and subtropical southern Africa (indicative of positive anomalies of rainfall over the southeast regions of the subcontinent), suggest that both the positive SIOD and the position of the SICZ over land are forced by the same atmospheric circulation patterns. The atmospheric forcing is

mainly associated with the strengthening of the easterly winds over the tropical and subtropical South Indian Ocean. The role of the easterly winds was observed to be stronger in the late (JFM) summer than in the early (OND) summer, which may explain the weak correlations observed between rainfall over south and central Mozambique and the positive SIOD in the early summer as compared with the late summer.

The analyses in this thesis do not exclude the possible role of the SST patterns analysed here in forcing the positive anomalies of rainfall over other parts of southern Africa. However, in terms of the particular context of the SICZ over southern Africa, the role of the SST anomalies in the South Indian Ocean appears to be modest.

The Angola low was observed in this thesis to be important for SICZ (when this system is located over southern Africa) through strengthening the low level convergence of wind and moisture (sourced from the tropical Atlantic) over the south-eastern regions of southern Africa. This low pressure cell appeared to be strongly linked to ENSO, as indicated in other studies (e.g. Reason et al., 2006a).

The composites of SST associated with the negative anomalies of rainfall over south and central Mozambique (cluster2- JFM) were characterised mainly by warming over the tropical and subtropical Indian Ocean, typical of ENSO (e.g. Reason et al., 2000). The correlations were negative (positive) and significant with rainfall (OLR) from 2 months up to 0 month lag. Low level westerly winds were observed to converge over the position of the largest warm SST anomalies in the central South Indian Ocean. This result suggests that the SST anomalies are forcing the atmosphere and is in agreement with the Lindzen and Nigam (1987) model. The results from this model suggest that, if the tropical lower troposphere is well mixed in the vertical, the horizontal gradients of temperature beneath the trade inversion are expected to resemble their surface pattern,

hence pressure gradients, proportional to sea surface temperature would arise in the boundary layer and drive low level winds.

Given the fact that other rainfall characteristics such as wet spells are very important for rain-fed agriculture in Mozambique, the inter-annual variability in the annual frequency of wet spells and of dry days for ten stations over Mozambique were analysed and their relationships with the JFM clusters were explored.

The annual frequencies of wet spells and dry days for three stations over southern Mozambique (station 1-3) and one over central (station 7) Mozambique showed significant links with the two clusters. Cluster2 was positively (negatively) correlated with the annual frequencies of dry days (wet spells) in these four stations. Cluster3 displayed a reversed pattern of correlations. Composites of SST associated with annual frequencies of wet spells and of dry days in these four stations, displayed patterns consistent with the patterns of annual frequencies of the clusters. The composites of SST for the annual frequencies of dry days showed warm SST anomalies over the tropical Indian Ocean, as in the patterns of cluster2. The composites of SST associated with wet spells showed mainly cool SST anomalies over the tropical Indian Ocean, typical of La Niña and also consistent with composite patterns of cluster3. The positive SIOD observed in composites of cluster3 was only significant for two stations (st2 and st7).

The correlations between the annual frequencies of the clusters and annual frequencies of dry days and wet spells over southern and central parts of Mozambique and also the similarity in the patterns of SST suggest strong links between the large scale atmospheric circulations described by the two clusters and the mechanisms associated with rainfall anomalies for the four stations in the southern (stations 1-3) and central (station 7) Mozambique. The northern stations and some central stations displayed weak links with the TTT clusters.

In summary, the atmospheric circulation associated with the two JFM clusters analysed in this thesis, may explain a significant portion of the rainfall anomalies observed over southern Mozambique and possibility central Mozambique, but not over northern Mozambique.

The few number of stations used in the analyses is a significant drawback, particularly over central Mozambique, where mixed signals were observed. For the southern stations, the results appear to be robust, given the significant coherence observed among the three station used in the analyses.

The analyses of the atmospheric circulation, SST and rainfall in this thesis were performed within the context of the TTT clusters considered here. However, these clusters captured most aspects of the large scale atmospheric circulation and SST associated with wet and dry years over southeast southern Africa (particularly the late summer-JFM variability), consistent with many previous studies of large scale rainfall/SST/circulation patterns.

While the influence of ENSO in summer rainfall over southern Africa is fairly well understood, large scale Southern Hemisphere planetary waves appear to play a significant role as well, an aspect that has not been sufficiently explored in previous work. It appears from the analyses in this thesis that these planetary waves may also explain much of the statistical relationship between the SIOD and rainfall over south and central Mozambique, as they have impact on both. These links may be better explored in fully coupled numerical models as they may allow the feedbacks in the evolution of the atmospheric circulation and SST modes.

Appendix A Dates of occurrence of each selected cluster for OND and JFM

Table 1 Dates of occurrence of each selected cluster for OND and JFM

Years	Cluster1_OND	Cluster2_JFM	Cluster3_JFM
1979	06:08-Oct; 16:18-Oct; 01:07-Nov; 10:15-Nov; 17:23-Nov-; 06:08-Dec; 28:31-Dec	07:13-Feb; 18:25-Feb; 22:29-Mar	02:08-Mar
1980	01:03-Oct; 20:29-Oct; 05:07-Nov; 09:11-Nov; 04:10-Dec; 17:21-Dec	26:28-Jan; 31-Jan:03-Feb; 26:13-Feb; 15:17-Mar	07:09-Jan; 12:15-Feb; 19:23-Feb; 18:20-Mar
1981	01:03-Oct; 05:09-Oct; 12:16-Oct; 19:22-Oct; 26:30-Oct; 11:13-Nov; 20:22-Nov; 10:12-Dec; 26:30-Dec	----------	06:08-Jan; 14:26-Jan; 30-Jan:-22-Feb
1982	----------	16:18-Jan; 06:08-Feb	03:08-Jan; 20:26-Feb; 24:26-Mar
1983	16:18-Oct; 21:23-Oct; 10:12-Nov; 14:19-Nov; 22:25-Nov ; 09:13-Dec	12:16-Feb; 08:10-Mar	15:17-Jan; 07:10-Feb
1984	07:09-Oct; 16:19-Oct; 04:09-Nov; 22:28-Dec	----------	30-Jan: 01-Feb ; 21:23-Feb; 23:31-Mar
1985	10:13-Oct; 20:22-Oct; 31-Oct: 06-Nov; 12:15-Nov; 16:18-Dec; 20:26-Dec	----------	06:11-Jan; 20:22-Jan; 17:20-Mar
1986	07:14-Oct; 17:21-Oct; 23:27-Oct; 10:14-Nov	12:16-Jan; 09:11-Feb; 13:18-Mar	30-Jan: 01-Feb; 25:28-Feb
1987	01:06-Oct; 15:19-Oct; 03:05-Dec; 18:21-Dec	01:06-Jan; 12:16-Feb; 05:07-Mar; 11:15-Mar; 17:20-Mar	17:19-Jan; 26:28-Jan
1988	13:16-Oct; 20:26-Oct; 02:09-Dec; 18:20-Dec	22-Feb: 03-Mar; 21:23-Mar	09:11-Jan; 01:03-Feb; 12:14-Feb; 09:14-Mar
1989	11:15-Oct; 24:28-Oct; 04:07-Nov; 09:15-Nov; 18:21-Nov; 29-Nov: 02-Dec; 07:10-Dec	21:24-Mar	16:22-Feb-89
1990	01:10-Oct; 20:22-Oct ; 27:29-Oct; 26:28-Nov; 20:22-Dec; 28:30-Dec	13:18-Feb; 20:23-Feb	12:16-Jan; 25:31-Jan; 20:22-Mar; 26:30-Mar
1991	01:05-Oct; 15:19-Nov	30-Jan: 03-Feb	10:13-Jan; 08:11-Feb; 19:22-Feb; 24:28-Feb; 16:18-Mar; 21:27-Mar
1992	03:07-Oct; 27:29-Oct; 31-Oct: 03-Nov; 05:07-Nov; 15:19-Nov; 27:29-Nov; 14:17-Dec; 25:30-Dec	16:19-Jan; 07:19-Feb; 24-Feb: 04-Mar; 14:17-Mar; 21:23-Mar	24:26-Mar-92
1993	03:10-Oct-93; 14:16-Nov; 26-Nov: 01-Dec	01:10-Mar	26:28-Jan; 25:28-Mar
1994	02:07-Oct; 14:17-Oct; 25:27-Nov; 13:16-Dec; 27:29-Dec	05:08-Feb; 26:28-Mar	04:06-Jan; 25:28-Jan; 16:18-Mar
1995	08:12-Oct; 20:23-Nov; 26:29-Nov; 02:04-Dec; 08:14-Dec; 19:27-Dec	02:12-Jan; 25:29-Jan; 27-Feb: 01-Mar	09:11-Feb-95
1996	16:24-Nov; 20:27-Dec	14:19-Jan; 22:28-Feb	20:22-Jan; 27:31-Jan; 11:16-Feb; 05:07-Mar; 15:19-Mar

Table 1 continued

1997	25:30-Nov; 08:10-Dec	23:29-Jan; 13:15-Mar	03:06-Jan; 12:14-Jan; 30-Jan: 01-Feb; 28-Feb: 05-Mar; 07:09-Mar; 22:24-Mar
1998	03: 06-Oct; 09:11-Oct; 16:19-Oct; 09:11-Nov; 28-Nov: 01-Dec; 03:07-Dec; 13:20-Dec; 23:26-Dec; 29:31-Dec	11-14Feb; 23-Feb: 03-Mar-98; 06:13-Mar; 26:29-Mar	09:12-Jan; 20:23-Jan; 26:28-Jan
1999	01:04-Oct; 26:31-Oct; 23:25-Nov ; 13:16-Dec	----------	07:09-Jan; 31-Jan: 11-Feb; 22:25-Feb
2000	28-Oct: 06-Nov; 01:03-Dec; 14:17-Dec; 23:25-Dec	11:16-Jan	18:21-Jan; 04:11-Feb; 13:18-Feb; 16:23-Mar; 28:31-Mar
2001	20:24-Oct; 27:29-Oct; 14:19-Nov; 21:24-Nov; 03:09-Dec; 13:19-Dec; 21:25-Dec; 28:31-Dec	----------	06:08-Feb; 15:28-Feb; 02:04-Mar; 11:16-Mar; 20:23-Mar
2002	08:11-Oct; 31-Oct: 04-Nov	01:06-Jan; 11:15-Jan; 17:19-Feb; 28:30-Mar	02:06-Feb; 09:11-Feb
2003	08:10-Oct; 19:25-Oct; 07:09-Nov; 30-Nov: 02-Dec	08:11-Jan; 22:24-Jan; 10:17-Feb; 23:26-Mar	27-Feb: 10-Mar

Appendix B

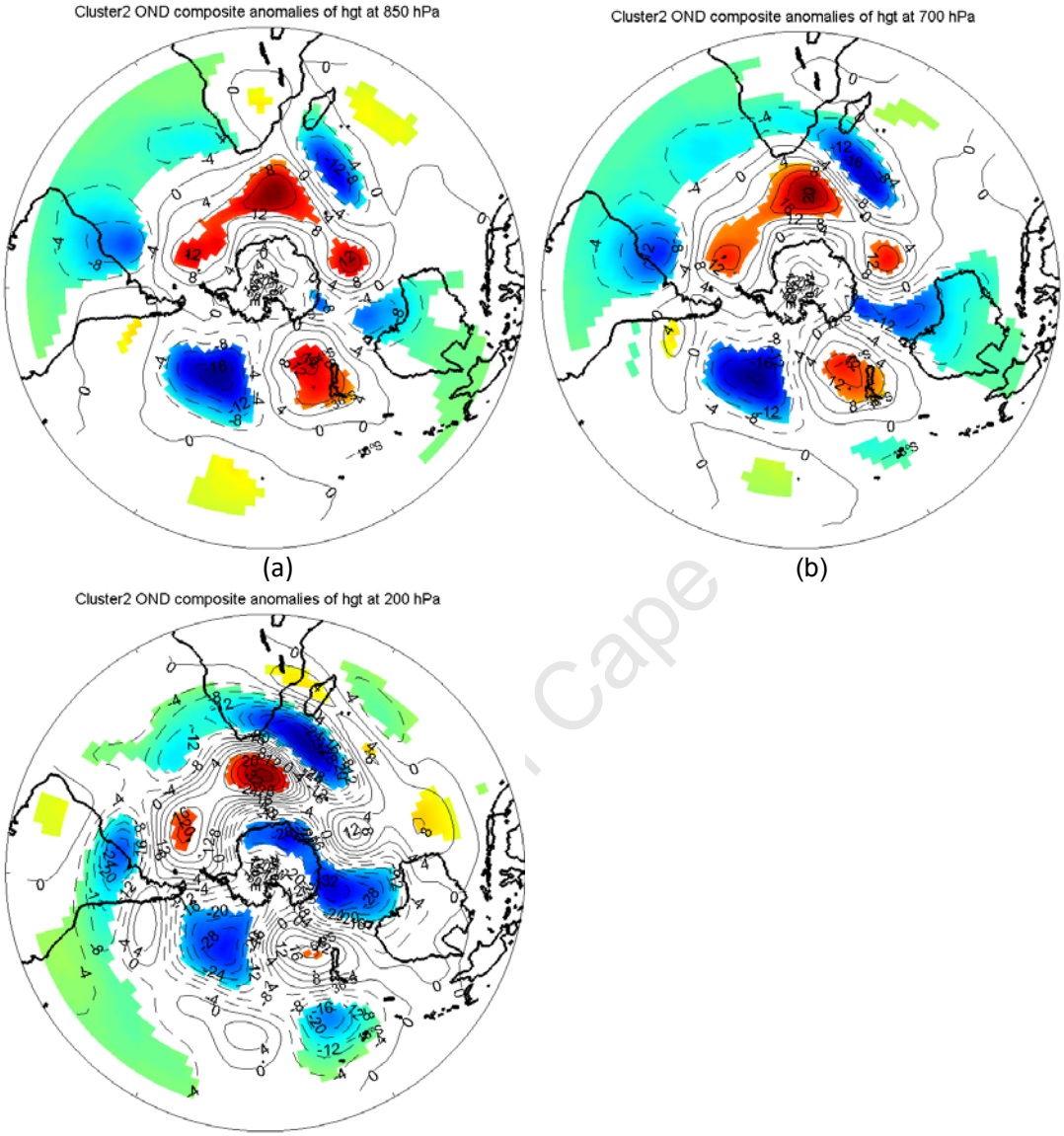

Fig.1 Geopotential height anomalies associated with cluster2 (OND) at 850 hPa (a), 700 hPa (b) and 200 hPa (c). Contour interval is 4 m.

Appendix B

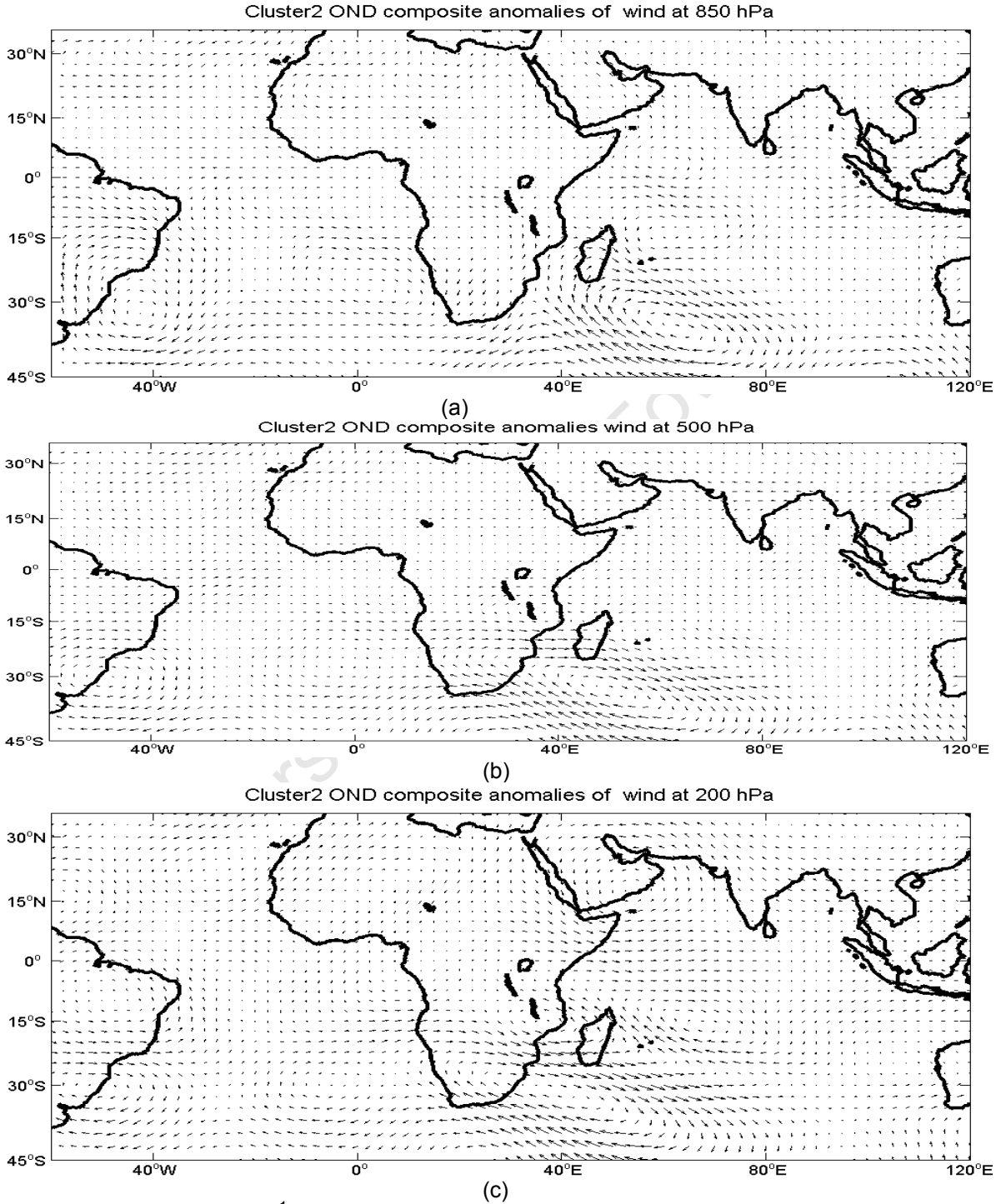

Fig.2 Wind anomalies ($m*s^{-1}$, with arrows scaled at 1 unit/degree latitude) associated with cluster2 (OND) at 700 hPa (a), 500hPa (b) and 200 hPa (c).

Appendix B

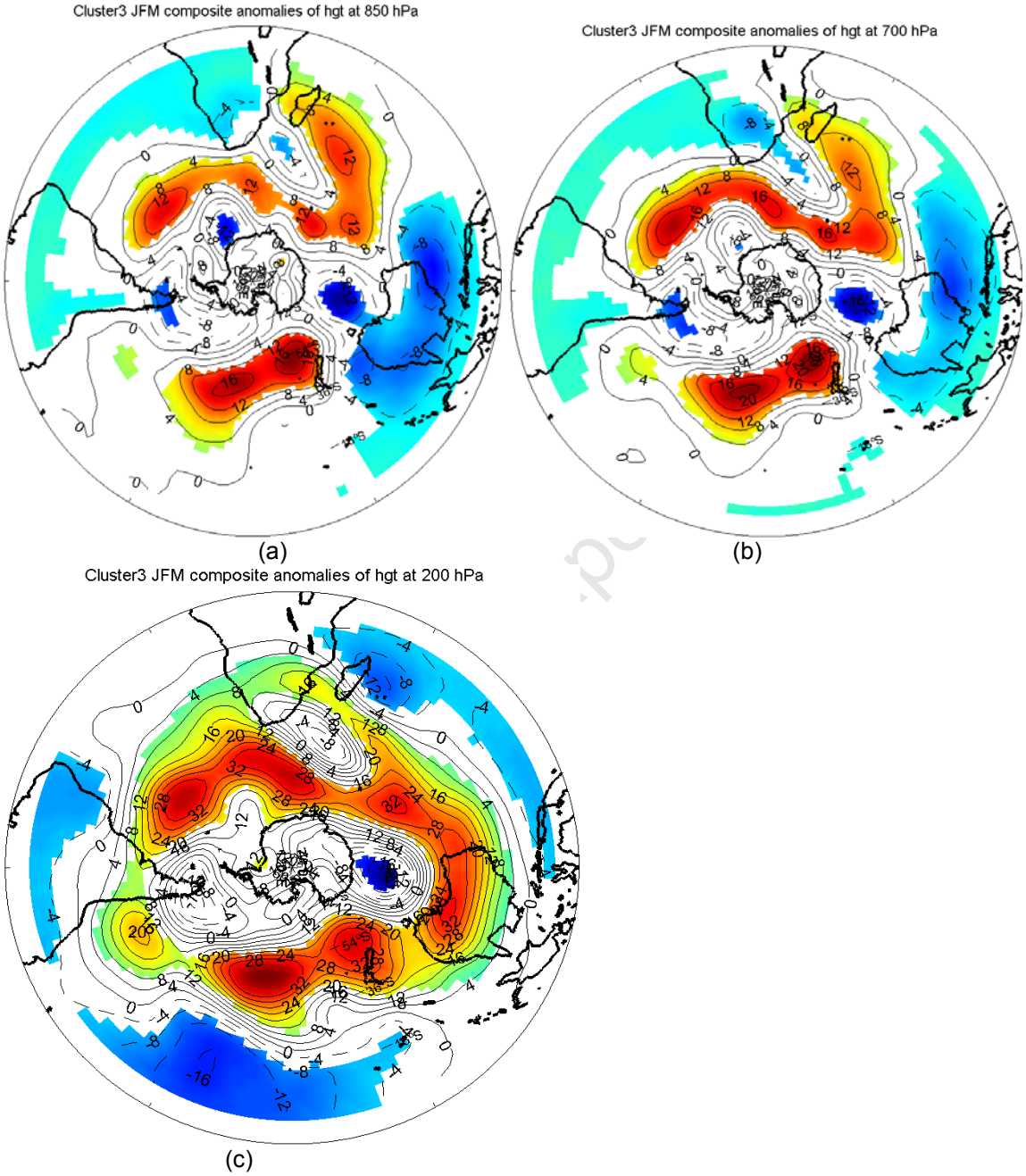

Fig.3 Same as Fig.1 except for cluster3 in JFM

Appendix B

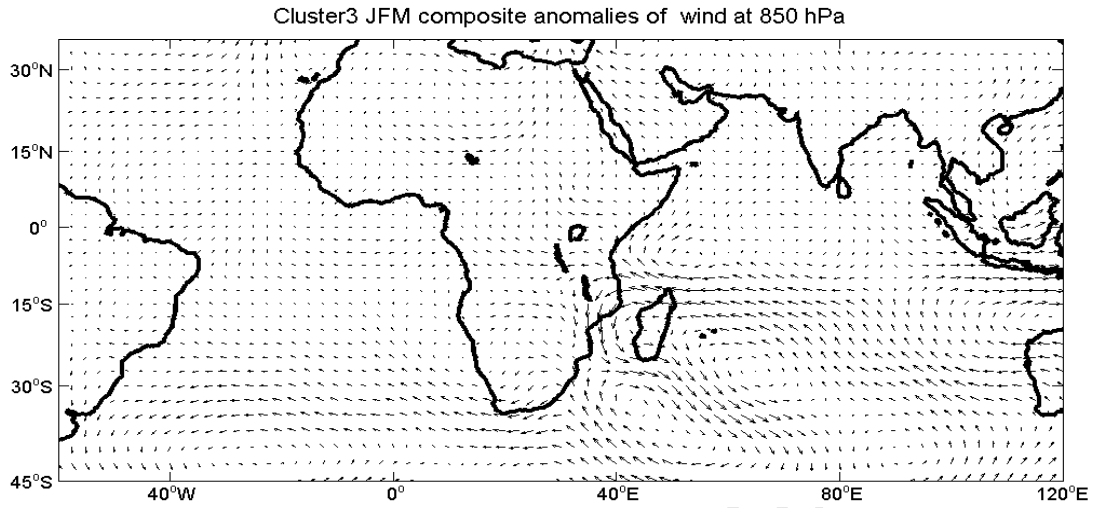

(a)

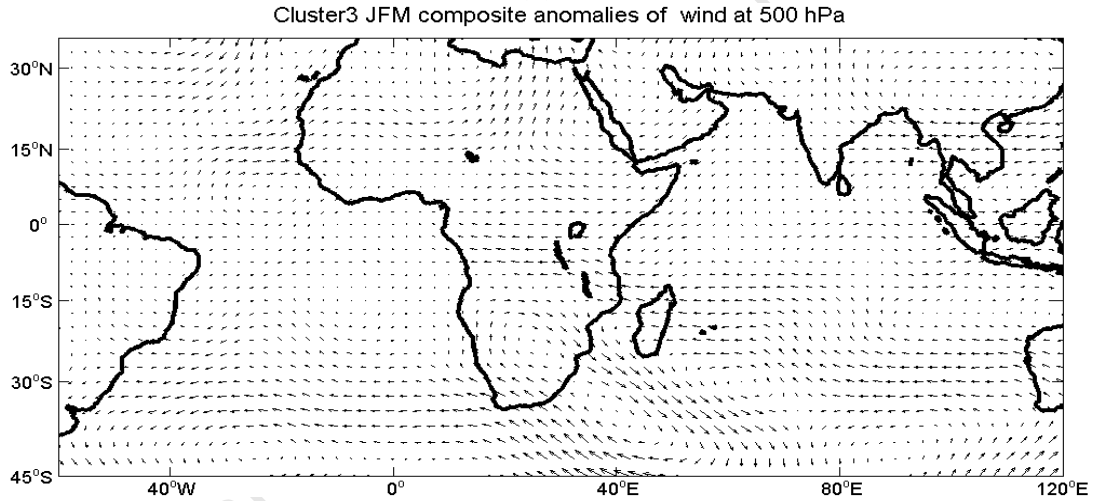

(b)

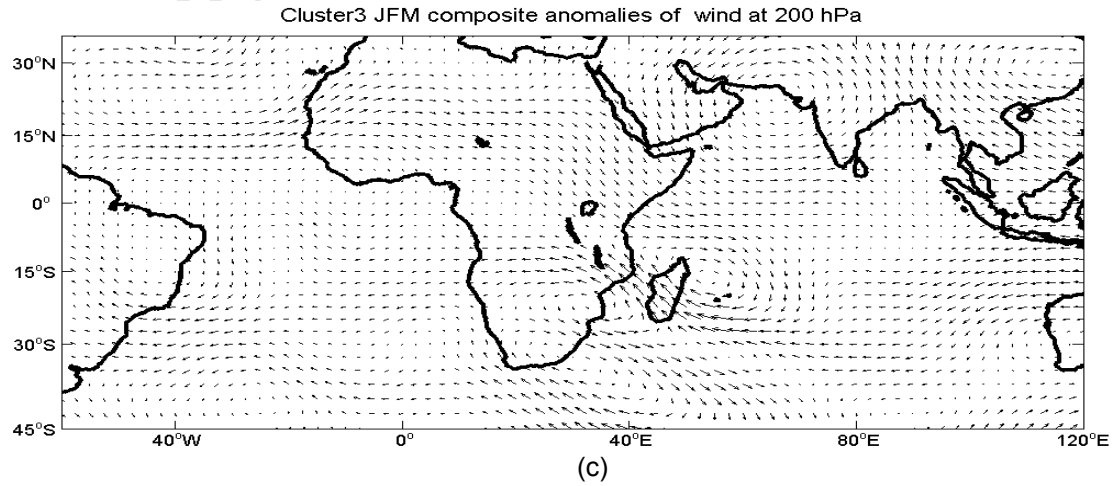

(c)

Fig.4 Same as Fig.2 except for cluster3 (JFM)

Appendix B

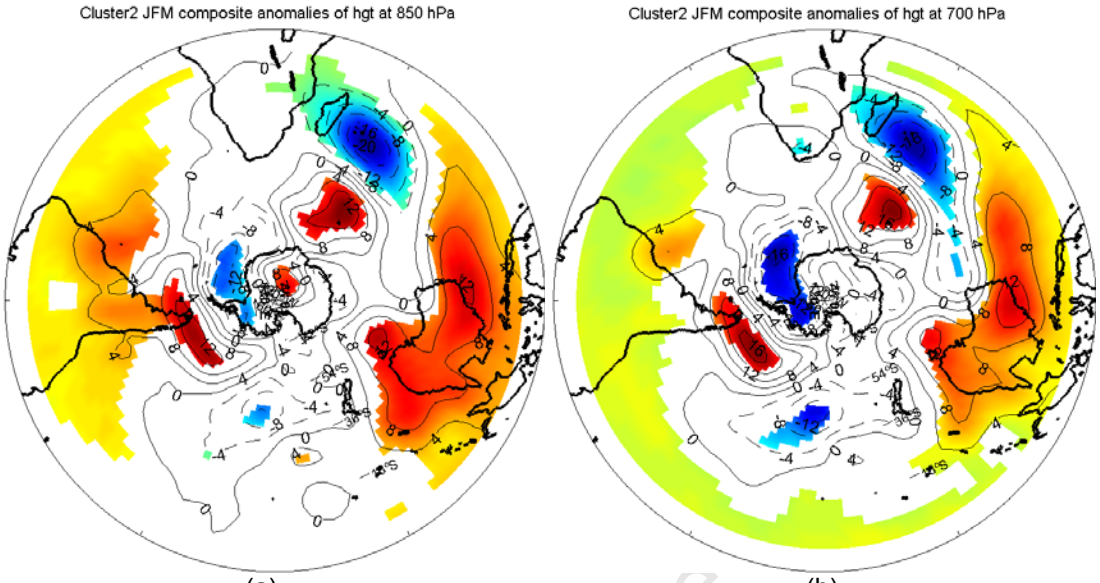

(a)

(b)

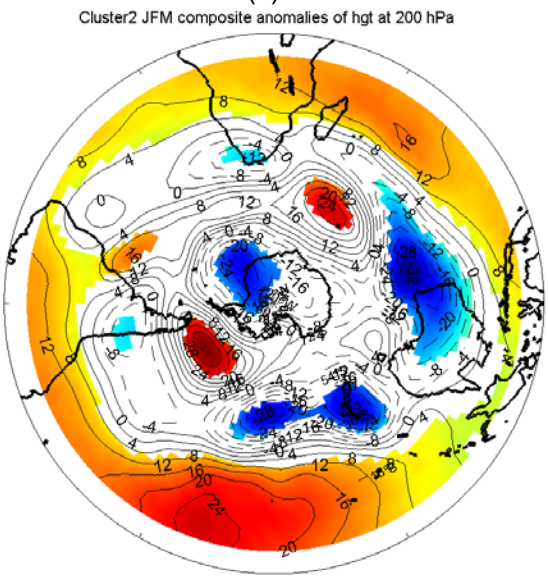

(c)

Fig.5 Same as Fig.1 except for cluster2 in JFM

Appendix B

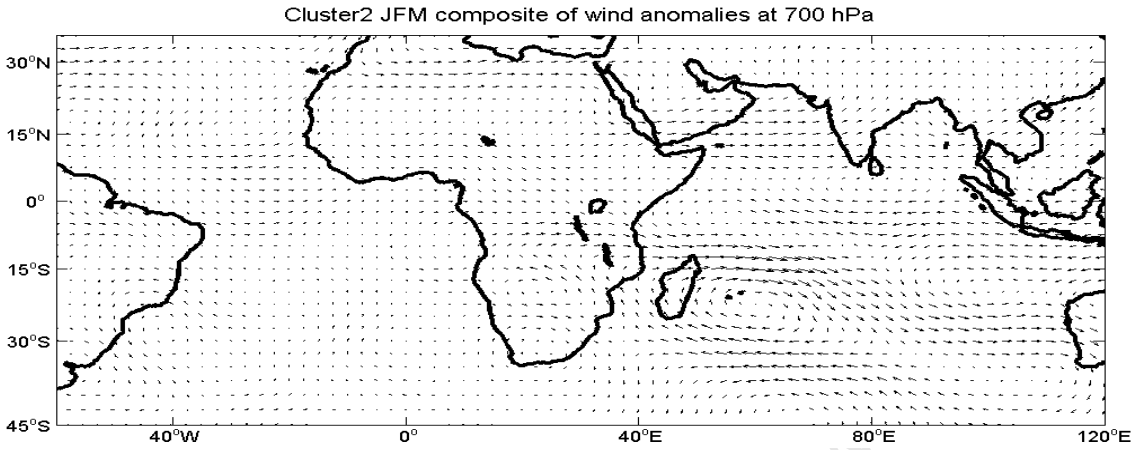

(a)

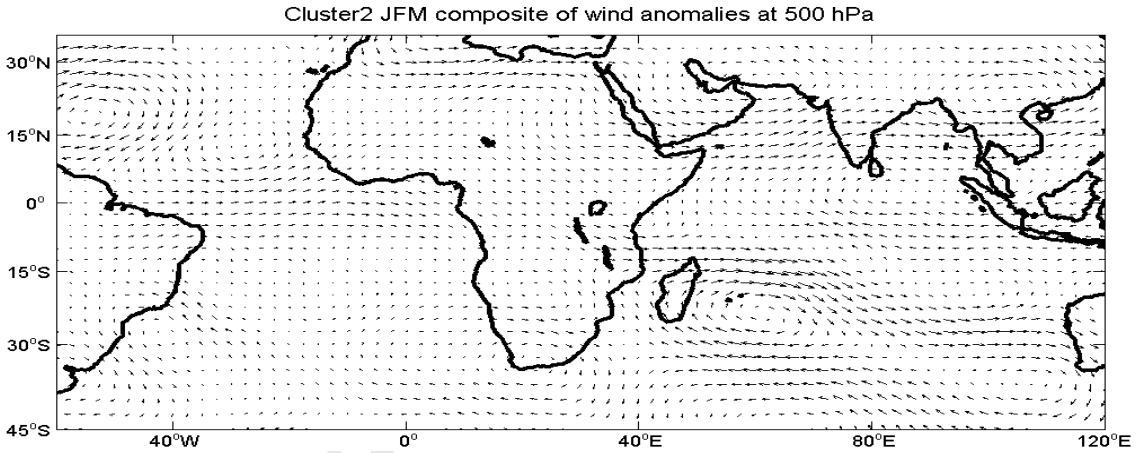

(b)

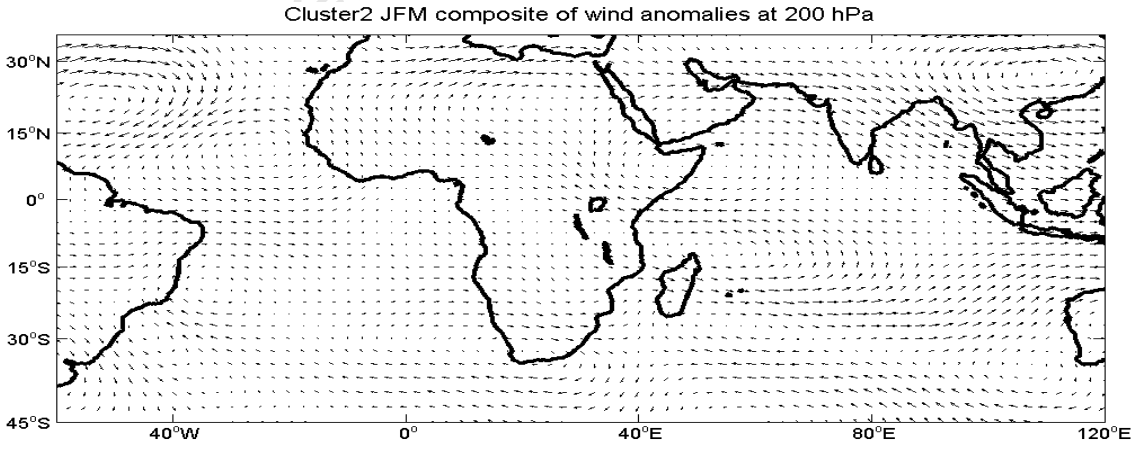

(c)

Fig.6 Same as Fig.2 except for cluster2 (JFM)

Appendix C

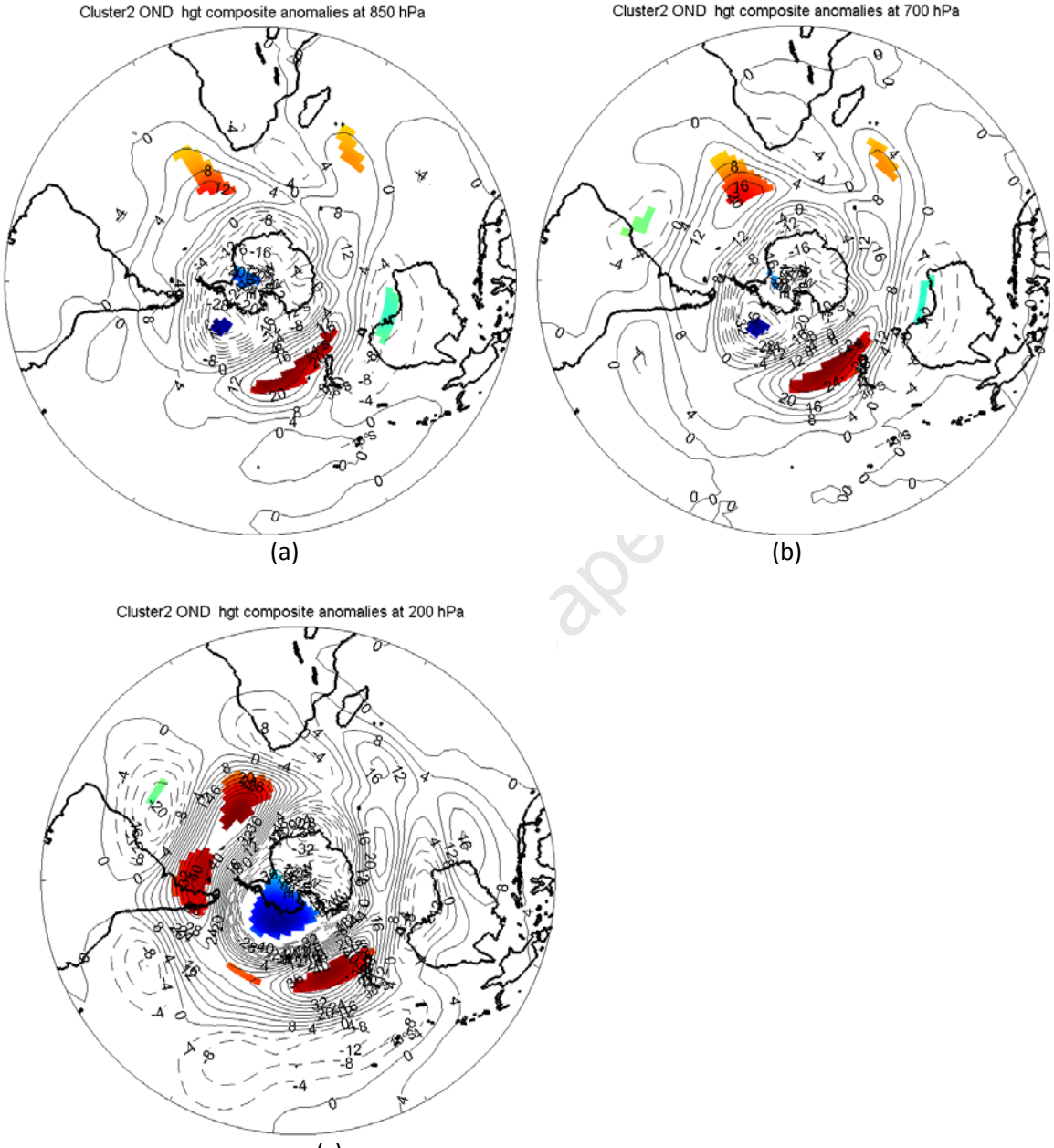

Fig.7 Composite of geopotential height anomalies for the annual frequecies of cluster2(OND) at 850 hPa (a), 700 hPa (b) and 200 hPa (c). Contour interval is 4m.

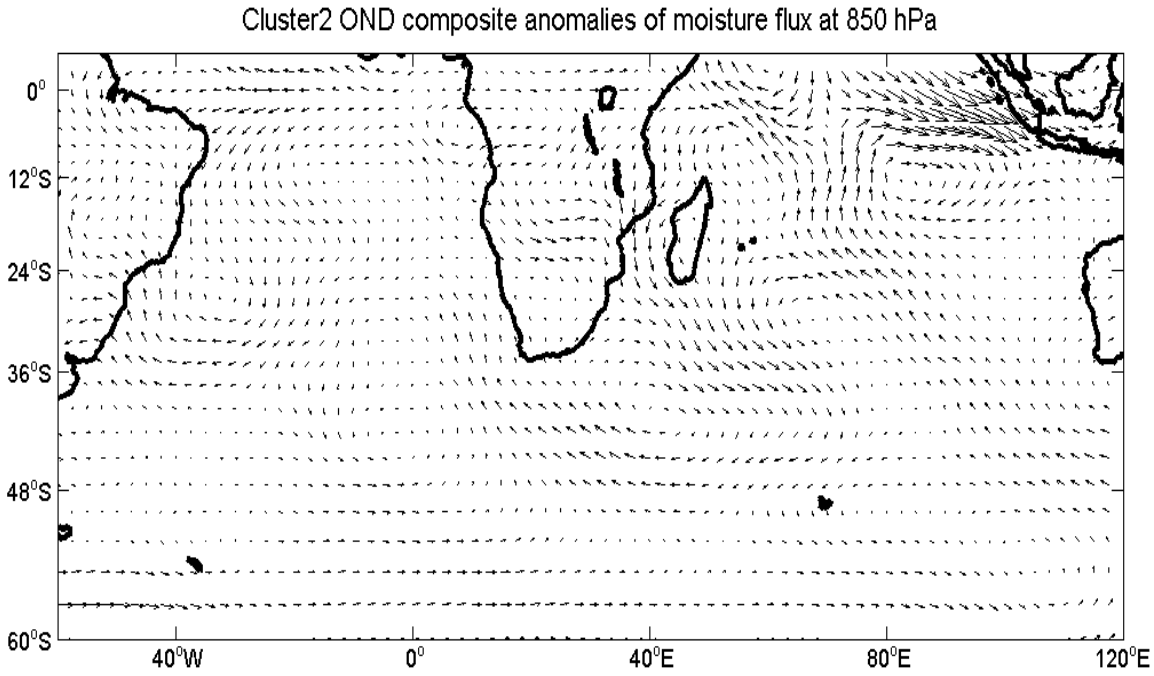

Fig.8 Composite of moisture fluxes (Kg*m*s^{-1}, with arrows scaled at 1 unit/degree latitude) for the annual frequency of cluster2 (OND)

Appendix C

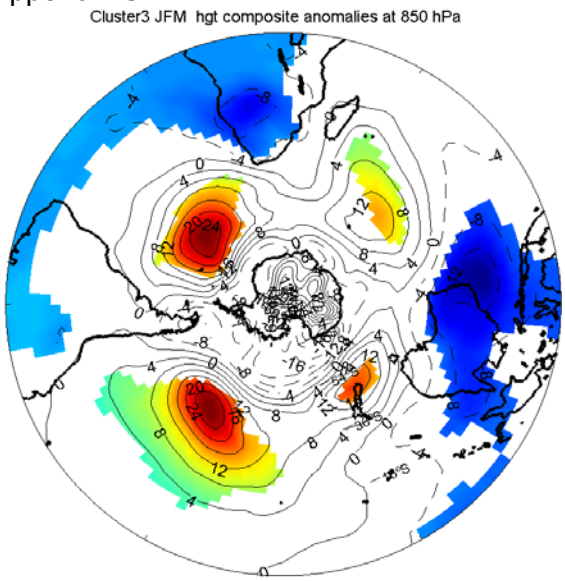

(a)

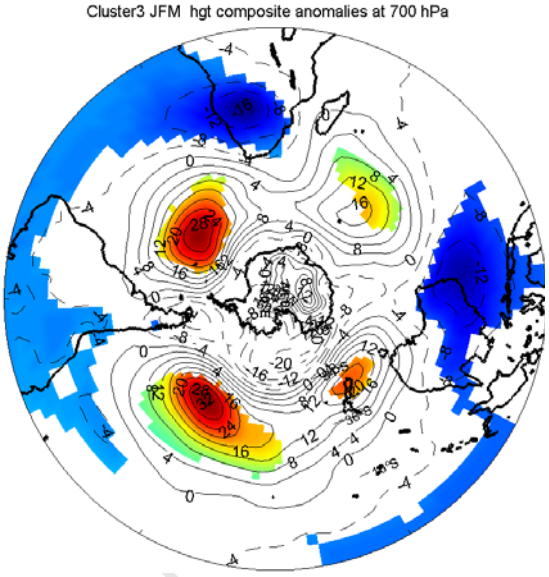

(b)

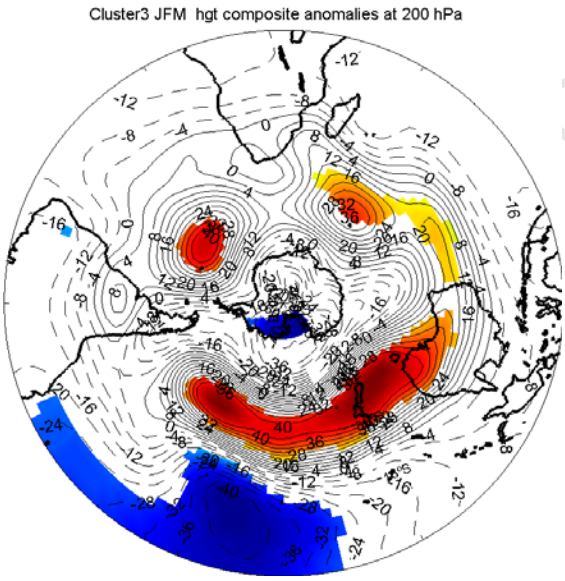

(c)

Fig.9 Same as Fig.4 except for cluster3 (JFM)

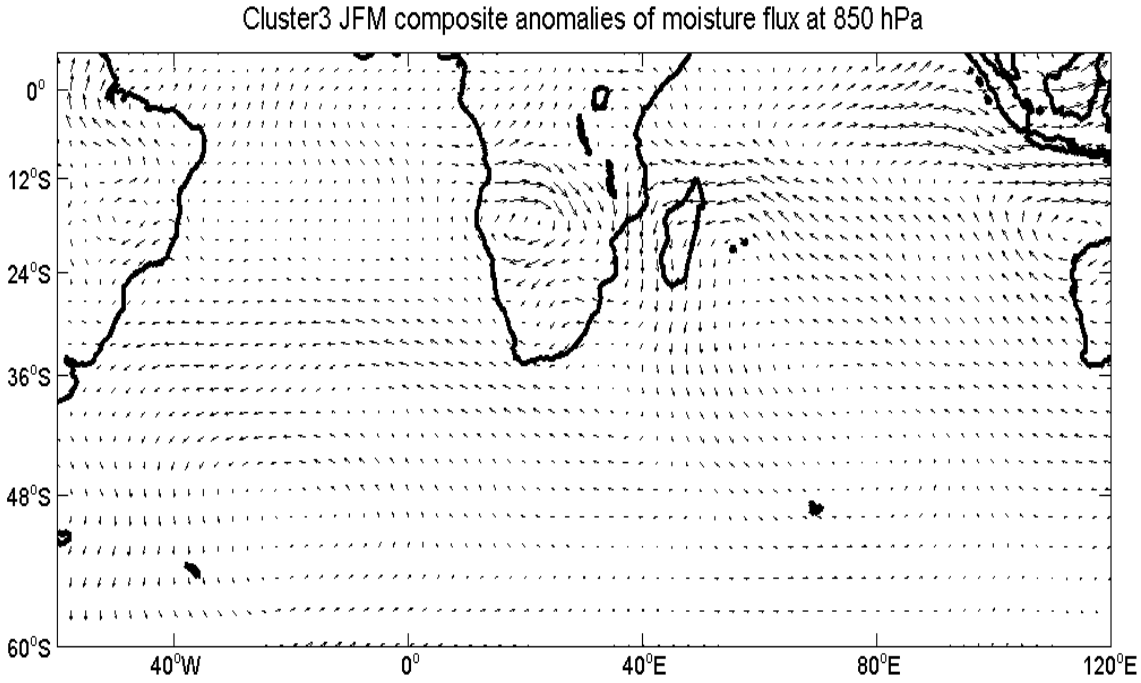

Fig.10 Same as Fig. 8 except for cluster3 (JFM).

Appendix C

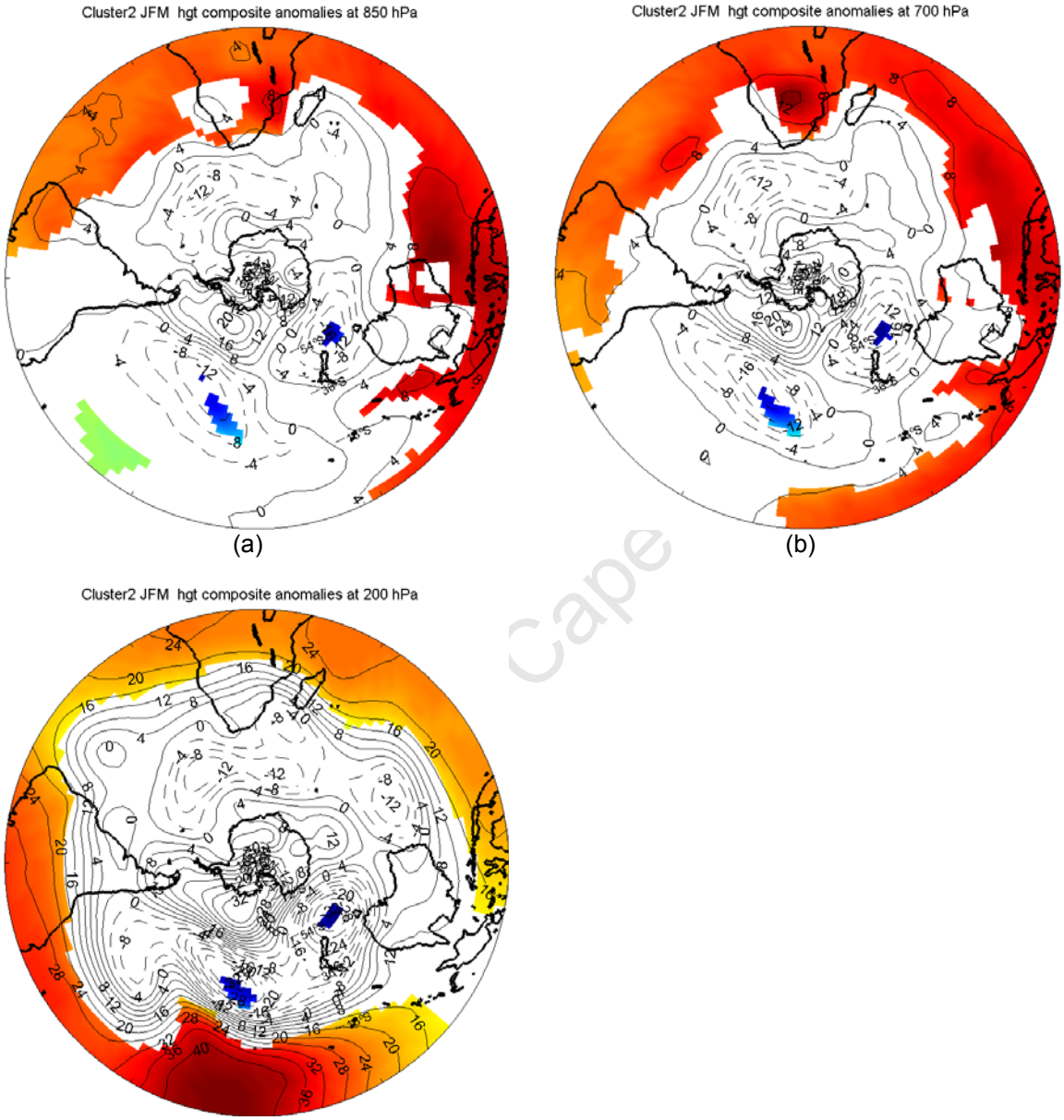

Fig.11 Same as Fig.4 except for cluster2 (JFM)

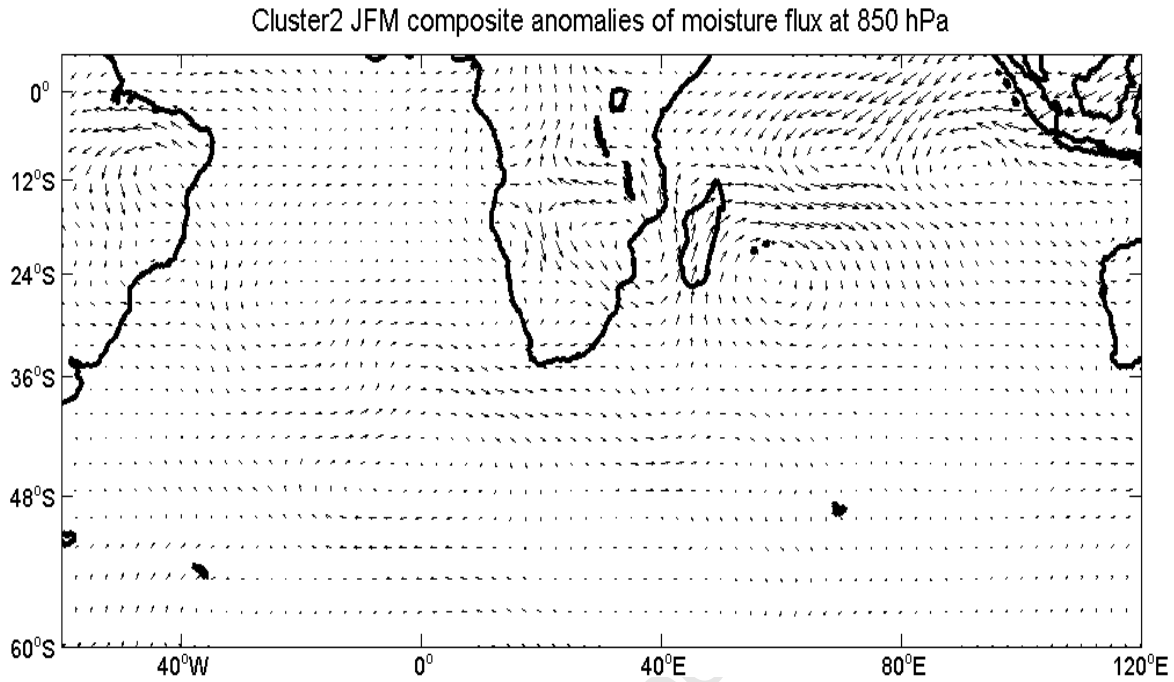

Fig.12 Same as Fig.8 except for cluster2 (JFM)

Appendix C

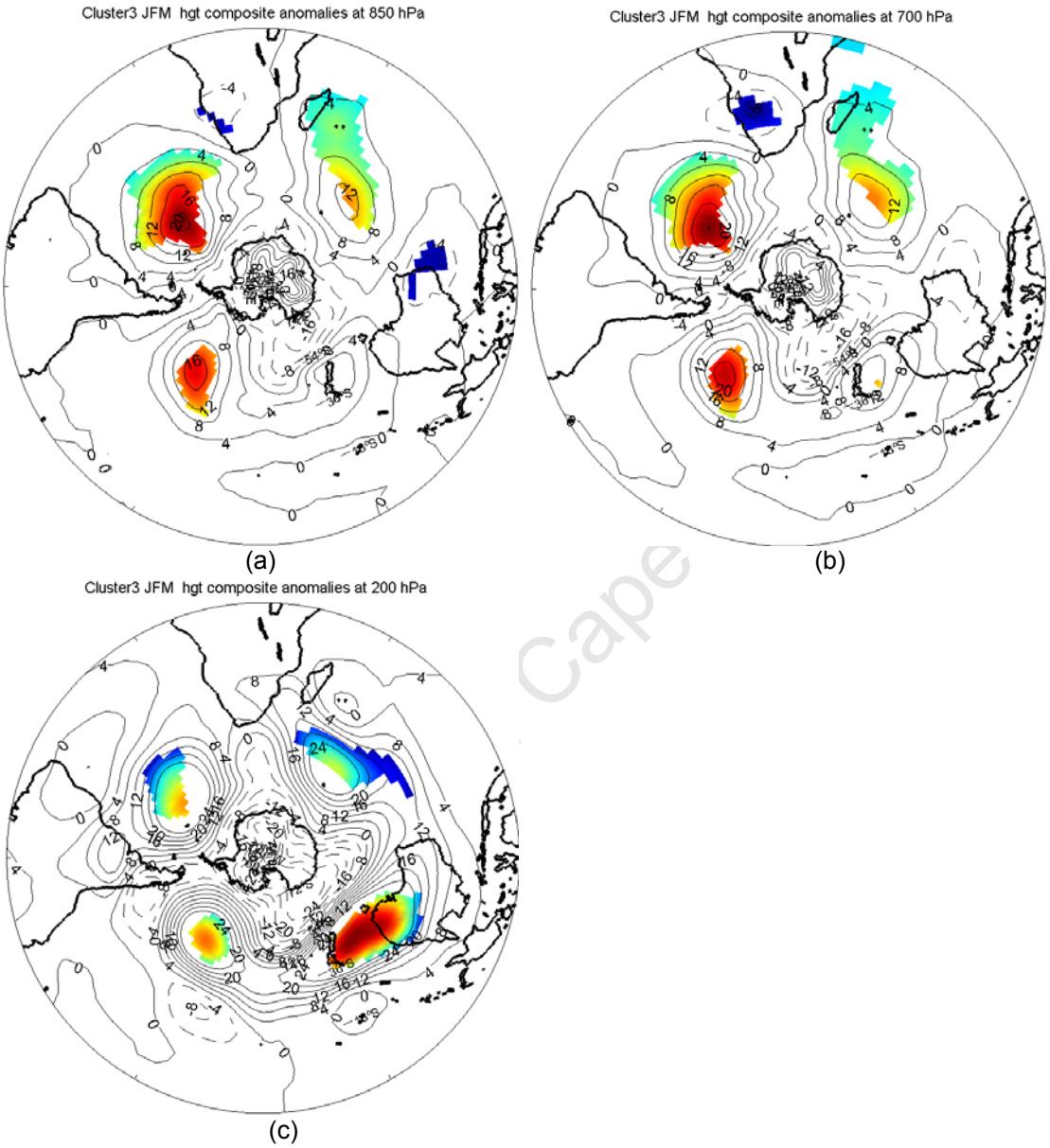

Fig.13 Same as Fig.9 except with the linear influence of ENSO removed by linear regression.

Appendix D

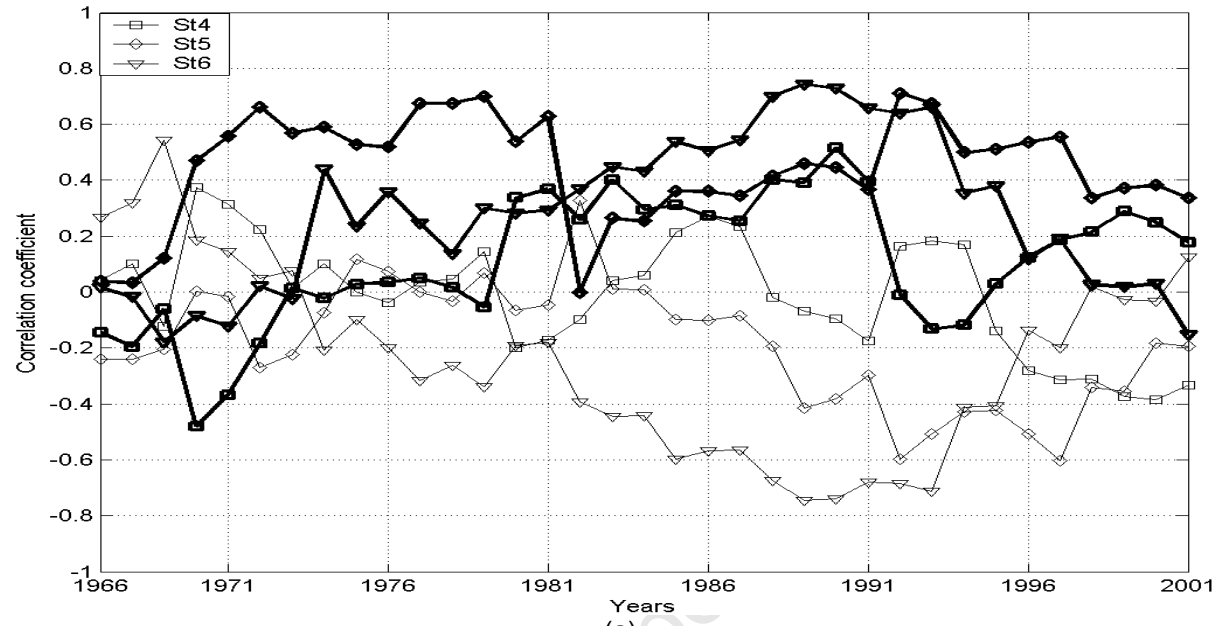

(a)

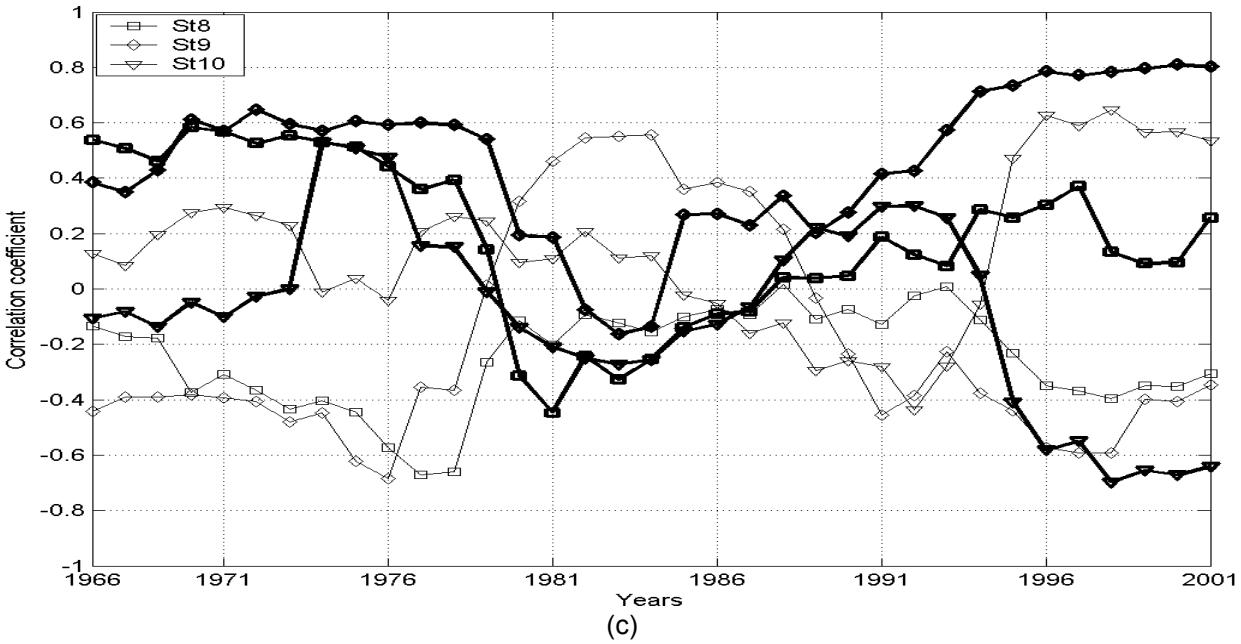

(c)

Fig.1 Running correlation (10 years window) between wet spells (light lines) and frequency of dry days (heavy lines) with anomalies in Niño 3.4 index for the period 1962-2004. Upper panel shows central Mozambique stations and lower panel shows northern Mozambique stations.

REFERENCES

Allan, R. J., and Coauthors, 2001: Is there an Indian Ocean dipole, and is it independent of the El Niño–Southern Oscillation? *CLIVARExchanges,* Vol. 6, No. 3, International CLIVAR Project Office, Southampton, United Kingdom, 18–22.

Ashok, K., Guan, Z. and Yamagata T., 2003. Influence of the Indian Ocean Dipole on the Australian winter rainfall. *Geophys. Res. Lett*., **30**, doi:10.1029/2003GL017926.

Baquero-Bernal A., Latif M. and Legutke, S., 2002. On dipolelike variability of sea surface temperature in the tropical Indian Ocean. *J. Climate*, **15**, 1358-1368.

Barreiro, M., Chang, P. and Saravanan, R., 2002. Variability of the South Atlantic Convergence Zone simulated by an atmospheric general circulation model. *J. Climate*, **15**, 745-763.

Behera, S.K. , Salvekar, P. S. and Yamahagata, T., 2001. Simulation of the interannual SST variability in the tropical Indian Ocean. *J. Climate*, **13**, 3487-3499.

Behera, S.K. and Yamagata, T., 2001. Subtropical SST dipole events in the southern Indian Ocean. *Geophys. Res. Lett*., **28**, 327-330.

Cai, W. and Watterson I.G., 2002. Modes of interannual variability of the Southern Hemisphere circulation simulated by the CSIRO climate model. *J. Climate*, **15**, 1159-1174.

Carvalho, L. M. V., Jones C. and Liebmann B., 2004. The South Atlantic convergence zone: Intensity, form, persistence, and relationships with intraseasonal to interannual activity and extreme rainfall. *J. Climate*, **17**, 88-108.

Cook, K.H., 2000. The Southern Indian convergence zone and interannual rainfall variability over southern Africa. *J. Climate*, **13**, 3789-3804.

Cook, K.H., 2001. A Southern Hemisphere Wave Response to ENSO with implications for Southern Africa Precipitation. *J. Atmos. Sci.*, **58**, 2146-2162.

Crimp, S. J., Lutjeharms, J. R. E. and Mason, S. J., 1998. Sensitivity of a tropical-temperate trough to sea-surface temperature anomalies in the Agulhas Current retroflection region. Water SA, **24**, 93-100.

D'Abreton, P. C. and Lindesay J. A., 1993. Water vapour transport over southern Africa during wet and dry early and late summer months. *Int. J. Climate*, **12**, 151-170.

Enfield, D. B. and Mestas-Nuñez, A. M., 1999. Multiscale variabilities in global sea surface temperatures and their relationships with tropospheric climate patterns. *J. Climate*, **13**, 2719-2733.

Fauchereau, N. Trzaska, S., Richard, Y., Roucou, P. and Camberlin, P., 2003. Sea-surface temperature co-variability in the southern Atlantic and Indian Oceans in connections with the atmospheric circulation in Southern Hemisphere. *Int. J. Climatol*., **23**, 663-677.

Fauchereau, N., Pohl, B., Reason, CJC, Rouault, M. and Richard, Y., 2008. Recurrent daily OLR patterns in the Southern Africa / Southwest Indian Ocean region, implications for South African rainfall and teleconnections. *Climate Dyn*., DOI 10.1007/S00382-008-0426-2.

Ghil, M. and Mo K., 1991. Intraseasonal oscillations in the global atmosphere. Part II: Southern Hemisphere. *J. Atmos. Sci.*, **48**, 780-790.

Gill, A. E., 1982. Atmosphere – ocean dynamics. Academic Press, California, 662 pp.

Goddard, L. and Graham, E., 1999. Importance of the Indian Ocean for simulating rainfall anomalies over eastern and southern Africa. *J. Geophys. Res.*, **104**, 19099-19116

Gong, D. and Wang, S., 1999. Definition of Antarctic Oscillation Index. *Geophys. Res. Lett*., **26**, 459-462.

Gong, X. and Richman, M. B., 1995. On the application of Cluster Analysis to growing season precipitation data in North America east of the Rockies. *J. Climate* **8**, 897-931

Goni, G. J., Mavume, A. F., Rouault, M., Lutjeharms, J.R. E., Rydberg L., 2008. Intensification and sea surface cooling in relation to tropical cyclones in the Mozambique Channel. Submitted to JGR: 2008JC004823

Grodsky A. S., Carton, J. A., 2003. The Intertropical Convergence Zone in the South Atlantic and the equatorial cold tongue. *J. Climate* **16**, 723-733

Harrison, M. S. J., 1984. A generalised classification of South African summer rain-bearing systems. *J. Climatol*., **4**, 547-560.

Hermes, J.C. and Reason, C.J.C., 2005. Ocean model diagnosis of interannual co-evolving SST variability in the South Indian and South Atlantic Oceans. *J. Climate*, **18**, 2864-2882.

Hermes, J.C. and Reason, C.J.C., 2008. Annual cycle of the South Indian Ocean (Seychelles-Chagos) thermocline ridge in a regional model. *J. Geophys. Res.*, **113**, C04035, doi 10.1029/2007JCOO4363.

Janowiak, J. E., 1988. An investigation of interannual rainfall variability in Africa. *J. Climate*, **1**, 240-255.

Johnson, R. A., and Wichern, D. W., 1982. Applied Multivariate Statistical Analysis. Prentice-Hall, 594 pp.

Jury, M. R., 1992. A climatic dipole governing the interannual rainfall variability of convection over the SW Indian Ocean and SE Africa region. *Trends Geophys. Res.*,**1**, 165-172.

Jury, M. R., Valentine, H. R. and Lutjeharms, J.R. E., 1993. Influence of the Agulhas Current on summer rainfall along the southeast coast of South Africa. *J. Appl. Meteor.*, **32**, 1282-1287.

Jury, M. R., Pathack, B., Rautenbach, C.J. de W., and Van Heerden J., 1996. Drought over South Africa and Indian Ocean SST: Statistical and GCM results. *Global Atmos. and Ocean System*, **4**, 47-63.

Jury, M. R., White, W. B., Reason, C.J.C., 2004. Modelling the dominant climate signals around southern Africa. *Climate Dyn*., **23**, 717-726.

.

Kalnay, E. and 21 others, 1996. The NCEP/NCAR 40 – year reanalysis project. *Bull. Amer. Meteor. Soc*., **77**, 437–471.

Kanamitsu, M., Ebisuzaki, W., Woollen, J., Yang, S.-K., Hnilo, J.J., Fiorino, M., and Potter G. L., 2002. NCEP – DOE AMIP-II REANALYSIS (R-2). *Bull. Amer. Meteor. Soc*., **83**, 1631–1643.

Kidson, J. W., 1988. Interannual variations in the Southern Hemisphere circulation. *J. Climate*, **1**, 1177 – 1198.

Kidson, J. W., 1991. Intraseasonal variations in the Southern Hemisphere circulation. *J. Climate*, **4**, 939 – 953.

Kidson, J. W., 1999. Principal modes of Southern Hemisphere low-frequency variability obtained from NCEP-NCAR Reanalyses. *J. Climate*, **12**, 2808 – 2830.

Kiladis, G. N.; Storch, H. V., and Loon, H. V., 1989. Origin of the South Pacific convergence zone. *J. Climate*, **2**, 1185 – 1195.

Kodama, Y-M, 1999. Roles of the atmospheric heat sources in maintaining the subtropical convergence zones: An Aqua-Planet GCM study. *J. Atmos. Sci.*, **59**, 4032-4049.

Kuleshov, Y., Qi, L., Fawcett, R. and Jones, D., 2008. On tropical cyclone activity in the Southern Hemisphere: Trends and ENSO connection. *Geophys. Res. Lett*., **35**, doi:10.1029/2007GL032983.

Lee, T., and Marotzke, J., 1998. Seasonal cycles of meridional overturning and heat transport of the Indian Ocean. *J. Phys. Oceanogr*., **29**, 217-230.

Lenters, J. D. and Cook, K. H., 1995. Simulation and diagnosis of the regional summertime precipitation climateology of South America. *J. Climate*, **8**, 2988-2999.

Liebmann, B. and Smith, C. A., 1996. Description of a complete (Interpolated) Outgoing Longawave Radiation Dataset. *Bull. Amer. Met. Soc*., **77**, 6, 1275-1277.

Liebmann, B., Kiladis G. N., Marengo, J. A., Ambrizzi, T. and Glick D. G., 1999. Submonthly convective variability over South America and the South Atlantic convergence zone. *J. Climate*, **12**, 1877-1891.

Lindesay, J. A., 1988a. South African rainfall, the Southern Oscillation and a Southern Hemisphere semi-annual cycle. *J. Climatol.*, **8**, 17-30.

Lindesay, J. A., 1988b. The southern Oscillation and atmospheric circulation changes over southern Africa, *PhD Thesis*, Univ. Witwatersrand, Johannesburg, 284 pp.

Lindzen, R. S. and Nigam, S., 1987. On the role of sea surface temperature gradients in forcing low-level winds and converegence in tropics. *J. Atmos. Sci.*, **44**, 2418-2436.

Loschnigg, J. and Webster, P. J., 2000. A coupled ocean-atmosphere system of SST modulation for the Indian Ocean. *J. Climate*, **13**, 3342-3360.

Lutjeharms, J.R.E., 2006. The Agulhas Current. Springer-Verlag Heidelberg. 329 pp.

Makarau , A. and Jury, M. R., 1997. Seasonal cycle of convective spells over southern Africa during austral summer. *Int. J. Climatol.*, **17**, 1317-1332.

Mapande, A. T. and Reason, C. J. C., 2005. Links between rainfall variability on intraseasonal and interannual scales over western Tanzania and regional circulation and SST patterns. *Met. and Atmos. Physics*, **89**, 215-234.

Mason, S. J. and Jurry, M. R., 1997. Climatic variability and change over southern Africa: a reflection on underlying processes. *Progress in Physical Geography*, **21**, 23-50.

Mestas-Nuñez, A. M. and Enfield, D. B., 2001. Eastern Equatorial Pacific SST variability: ENSO and non-ENSO components and their climatic associations. *J. Climate*, **14**, 391-402.

Michelangeli, P. A., Vautard, R., and Legras, B., 1995. Weather regimes: Recurrence and quasi-stationarity. *J. Atmos. Sci.*, **52**, 1237-1256.

Mitchell, T. D, Carter, T. R., Jones, P. D., Hulme, M. and New M., 2004. A comprehensive set of high-resolution grids of monthly climate for Europe and the globe: the observed record (1901-2000) and scenarios (2001-2100). Tyndall Centre working paper n° 55.

Mo, K. C., 2000. Relationship between low-frequency variability in the Southern Hemisphere and sea surface temperature anomalies. *J. Climate*, **13**, 3599-3610

Mozambique News Agency reports, 2000, 2001 and 2007. Reports numbers: 176-180, 194, 200-203, 333-336.

Mulenga, H. M., Rouault, M. and Reason, C.J.C., 2003. Dry summers over northeasren South Africa and associated circulation anomalies. *Clim. Res*., **25**, 29-41.

Neelin, J. D., 1989. On the interpretation of the Gill Model. *J. Atmos. Sci.*, **46**, 2466-2468.

Neelin, J. D., Battisti, D. S., Hirst, A. C., Jin, F., Wakata, Y., Yamagata, T., and Zebiak, S. E., 1998. ENSO theory. *J. Geophys. Res.*, **103**, 14261- 14290.

New, M., Hulme, M. and P., Jones, 1999. Representing twentieth-century space-time climate variability. Part I: Development of a 1961- 90 mean monthly terrestrial climatology. *J. Climate*, **12**, 829-856.

Nicholson, S. E., and Kim, J., 1997. The relationship of the El Niño –Southern Oscillation to African rainfall. *Int. J. Climatol.*, **17**, 117-135.

Peixoto P. J. and Oort A. H., 1992. Physics of climate. American Institute of Physics, 335 E. 45th Street, New York, NY 10017-3483, 520 pp.

Preisendorfer, R. W., 1988. Principal Component Analysis in Meteorology and Oceanography. C. D. Mobley, ed., Elsevier, Amsterdam, 425 pp.

Rayner, N. A., Brohan, P. Parker, D.E., Folland, C.K., Kennedy, Vanicek, M., Ansell, T. J. and Tett, S. F. B., 2006. Improved analyses of changes and uncertainties in sea surface temperature measured in situ since the mid-nineteeth century: The HadSST2 dataset. *J. Climate*, **19**, 446-469

Rao S. A., Behera, S. K., Masumoto, Y. and Yamagata, T. 2002. Interannual subsurface variability in the tropical Indian Ocean with a special emphasis on the Indian Ocean Dipole. *Deep –Sea Res*. Part II, **49**, 1549-1572.

Reason, C.J.C., 1998. Warm and cold events in the southwest Atlantic/ Southwest Indian Ocean region and potential impacts on circulation and rainfall over southern Africa. *Meteorl. Atmos. Phys.*, **69**, 49-65.

Reason, C.J.C. and Mulenga H., 1999. Relatioship between South African rainfall and SST anomalies in the Southwest Indian Ocean. Int. J. Climatol., 19, 1651-1673.

Reason, C.J.C., Allan, R.J., Lindesay, J.A. and Ansell, T.J., 2000. ENSO and climateic signals across the Indian Ocean basin in the global context: Part I, interannual composite patterns. *Int. J. Climatol.*, **20**, 1285-1327.

Reason, C.J.C., 2001. Subtropical Indian Ocean SST dipole events and southern African rainfall. *Geophys. Res. Lett*., **28**, 2225-2227.

Reason, C.J.C., 2002. Sensitivity of the southern African circulation to dipole sea-surface temperature patterns in the South Indian Ocean. *Int. J. Climatol.*, **22**, 377-393.

Reason, C.J.C., and Jagadheesha, D., 2005. A model investigation of recent ENSO impacts over southern Africa. *Meteorol Atmos Phys*, **89**, 181-205.

Reason , C.J.C., Landman, W. A. and Tennant, W., 2006a. Seasonal to decadal prediction of the southern African climate and its links with the variability of the Atlantic Ocean. *Bull. Amer. Meteor. Soc*., **87**, 941–955.

Reason , C.J.C., Engelbrecht, F., Landman, W. A., Lutjeharms, J.R.E, Piketh, S., Rautenbach, C. J. de W., and Hewitson, B.C., 2006b. A review of South African research in atmospheric science and physical oceanography during 2000-2005. *S. Afr. J. Sci*., **102**, 35-45.

Richard, Y., Trzaska, S., Roucou, P. and Rouault, M., 2000. Modification of southern African rainfall variability/ENSO relationship since late 1960s. *Climate Dyn*., **16**, 883-895.

Richard, Y., Fauchereau, N., Poccard, I., Rouault, M. and Trzaska, S., 2001. 20th Century droughts in Southern Africa: Spatial and temporal variability, teleconnections with oceanic and atmospheric conditions. *Int. J. Climatol.*, **21**, 873-885.

Rocha, A. M. C. and Simmonds I., 1997. Interannual variability of south-eastern African summer rainfall. Part 1: Relationships with air-sea interactions processes. *Int. J. Climatol.*, **17**, 235-265.

Rocha, A. M. C. and Simmonds, I., 1997. Interannual variability of south-eastern African summer rainfall. Part II: Modeling the impact of sea-surface temperatures on rainfall and circulation. *Int. J. Climatol.*, **17**, 267-290.

Rouault, M., White, S. A., Reason , C.J.C., Jobard , and Lutjeharms, J.R.E., 2002. Ocean-atmosphere interactions in the Agulhas Current region and a South African extreme weather event. *Weather forecasting*, **17**, 655-669.

Rouault, M., Reason , C.J.C., Lutjeharms, J.R.E. and Beljaars, A. C.CM., 2003. Underestimation of latent and sensible heat fluxes above the Agulhas Current in NCEP and ECMWF analyses. *J. Climate*, **16**, 776-782.

Saji, N. H., Goswami, B. N., Vinayachandran P.N. and Yamagata T., 1999. A dipole mode in the tropical Indian Ocean. *Nature*, **401**, 360-363.

Saji, N. H. and Yamagata T., 2003. Possible impacts of the Indian Ocean Dipole mode events on global climate *Clim. Res,* **25**, 151-169.

Schott, F. A., and McCreary Jr., J. P., 2001. The monsoon circulation of the Indian Ocean, *Prog. Oceanogr.*, 51, 1-123.

Shinoda, M. and Kawamura, R., 1996. Relationships between rainfall over semi-arid southern Africa, geopotential heights, and sea surface temperatures. *Journal of Meteorological Society of Japan*, 74, **1**, 21-36.

Solman, A. S. and Menéndez, C. G., 2003. Weather regimes in the South American sector and neighbouring oceans during winter. *Climate Dyn*., **21**, 91-104.

Thompson, D. W. J. and Wallace J. M., 2000. Annular modes in the extratropical circulation. Part I: Month-to-month variability. *J. Climate*, **13**, 1000-10016.

Todd, M. C. and Washington R., 1999. Circulation anomalies associated with tropical-temperate troughs in southern Africa and the southwest Indian Ocean. *Climate Dyn***, 15,** 937-951

Todd, M. C. , Washington R., and Palmer P. I, 2004. water vapour transport associated with tropical–temperate trough systems over southern Africa and the southwest Indian Ocean. *Int. J. Climatol.*, **24**, 555-568.

Tomczak, M. and Godfrey, J.S., 1994. Regional Oceanography: An introduction. Pergamon Press, Oxford, 422pp.

Tyson, P.D. and Preston-Whyte, R.A., 2000. The weather and climate of southern Africa, Oxford Univ. Press, Cape Town, 396 pp.

Ummenhofer, C.C., Gupta, A. S., England, M. H. and Reason, C.J.C., 2008. Contribution of Indian Ocean sea surface temperatures to enhanced east African rainfall. To be submitted to *J. Climate.*

Usman M. T. and Reason C.J.C., 2004. Dry spells frequencies and their variability over southern Africa. *Clim. Res*., **26**,199-211.

Van Loon, H., Kidson, J. W., and Mullan, A. B., 1993. Decadal variation of the annual cycle in the Australian dataset. *J. Climate*, **6**, 1227-1231.

Venzke, S., Latif, M. and Villwock, A., 2000. The coupled GCM ECHO –2. Part II: Indian Ocean Response to ENSO. *J. Climate*, **13**, 1371-1383.

Vigaud, N., Richard, Y., Rouault, M. and Fauchereau, N., 2007. Water vapour transport from the tropical Atlantic and summer rainfall in tropical southern Africa. *Climate Dyn***,** **28**, 113-123

Vincent, D. G., 1994. The South Pacific Convergence Zone: A review. *Mon. Wea. Rev.*, **122**, 1949-1970.

Von Storch, H. and Navarra, A., 1999. Analysis of climate variability, application of statistical techniques. Second updated and extended edition, Springer, 342 pp.

Von Storch, H. and Zwiers, F. W., 2000. Statistical analysis in climate research, Cambridge University Press, reprinted 484 pp.

Von Loon, H., Kidson, J. W., and Mullan, A. B., 1993. Decadal variation of the annual cycle in the Australian dataset. *J. Climate*, **6**, 1227-1231.

Waliser, D. E., and Gautier, C. 1993. A Satellite-derived Climateology of the ITCZ. *J. Climate*, **6**, 2162-2174.

Walker, N. D., 1989. Sea surface temperatures and relationships and associated ocean-atmosphere coupling mechanisms in the southern African region. PhD thesis, University of Cape Town, 173 pp.

Washington, R., and Preston A, 2006. Extreme wet years over southern Africa: Role of the Indian Ocean sea surface temperatures. *J. Geophys. Res.*, **111**, D15104.

Washington, R. and Todd, M, 1999. Tropical-temperature links in southern Africa and southwest Indian Ocean satellite- derived daily rainfall. *Int. J. Climatol.*, **19**, 1601-1616.

Webster, P.J., 1981. Mechanisms determining the atmospheric response to sea surface temperatures. *J. Atmos. Sci.*, **38**, 554-57.

Webster, P.J., Moore, A. M., Loschnigg, J. P. and Leben R. R., 1999. Coupled ocean-atmosphere dynamics in the Indian Ocean during 1997-98. *Nature*, **401**, 356-359.

Wentz, F. J., Gentemann, C. Smith D. and Chelton D., 2000. Satellite measurements of sea surface temperature through clouds. *Science*, **288**, 847-850.

Wilks, D. S., 2006. Statistical Methods in Atmospheric Sciences. Academic Press, California, 627 pp.

Woodberry, E. K., Luther, M. E., and O'Brien , J. J., 1989. The wind-driven seasonal circulation in the Southern Tropical Indian Ocean. *J. Geophys. Res.*, **94**, C12, 17985-18002

Xie, P. and Arkin, P. A., 1997. Global Precipitation: A 17-year monthly analysis based on gauge observations, satellite estimates, and numerical model outputs. Bull. Amer. Meteor. Soc., **17**, 2539-2558

Xie, S.-P., Annamalai, H., Schott, F., McCreary, J. P. Jr., 2002. Structure and mechanisms of South Indian Ocean climate variability. *J. Climate*, **15**, 864-878.

Zhang, J. Z. and McPhaden, M. C.,1995. The relationship between sea surface temperature and latent heat flux in the Equatorial Pacific. *J. Climate*, **8**, 589-605.